RN-33

ATMOSPHERIC GENERAL CIRCULATION MODELS

SATISH CHANDRA

DIRECTOR

STUDY GROUP

K S RAMASASTRI

PRATAP SINGH

NATIONAL INSTITUTE OF HYDROLOGY
JAL VIGYAN BHAVAN
ROORKEE-247667 (U.P.)

1985-86

CONTENTS

LIST OF SYMBOLS

u	Zonal (X direction) component of the wind vector V
v	Meridional (Y direction) component of the wind vector V
Ω	Angular velocity of spin of earth
ϕ	The latitude (of earth)
g	The acceleration due to gravity cm/sec^2
ρ	Density of dry air
f	Coriolis parameter
ψ	Stream function
C_p	Specific heat at constant pressure $cal/gm/^oK$
ζ	Relative Vorticity
∇^2	Horizontal Laplacian Operator
J	Jacobian operator
dp	Increment of pressure along the vertical axis mb
dh	Increment of height in the atmosphere
m	Map scale factor
ω	Vertical velocity cm/sec
ϕ	Geopotential
Z	Geopotential height

LIST OF FIGURES

LIST OF TABLES

ABSTRACT

Hydrological cycle encompasses in itself two major processes; the atmosphere phase and the ocean-land surface phase. Mathematical and conceptual modelling of these two processes independently have been accomplished for a long time now Combined models for the representation of the hydrological processes and atmospheric general circulation have been in the process of development since the last 15 years.

Precipitation is the most important climatic element for hydrological processes. The General Circulation Models (GCMs) simulate precipitation as a result of large scale convective motion. Several atmospheric GCMs have been integrated in the last 10 to 15 years and have shown themselves capable of simulating not only the average seasonal oscillation but also the inter annual variability.

Some GCMs have also been made operational by India Meteorological Department and Indian Institute of Technology, Delhi for prediction of weather from 2 to 7 days in advance. Attempts have also been going on for introducing further sophistication into combined Atmospheric General Circulation-Land surface process models.

The atmospheric general circulation is a largest and most persistent scale of motion and serves to transport the hot air from the equatorial region toward poles and to maintain return flow of cold air from polar to tropical latitudes.

The GCMs synthesize the large scale distribution of the climate by application of the physical laws governing the atmospheric structure and behaviour. With realistic boundary conditions, the GCMs were successful in reproducing the continental - scale features of the observed distribution of temperature and pressure and other circulation patterns. Some of the GCMs developed for tropical regions were able to simulate the seasonal shifts of surface temperatures and precipitation which accompany the monsoons.

A review of the available general circulation models is carried out in this note with a view to identify such models which have the necessary space-time structure and requisite output so that they could be coupled with suitable hydrological models.

A number of regional and general circulation models made operational in India with various constraints and forcing introduced into them are reviewed in particular.

1.0 INTRODUCTION

The planning meeting of the World Climate Programme (WCP) - Water was held at Paris in 1982 when the current and planned activities of WCP-Water were reviewed. The committee formulated the following project heads.

i) studies of climate variability using hydrological data,

ii) modelling of the hydrological cycle,

iii) application of climate information to hydrological forecasts in the operation of water resources systems,

iv) inventory of water resources and their dynamics,

v) studies of the influence of climate variations on water resources,

vi) impact of climate on society through water resources

vii) influence of man's activities on climate.

While detailing the projects under the head 'Application of climate information to hydrological forecasts in the operation of water resources systems' one project was identified for implementation by India namely 'Pilot study for application of climate information to operation of Irrigation, Hydropower and flood control systems in India'. WMO wanted a feasibility study to be carried out first.

This review report is an attempt in this direction to identify such of the general circulation models which could be

used for coupling with the hydrologic (land surface) process models to achieve the desired objective of using climate information for hydrological forecasts.

The hydrologic cycle on one hand and the global general circulation on the other are nature's mechanism to maintain balance of water and temperature on earth. The general circulation of the atmosphere and the atmospheric disturbances set the atmosphere in constant motion whereby heat is transported from the lower latitudes to high latitude regions. Nearly 90 per cent of the heat exchange is due to atmosphere, the remaining 10 per cent is carried by the oceanic circulation.

Conceptually, the hydrologic cycle is visualised as beginning with evaporation from the oceans. The resulting water vapour condensed to form clouds. Under some favourable conditions the clouds precipitate. The precipitation falling on earth is dispersed on land in several ways through soil, overland and under ground. The surface stream flow and ground water move towards ocean under gravity. Substantial quantities of water are returned to the atmosphere by evaporation and transpiration before the waters reach the ocean.

The movement of water through the various phases of the cycle is erratic, both in time and space. The hydrologist's interests extend far beyond the qualitative understanding of the hydrologic cycle and the quantitative estimates of the water in constant motion in the different phases of the cycle. A thorough understanding of the inter-relations between various factors is needed so that the hydrologist could accurately

predict the effect of one process on the other and plan to estimate the influence of man-made works on the system.

The hydrological cycle is shown in the form of a block diagram in figure 1. The boxes in the diagram represent forms of moisture storage and the directed arrows the transformation of moisture from one form of storage to another.

The water vapor flux and the water budget are major factors which affect the dynamic and thermodynamic state of the atmosphere on different scales

- Over short time scales they contribute to maintaining the energy balance of atmosphere
- Over medium time periods the behaviour of the atmosphere is indicated by anomalies in the parameters such as sea surface temperature, pressure etc.
- Over long term time scale the variations in the parameters are integrated.

The advent of General Circulation Models had made possible a better insight into the behavioural pattern of the atmosphere over different time and space scales.

General Circulation Models (GCMs) outlined in the sketch in fig. 2 are three dimensional atmospheric models for the time dependent turbulent large scale motions of the atmosphere. Atmospheric radiation depends on the amount and type of cloud which in turn is determined by the water evaporating from land surface. Atmosphere is thus coupled to the surface through the hydrological cycle with the vaporation at surface as source and condensation from clouds

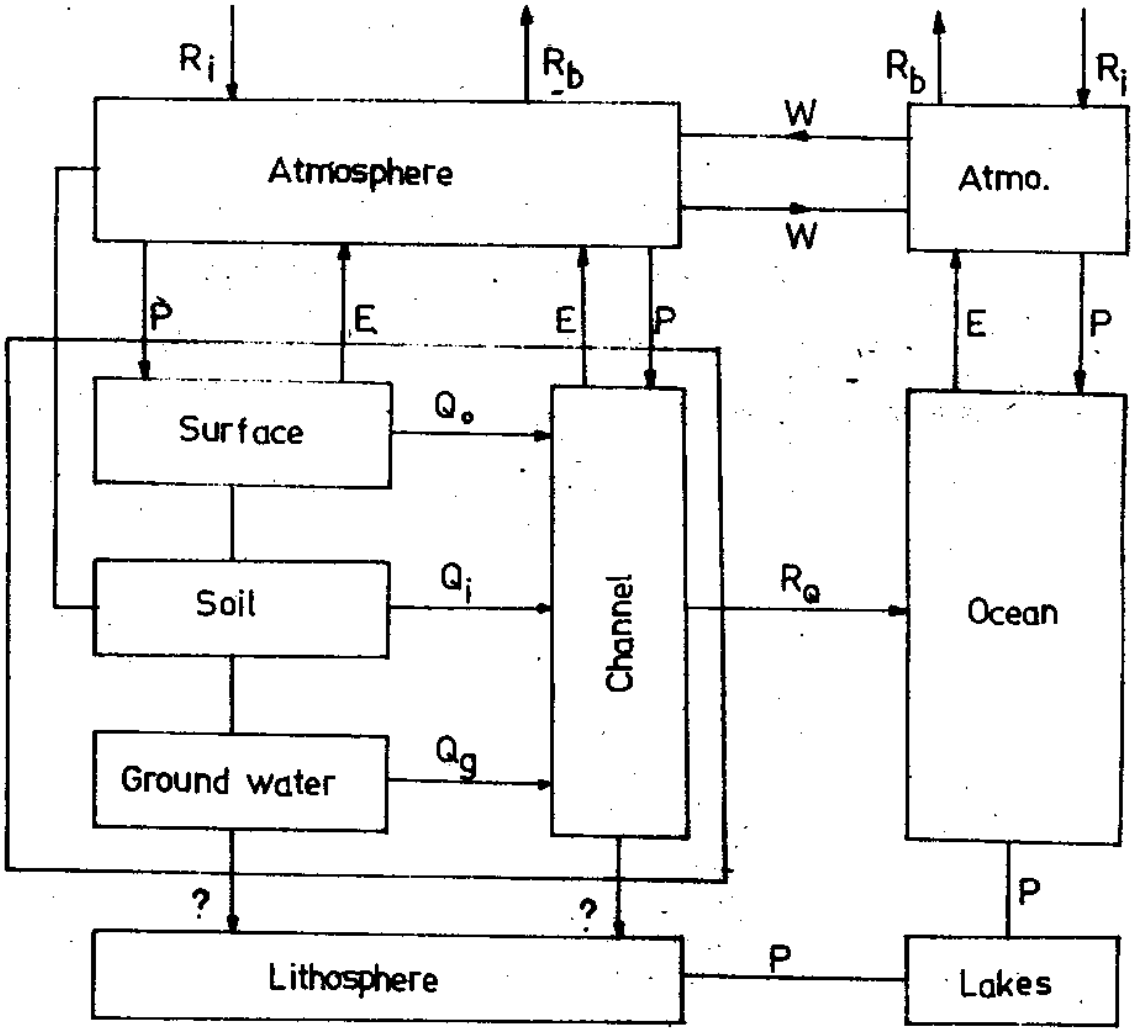

FIGURE 1 - BLOCK DIAGRAM OF HYDROLOGIC CYCLE

R_i - Incoming radiation

R_b - Back radiation

W - Transport precipitable water

P - Precipitation

E - Evaporation

T - Transpiration

F - Infiltration

R - Groundwater recharge

Q_o - Over land flow

Q_i - Inter flow

Q_g - Groundwater flow

R_Q - Total run-off

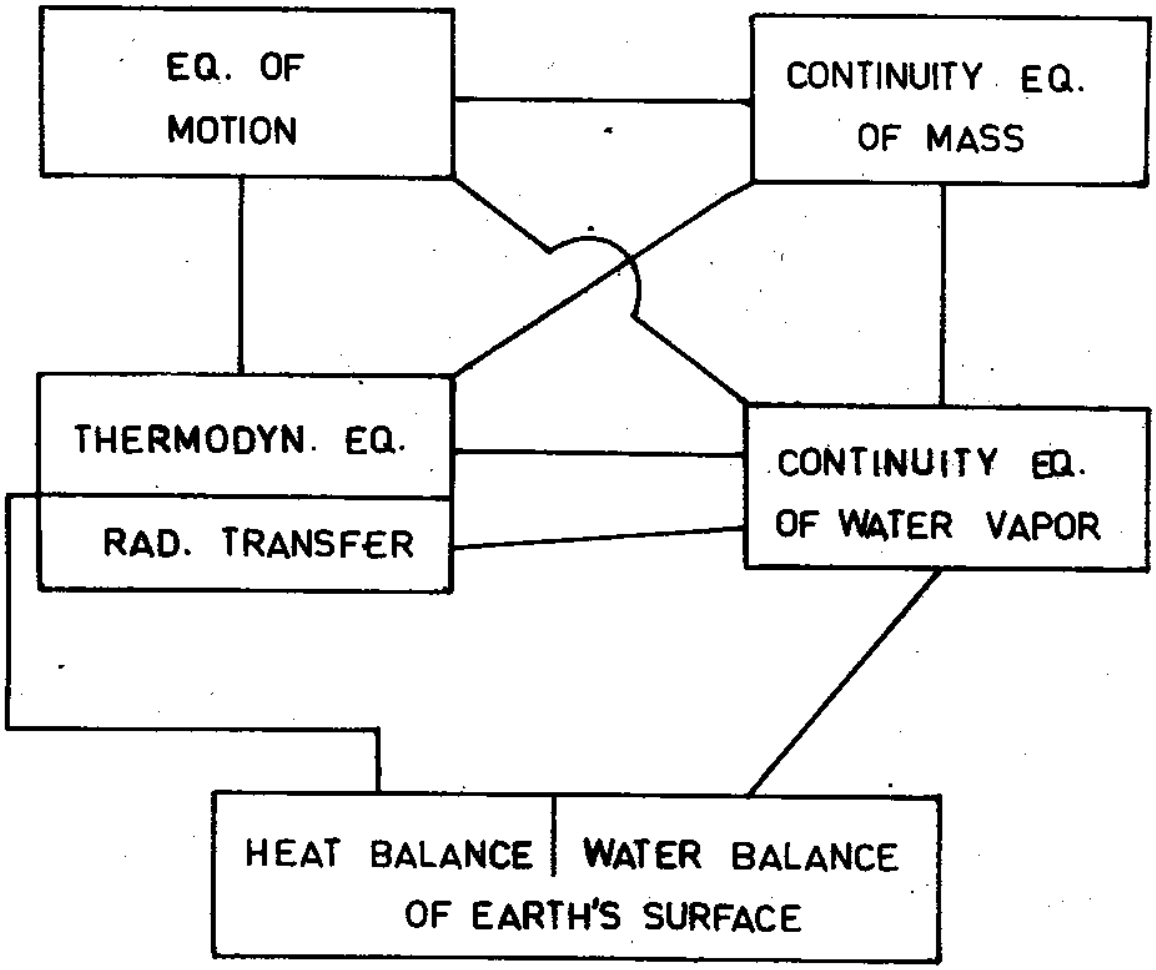

FIGURE 2 - BOX DIAGRAM OF A GENERAL CIRCULATION MODEL OF THE ATMOSPHERE

acting as sinks.

Initially, the GCMs have been developed to study the patterns of the climatic changes. The pioneering work in this direction has been made by Phillips (1956). Using a simple 2 layer weather prediction model of the atmosphere and assuming a latitudinal distribution of zonally uniform heating he succeeded in simulating the jet stream and the zonal mean cells of the meridional circulation i.e. Hadley cell, Ferrel cell and Polar cell (Figure 3). His model was, however, not suitable for dealing with the hydrological cycle.

The first ever efforts towards coupling the GCMs with surface hydrology was considered by Manabe (1969). Since then, many investigators have incorporated the hydrologic processes into their general circulation models (Holloway and Manabe, 1971, Kasahara and Washington, 1971, Gates and Schlesinger, 1977, Washington and Williamson, 1977 and Corby etal 1977). They were able to simulate the important characteristics of the global circulation and hydrologic variables.

This review note is concerned with the atmospheric phase of the Atmospheric-land surface coupling. A number of general circulation models developed in different parts of the world including India are reviewed and their features in relation to the land surface coupling examined.

2.0 REVIEW

The general circulation of the atmosphere, the largest and most persistent scale of motion represents the reaction of the atmosphere to the global features characterised by

i) Large latitudinal variation of atmospheric heating

ii) Northward and southward displacement of the zone of maximum heating because of earth's orbit around the sun during the course of an year.

iii) The strengthening of the north-south gradient of heating in the winter hemisphere and its weakening in summer hemisphere.

iv) The distribution of continents and oceans and

v) The rotation of earth.

The north-south variation in heating initiates the northward or south ward motion called the 'Meridional flow'. The flow towards east or west called the 'Zonal flow' is caused by earth's rotation. The general circulation is principally characterized by extensive zonal wind systems.

The large scale motion of the upper layers of ocean water also has a major influence on the general circulation of the atmosphere. The interaction of the ocean-atmospheric system is exceedingly complex, with large scale energy exchange taking place in the boundary layer.

2.1 Features of General Circulation

Scientists have been engaged in the study of general

circulation for nearly three centuries. One of the early theories of general circulation was put forth by George Hadley, a British layer in 1735. Hadley concluded that strong solar heating in equatorial latitudes causes a general rising motion of air along the equator, with the air flowing poleward at high elevations. As the poleward flowing air cools, it becomes heavier and sinks. At low elevations air then flows, equatorward to replace the rising warm air, thus forming a continuous circulation cell oriented north-south along the meridians. This meridional cell is known as 'Hadley cell' (Figure 3)

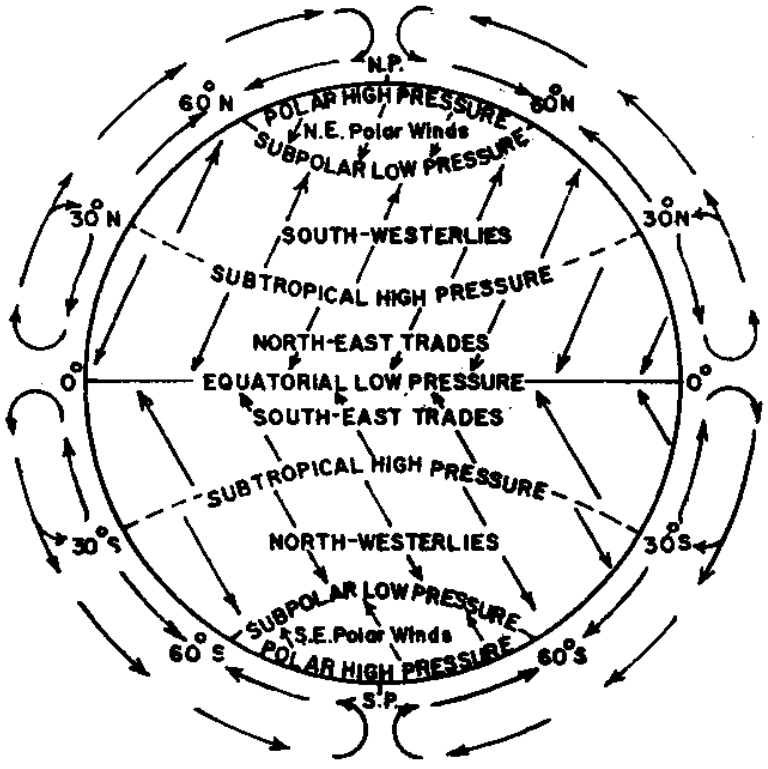

FIGURE 3 - HADLEY'S MERIDIONAL CIRCULATION

2.2.1 Hadley cells

Though the concept of 'Coriolis force' due to earth's rotation has not yet been recognized at the time of Hadley, he had postulated the north east and southeast 'trade' winds to be resulting due to the rotation of earth. Hadley thus concluded that as air in the lower branch of a meridional cell flows equatorward, it travels into a region of the earth which is moving more rapidly eastward. This gives the air an easterly component (relative to earth) which added to its equatorward motion produces the northeast trades of the southern hemisphere.

Since Hadley's time several other theories of the general circulation had employed meridional cells, often suggesting the existence of three cells between the equator and the poles. Hadley type cells were postulated in low latitudes and again in high latitudes. Between them in middle latitudes was an indirect meridional cell.

The rising equatorial air acquired an eastward component as it moves northward. At about 30^{o} latitude it tends to subside because of cooling. The subsiding air splits into two currents, one moving southward as the north-east trade winds and the second continuing northeastward. In the polar cell loss of heat in the lower layers results in subsidence, the subsiding air spreading south-westward. As it moves southward, the air is warmed and at about 60^{o} latitude , it rises and returns poleward as a south-westerly current. In the middle cell, the south-westerly current in

the lower layers meets the southern edge of the polar cell and is forced upward over the colder westward moving air.

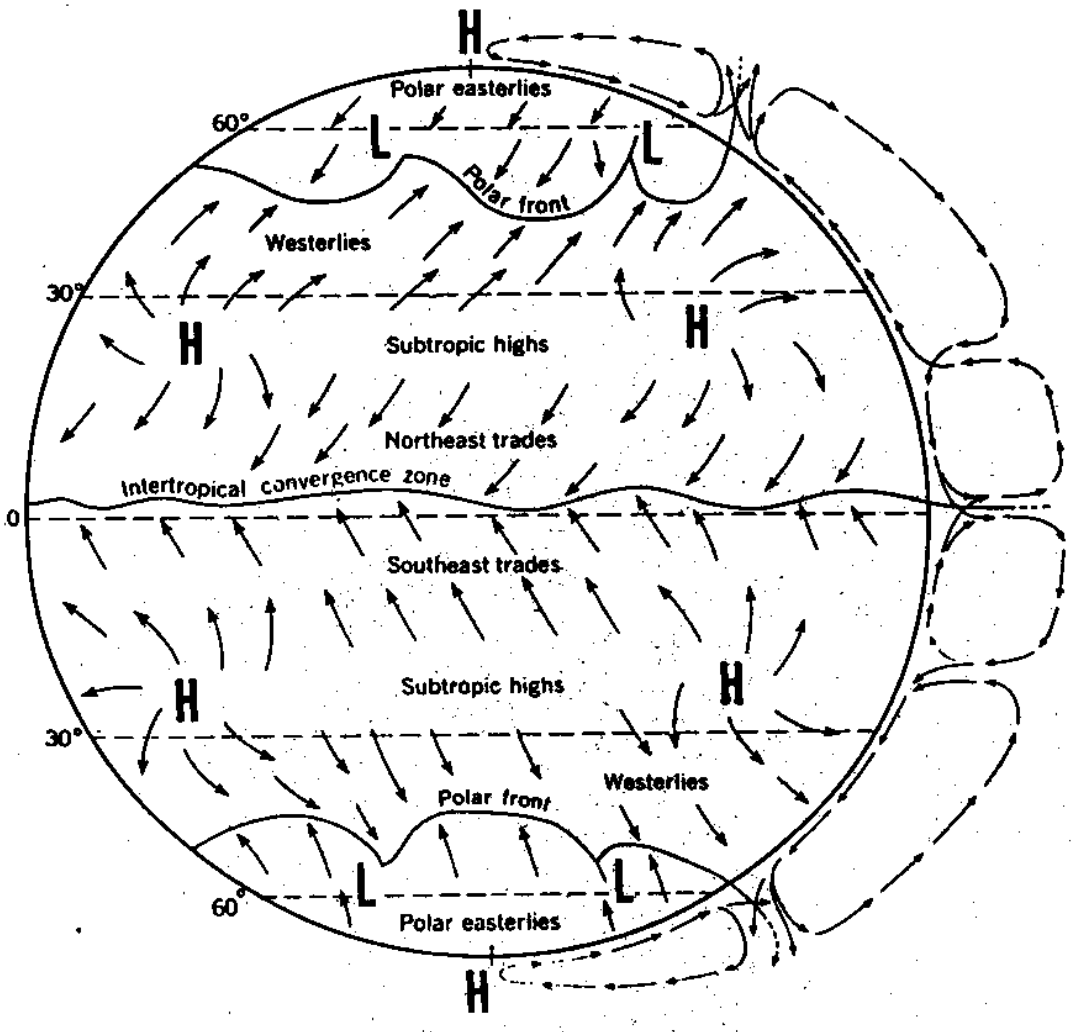

FIGURE 4 - SCHEMATIC ARRANGEMENT OF WINDS AND PRESSURE IN THE GENERAL CIRCULATION. EFFECTS OF DIFFERENTIAL HEATING OF LAND AND WATER SURFACES ARE NEGLECTED.

The major features of the 'General Circulation' as visualised at present is shown in figure 4. The Hadley cells accomplish certain major atmospheric processes:

i) Their upper level branches transport energy from equatorial latitudes to about 30^{o}N and 30^{o}S latitude.

10

ii) Their lower level branches transport moisture evaporated from the subtropical latitudes of equatorial latitudes, where it contributes to the heavy equatorial rains.

iii) The rising of warm air in equatorial latitudes and sinking of cooler air transforms total potential energy into kinetic energy.

The east-west circulations resulting from differential heating of ocean and land surfaces are particularly important in determining the precipitation distribution in the subtropics and tropics.

2.1.2 Observed circulation patterns

The general circulation pattern shown in figure 5 is an idealized situation when the earth's surface could be considered to be completely homogeneous. But the real earth has an irregular pattern of continents and oceans, particularly in the north hemisphere. This basic irregularity, which is further complicated by seasonal differences in the heating and cooling patterns, results in a circulation which departs from an ideal, symmetrical pattern. In spite of the complications of a non-homogeneous earth, there is nevertheless, a recognizable pattern both to the general circulation and to the earth's climates. In figures 5 and 6 the mean sea-level pressure pattern in the months of January and July is shown. The flow of winds is indicated by arrows. The existence of broad latitudinal zones of wind systems could be seen in these

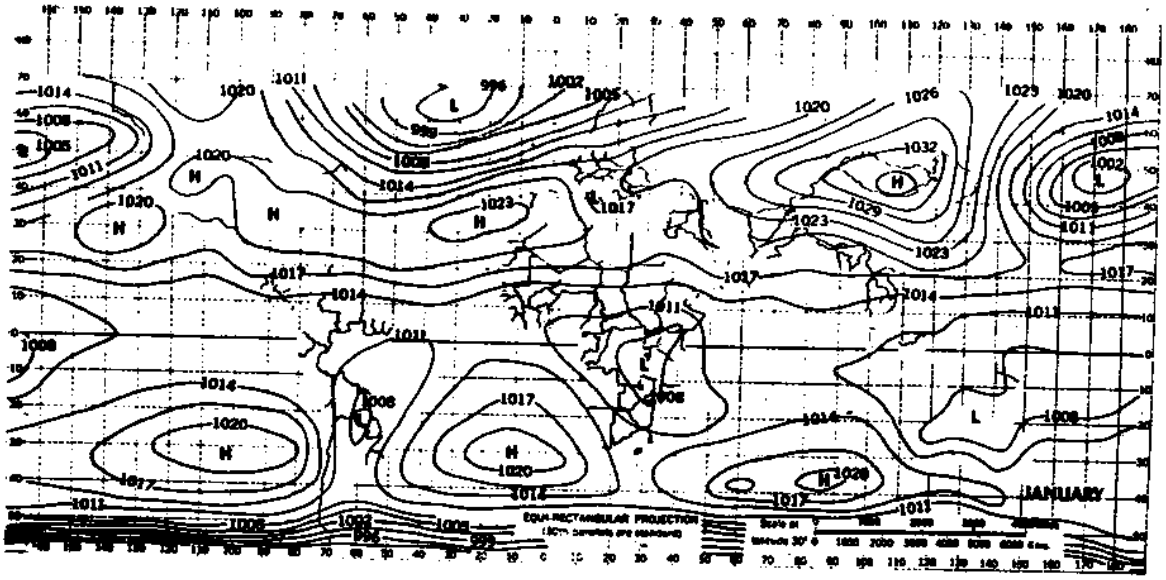

FIGURE 5 - JANUARY SEA-LEVEL PRESSURE, IN MILLIBARS (mb).

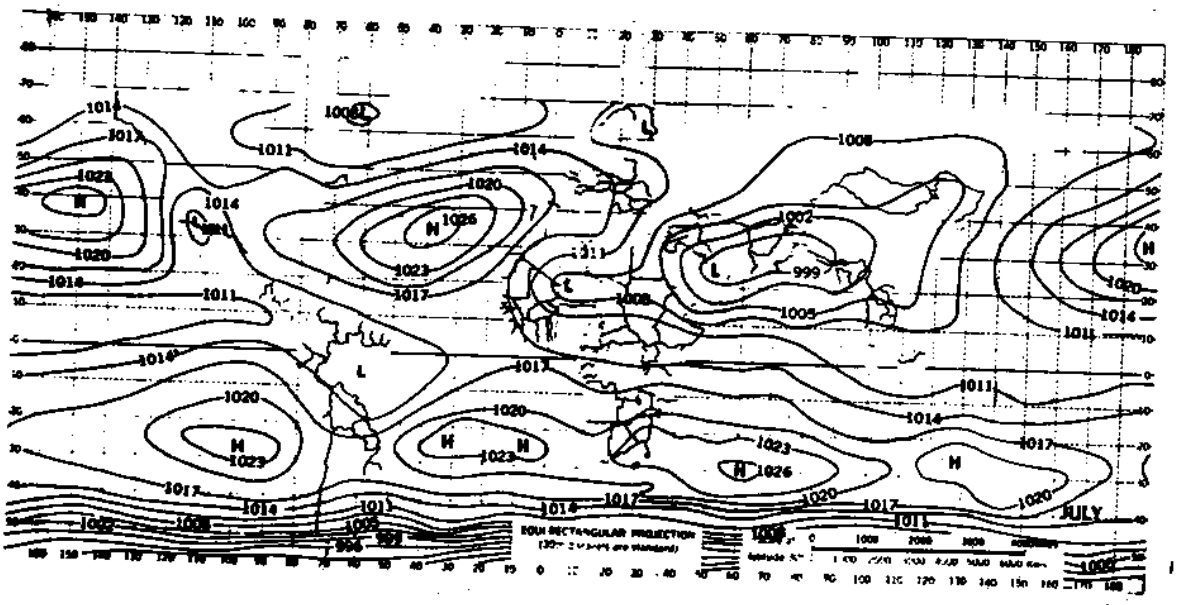

FIGURE 6 - JULY SEA-LEVEL PRESSURE, IN MILLIBARS (mb).

figures. The major zonal systems are:

i) The inter-tropical convergence zone

ii) The equatorial westerlies

iii) The tropical easterlies

iv) The subtropical highs

v) The middle latitude westerlies, and

vi) The polar easterlies

The shifting wind systems typical of monsoons are another important feature of the general circulation. Descripiton of the systems listed above could be seen in text books of climatology. Global analysis of January and July sea level pressure has also been presented by Godbole and Shukla (1981).

2.1.2.1 rossby waves

The very large scale wave features which are observed in the flow on the planetary scale are known as planetary waves. In their simplest form they occur because of the variation of the coriolis parameter with latitude and are known as 'Rossby Waves'.

The equation for Rossby wave in its simplest form is obtained for an atmosphere of constant density under the assumption of uniform zonal flow $\bar{U}$ and no vertical motion. The wave speed:

$$C = \bar{U} - \beta/(K^2 + m^2) \qquad \ldots \quad (1)$$

where β is the Rossby parameter given by $2\,\Omega \cos \phi/a$ where a is radius of earth. K and m are the wave numbers in

the x and y directions respectively.

2.1.2.2 gravity waves

These are vertical transverse waves whose primary driving force is that of gravity. Effects of compression, the earths rotation and friction are ignored to isolate the mechanisms at work in pure gravity waves. Consequently these are omitted from the u and w equations of motion and the two dimensional continuity equation. Thus the wave speed

$$c = U \pm \frac{g\lambda}{2\pi} \tan h \frac{2\pi h}{\lambda})^{1/2} \quad \ldots \quad (2)$$

where h is the height of the surface on which the wave forms. The most simple example of gravity waves is that of lee waves in mountains.

2.2 Forces Controlling the Horizontal Motion

The downward acting gravitational field of the earth sets up the decrease of pressure away from earth's surface. This mutual balance between the force of gravity and the vertical pressure gradient is referred to as hydrostatic equilibrium. The hydrostatic equation is written as:

$$dp = -g \rho \, dh \quad \ldots \quad (3)$$

In other words the pressure gradient force per unit height was given by $-\frac{1}{\rho} \frac{dp}{dh}$ Hence, the closer the isobar spacing, the more intense the pressure gradient and the greater the wind speed.

The other forces which control the motion of air include:

i) the coriolis force

ii) the centrepetal acceleration, and

iii) the frictional forces.

2.2.1 Coriolis force

Unlike the fixed coordinate system, in the case of rotating earth, there is apparent deflection of moving objects to the right of their line of motion in the northern hemisphere and to the left in the southern hemisphere as viewed by observers on earth. The coriolis force is expressed by:

$$f = -2\Omega V \sin \phi \qquad \ldots \qquad (4)$$

where,

V = the velocity of the mass

2.2.2 Geostrophic wind

Observations in the free atmosphere show that the wind blows more or less at right angles to the pressure gradient (i.e. parallel to the isobars). This implied that for steady motion, the pressure gradient force is exactly balanced by the coriolis force acting exactly in the opposite direction. This form of idealised wind is called 'geostrophic wind' and the geostrophic wind velocity Vg is given by:

$$Vg = \frac{1}{2\Omega \sin \phi \rho} \cdot \frac{dp}{dh} \qquad \ldots \qquad (5)$$

Thus, except in low latitudes, where the coriolis force approaches zero, the geostrophic wind is a close approximation to the observed air motion in the free atmosphere. Since pressure systems are rarely stationary, mutual adjustments of the wind and pressure fields take place constantly.

2.2.3 Centripetal acceleration

For a body to follow a curved path, there must be an inward acceleration towards the centre of rotation.

$$C = - \frac{mV^2}{r} \qquad \ldots \qquad (6)$$

where,

m = moving mass

V = its velocity

r = the radius of curvature

In the northern hemisphere flow in a low pressure system is maintained in a curved path by virtue of the coriolis force being weaker than pressure gradient wind.

2.2.4 Frictional forces

An important effect on the air movement is due to the friction caused by earth's surface. Near the surface of the earth the frictional force reduces the wind velocity thereby reducing the force of deflection with the result that the air tends to be guided more by the pressure gradient. This produces the spiraling effect of wind with increasing height

because of the decreasing of frictional force with height. This spiral is known after Ekman who has investigated similar effect in ocean currents.

2.3 Forces of Vertical Motion

Mass uplift or descent of air occurs primarily in response to dynamic factors related to horizontal flow and secondarily due to air-mass instability.

2.3.1 Divergence and vertical velocity

Convergence occurs when there is a net accumulation of air in a limited sector and divergence when there is net outflow. Thus, if all winds follow the geostrophic law, there could be neither convergence nor divergence and hence no weather. Other ways in which convergence or divergence can occur are the result of surface friction effects.

The relationship for vertical motion is derived from the equation of continuity :

$$\frac{1}{\rho}\frac{\partial p}{\partial h} + \nabla_H \cdot V + \frac{\partial \rho}{\partial h} = 0 \qquad \ldots (7)$$

Assuming no change in density ρ, $\frac{\partial \rho}{\partial h}$ would be zero.

Hence, $W = -\int_0^z \nabla_H \cdot V \, dh$ ... (8)

where,

$\nabla_H \cdot V$ is the horizontal divergence and is written as $\nabla_H \cdot V = \frac{\partial u}{\partial x} + \frac{\partial v}{\partial y}$ ... (9)

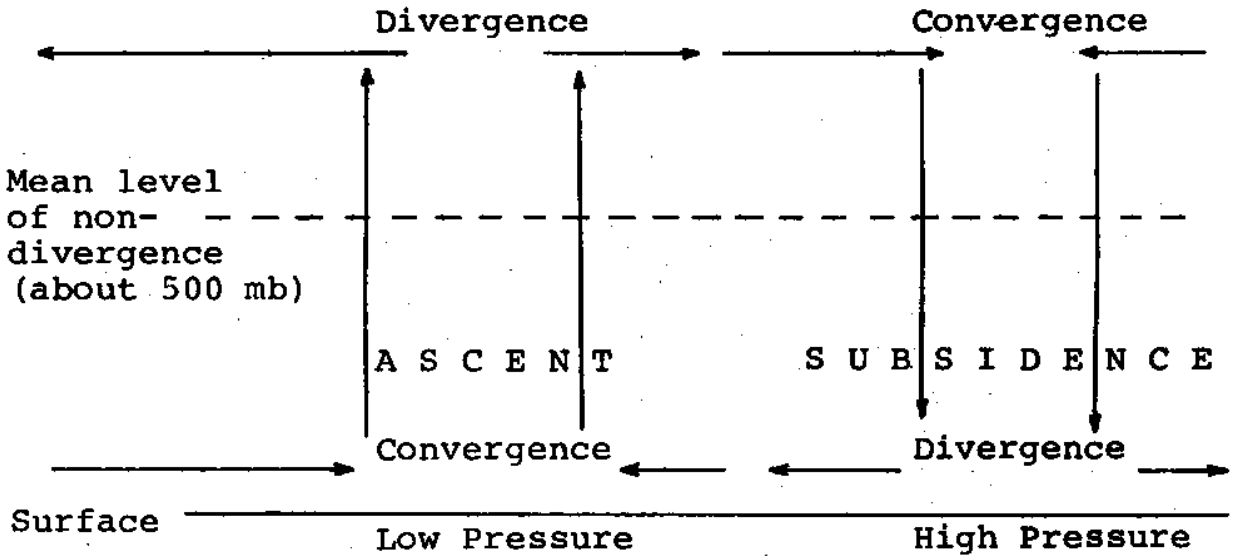

FIGURE 7 - SCHEMATIC DIAGRAM OF CONVERGENCE AND DIVERGENCE.

Horizontal inflow and outflow near the surface has to be compensated by vertical motion. As shown in figure 7, air rises above a low pressure cell and subsides over a high pressure with compensating divergence and convergence respectively in the upper troposphere. Thus, at some level in the atmosphere the divergence or convergence is effectively zero. Generally 500 mb is identified with this level. The vertical velocities in large scale motion are less as compared to those in the convective storms. For example, the vertical velocities in cumulus may exceed 10 m/sec. as compared to 5-10 m/sec. in depressions and cyclones.

2.3.2 Vorticity

Vorticity represents the rotational or angular velocity of minute particles in any fluid system. Vorticity has three elements. Magnitude, direction and sense of rotation. Thus cyclonic vorticity may result from cyclonic curvature and anticyclonic vorticity from an anticyclonic situation.

The vorticity or circulation about a rotating circular fluid disc is given by the product of the rotation on its boundary (ωR) and the circumference $2\pi R$.

The vorticity is equal to $2\pi R^2$ where R is the radius of disc.

2.4 Other Forces

Some of the local conditions exert more influence some times than the planetary scale systems. Some of these are:

i) Land and sea contrast

ii) Irregular terrain, and

iii) Barrier effect of mountains

2.5 Upper Air Wind System

Above the level of surface frictional effects (about 500-2000 m), the wind increases in speed and becomes more or less geostrophic. With further height increase, the reduction of air density leads to a general increase in wind speed. There is also a seasonal variation in wind speed

aloft, these being much greater during winter months when the meridional temperature gradients are at a maximum. The mean contours of the geopotential at 700 mb in the northern hemisphere and southern hemisphere respectively are indicated in figures 8 and 9. The charts show strong cyclonic vortex over Canadian Arctic and eastern Siberia in the northern hemisphere and over the subpolar regions in southern hemisphere.

In the northern hemisphere most upper geostrophic winds are dominantly westerly between the subtropical high pressure cells and the polar low pressure centre aloft. Between the subtropical high pressure cells and the equator they are easterly. This westerly circulation reaches maximum speeds of 150-250 kmph which even increase to 300 kmph. These maximum speeds are concentrated in a narrow band and are often situated at about 30^{o}N between 9 and 15 km and are called the 'Jet Stream'. Observational study of wind and temperature distribution in the troposphere in winter suggested that these are two westerly jet streams. The more northerly one is termed the Polar Front Jet Stream. The polar jet stream is irregular whereas the subtropical jet stream is much more consistent. During the monsoon season two easterly jet streams set over India and displace the subtropical jet to north. The easterly jet is a semipermanent summer time feature with air entering it from the east, speeding up as it moves into the core of jet, and then slowing

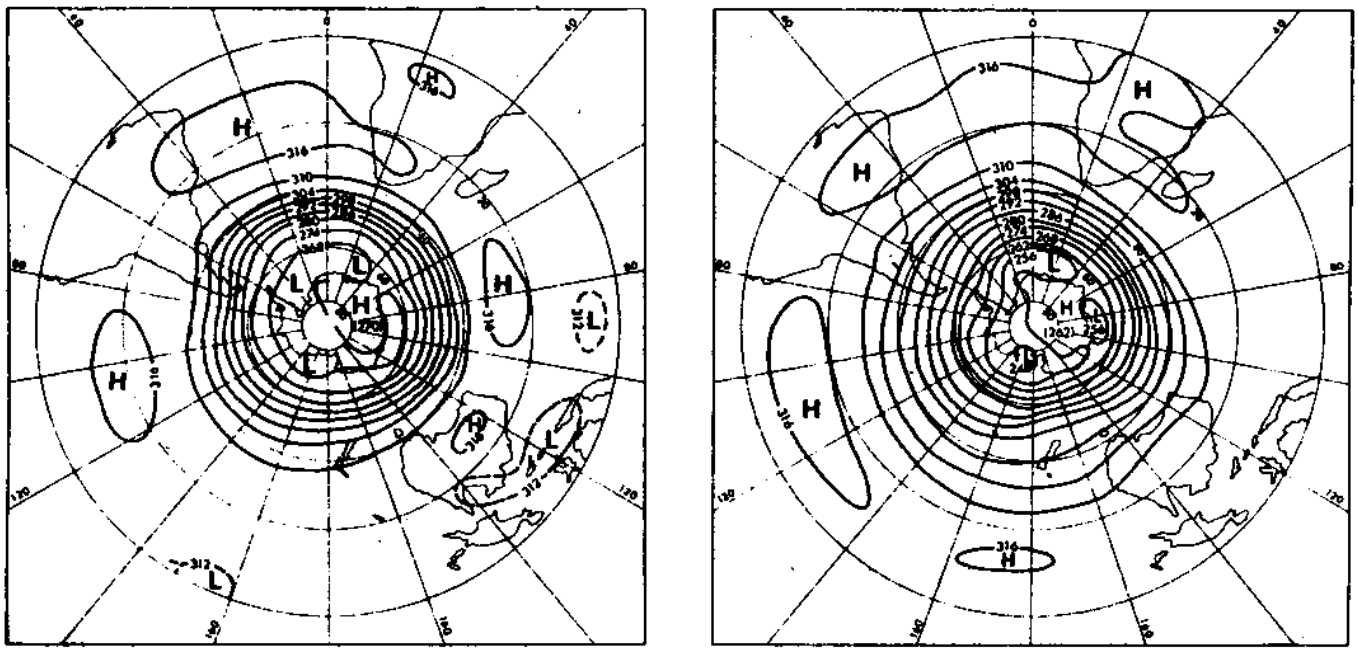

FIGURE 8 - THE MEAN CONTOURS (g.p.dkm) OF THE 700 mb PRESSURE SURFACE IN JANUARY (LEFT) AND JULY (RIGHT) FOR THE SOUTHERN HEMISPHERE .

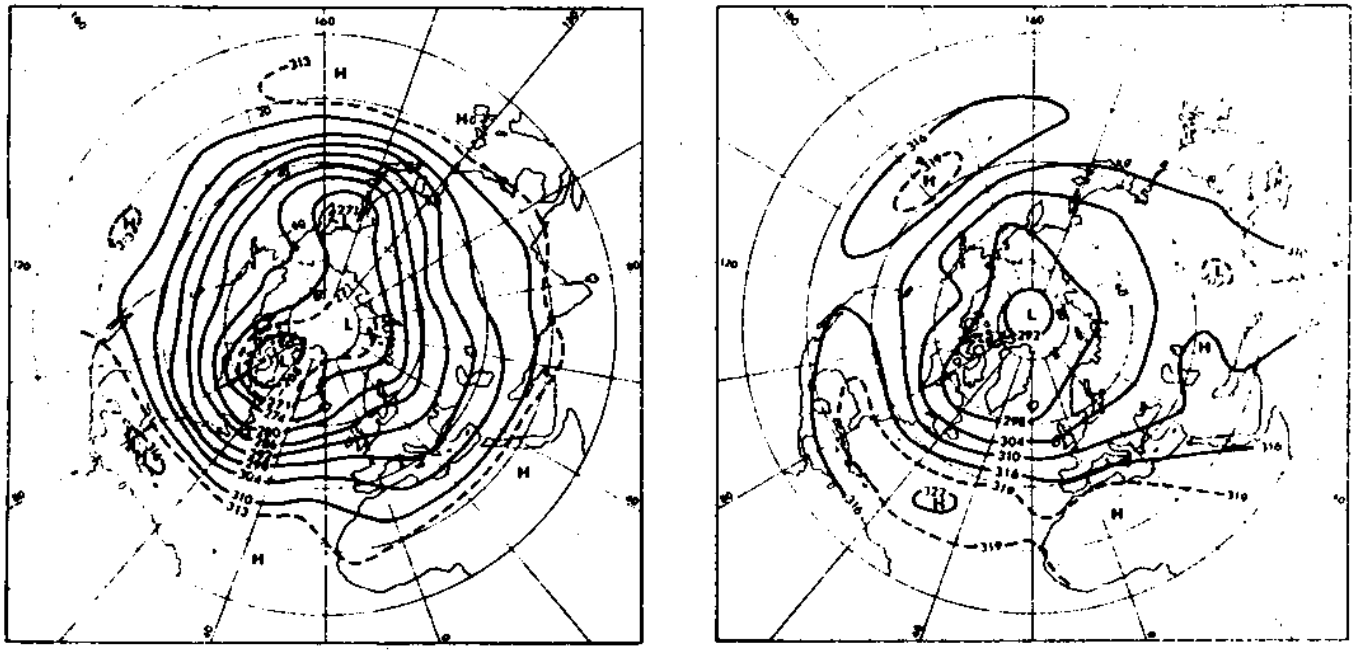

FIGURE 9 - THE MEAN CONTOURS (g.p.dkm.) OF THE 700 mb PRESSURE SURFACE IN JANUARY (LEFT) AND JULY (RIGHT) FOR THE NORTHERN HEMISPHERE

down as it leaves the western end.

2.6 Laboratory Models

Information on the basic physical controls of the general circulation can be obtained by a study of models of the atmosphere in the laboratory. The laboratory experiments which most nearly duplicate the basic motions observed in the atmosphere are those involving a rotating annulus of fluid subjected to axisymmetric heating and cooling. The earliest experiments of this type were conducted by Vettain (1885) in which the apparatus was a rotating cylinder about 30 cm in diameter and 5 cm deep, containing air. In one experiment ice was placed at the centre and the resulting motion of air was, in its essential features, a simple direct cell like that envisaged for the atmospheric circulation by Hadley (1735).

The apparatus is rotated on a turntable, and the resulting motions in the fluid, which can be a mixture of water and glycerol, are made visible by the use of tiny neutrally buoyant reflecting solid particles such as polystyrene beads. The particle motions are recorded by a camera which rotates with the convection chamber, and so a time exposure will record particle motions relative to the rotating apparatus as streaks. Typically the radius of the outer surface of the inner cylinder varies from 0-4 cm, while the inner surface of the outer cylinder may have a radius of about 9 cm and the fluid depth is about 16 cm, while rotation rates vary from

0-4 cm, while the inner surface of the outer cylinder may have a radius of about 9 cm and the fluid depth is about 16 cm, while rotation rates vary from 0 to 7 rad/sec (Hide, 1969; Hide and Mason, 1970). In some such experiments dye was added to reveal the water motion. The dishpan was heated around its outer edge to correspond to the heating of the atmosphere in equatorial latitudes and cooled in the center to represent the cooling in polar latitudes. When the dishpan was rotated at slow speeds to represent the weak coriolis force at low latitudes, a Hadley type circulation called the Hadley regime developed. Water rising around the edge of the pan flowed towards the center near the top and sunk near the centre. However, when the pan was rotated more rapidly to produce a larger coriolis effect, corresponding to that found in the middle and high latitudes, a Hadley circulation does not develop. Rather, a vortex containing large amplitude waves similar to the Rossby waves was present. The dishpan experiments seem to indicate that for small values of the coriolis term (lower latitudes), a Hadley like regime was to be expected but that for larger values (middle and high latitudes), a wave like pattern called the Rossby regime would exist.

Douglas, Hide and Mason (1972) made laboratory experiments on the three dimensional structure of thermal convection in a rotating fluid subject to a horizontal temperature gradient. The experiments were made possible by a straight forward application of the method of streak

photography to determine the motion of tiny neutrally buoyant reflecting solid particles. The convection chamber has the annular space of total height 22.07 cm between two cylinders, the outer one with inner radius of 8.44 cm and the inner one with outer radius of 3.80 cm. The top of the convection chamber carried a fix clear acrylic lid. In experiments with a rigid upper surface the bottom of the lid was used in contact with the upper surface of the liquid in the convection chamber. In other experiments, with a free liquid surface, a different lid was used which did not touch the liquid in the convection chamber, but served to eliminate wind stress and effects due to evaporation.

Though various experimental arrangements are possible, one of the greatest interests in the context of general circulation is that in which the central cylinder acts as a cold source (pole) while the outer cylinder is a warm source (equator). If the temperature gradient is kept constant and the rate of rotation is varied, a variety of interesting flow patterns become apparent. At low rates of rotation the flow is completely symmetrical about the axis of rotation, but as the rotation rate increases, the flow becomes non-axisymmetric and waves appear which are arranged around the central axis. The fluid flows through the waves in the direction of rotation, with the flow concentrated into narrow bands or streaks, since the velocity is not uniform over the whole wave. It is also observed that the waves progress around the axis in the direction of rotation, and the flow exhibits

regular periodic time variations, including a change in the number of waves, and shows the regular progression around the wave pattern of the sizable distortions and a wavering in the shape of the flow pattern. As the rate of rotation increases so does the number of waves until eventually the flow becomes irregular.

The waves observed in the non-axisymmetric case are fully developed baroclinic waves, which are responsible for the main heat transfer between the warm rim and the cool centre. A baroclinic wave is one which forms in a strongly baroclinic region of fluid, and the growth of the disturbance is characterized by the ascent of the warmer, and descent of the colder fluid masses, representing a decrease of potential energy and an associated release of kinetic energy. A three level streak photographs of regular baroclinic wave flow patterns are shown in figure 10.

Krishnamurti (1977) described a laboratory model of wind driven circulation in which various wind stress patterns were simulated. Both homogeneous and two layer fluids were used. In this experiment, a cylindrical tank was divided into three separate basins: a 180^{o} basin, a 120^{o} basin and a 60^{o} basin. The tank was placed in a rotating table and arrangement was made for rotating a 'cone' shaped lid relative to the tank. The physical basis for the model lies in the analogy between the vortex stretching by flow across constant depth contours, and the relative vorticity produced by the oceanic flow between latitudes of different coriolis

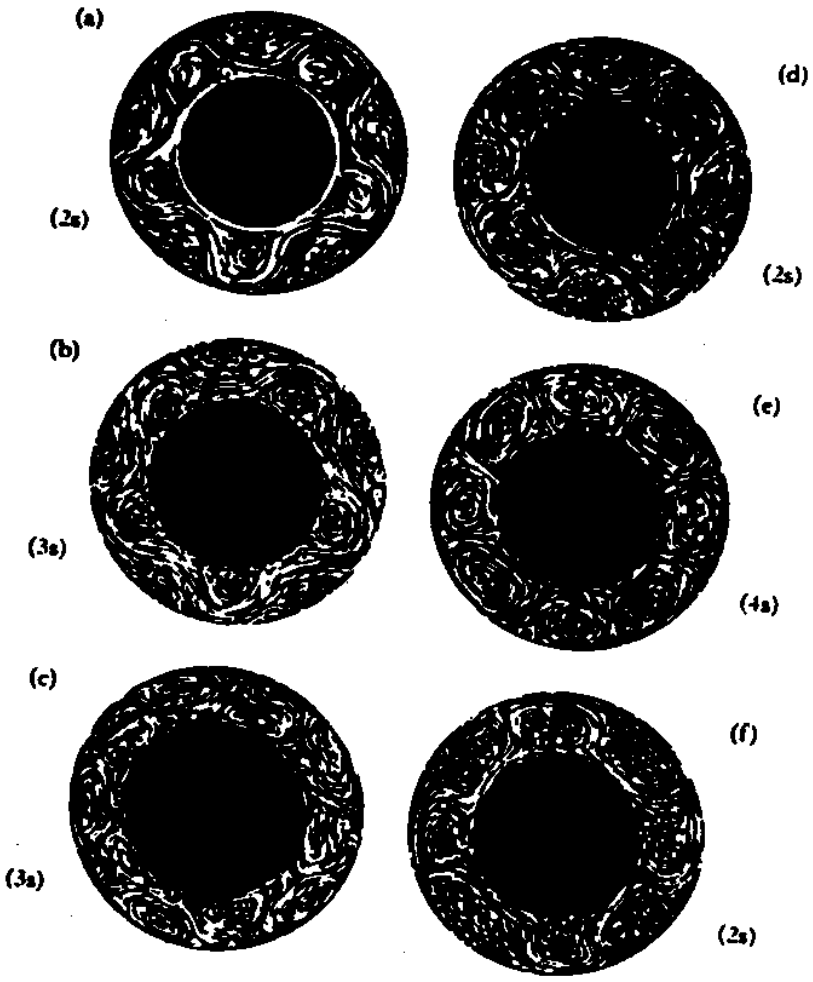

FIGURE 10 - GENERAL SENSE OF RELATIVE MOTION (a) ANTICLOCKWISE IN JET STREAM, (b) ANTICLOCKWISE IN JET STREAM, (c) CLOCKWISE IN EDDY AT '2 o'CLOCK', (d) ANTI-CLOCKWISE IN JET STREAM, (e) CLOCKWISE IN EDDY AT ' 12 o'CLOCK', (f) CLOCKWISE IN JET STREAM.

force. It was demonstrated that two layer laboratory model of a wind driven ocean circulation appears to be capable of simulating some of the gross features observed or expected from theories of the general circulation.

2.7 Numerical Models

The possibility of representing the atmospheric general circulation through a set of equations (equations of motion and thermodynamic equations) was realised about 75 years ago. By imposing certain boundary conditions and solving the equations with high speed digital computers, several numerical models were developed. Starting with a given atmospheric situation at a particular time, by integrating the basic equations with respect to time, the future state of the atmosphere could be predicted. The models calibrated by comparison with real atmospheric weather situations over a couple of years were validated for routine weather forecasting.

The first attempt to build a numerical weather model was made by L.T. Richardson in (1918). For a nonviscous adiabatic atmosphere the equations can be written in the form:

$$\frac{\partial u}{\partial t} = -\left(u\frac{\partial u}{\partial x} + v\frac{\partial u}{\partial y} + \omega\frac{\partial u}{\partial z}\right) - \frac{1}{\rho}\frac{\partial p}{\partial x} + 2\Omega\,(v\,\mathrm{Sin}\,\phi - \omega\,\mathrm{Cos}\,\phi)$$

$$\frac{\partial v}{\partial t} = -\left(u\frac{\partial v}{\partial x} + v\frac{\partial v}{\partial y} + \omega\frac{\partial v}{\partial z}\right) - \frac{1}{\rho}\frac{\partial p}{\partial y} - 2\Omega\, v\,\mathrm{Sin}\,\phi$$

$$\frac{\partial \omega}{\partial t} = -\left(u\frac{\partial \omega}{\partial x} + v\frac{\partial \omega}{\partial y} + \omega\frac{\partial \omega}{\partial z}\right) - \frac{1}{\rho}\frac{\partial p}{\partial z} - 2\Omega\, u\,\mathrm{Cos}\,\phi - g$$

$$\frac{\partial \rho}{\partial t} = -\left(u\frac{\partial \rho}{\partial x} + v\frac{\partial \rho}{\partial y} + \omega\frac{\partial \rho}{\partial z}\right) - \rho\left(\frac{\partial u}{\partial x} + \frac{\partial v}{\partial y} + \frac{\partial \omega}{\partial z}\right)$$

$$\frac{\partial p}{\partial t} = -\left(u\frac{\partial p}{\partial x} + v\frac{\partial p}{\partial y} + \omega\frac{\partial p}{\partial x}\right) - \nu\, p\left(\frac{\partial u}{\partial x} + \frac{\partial v}{\partial y} + \frac{\partial \omega}{\partial x}\right)$$

... (10)

where the first three are the equations of motion, and the other two are the equations of continuity and the law of conservation of energy for an adiabatic process.

Richardson realised that with the equations written in the form, the instantaneous local rates of changes of each of the dependent variables at a given moment could be computed from a knowledge of the variables in space. Further, these equations could be solved by the method of finite differences. Subsequent investigators found the set of equations solved by Richardson were having practical drawbacks. Besides, the solution using finite difference approach was also found to be mathematically inadequate.

2.7.1 Barotropic models

The first successful forecast was made by Charney, Fjortoft and Von Neumann (1950). The equation employed for this early forecast was the vorticity equation applied to a barotropic atmosphere i.e. an atmosphere which was assumed to be homogeneous and of uniform density and in which vertical motion ignored. Writing the components of the velocity V, the vorticity equation is:

$$\frac{\partial}{\partial t}(\nabla^2\psi) + V.\ \nabla(\nabla^2\psi + f) = 0 \qquad \ldots (11)$$

The equation (11) being a one parameter equation could be applied with some success in the mid troposphere where the horizontal divergence of the flow is negligible.

2.7.2 Baroclinic models

With barotropic models, it was not possible to predict the development of instabilities due to thermal gradients. Also the model has to allow for consideration of vertical motion.

Assuming a quasi-horizontal and quasi-geostrophic state, the vorticity equation at equation (10) is written in isobaric coordinates as:

$$\frac{\partial}{\partial t}(\nabla^2\psi) + V.\nabla(\nabla^2\psi + f) - f\frac{\partial \omega}{\partial p} = 0 \qquad \ldots (12)$$

and the thermodynamic equation is:

$$\frac{\partial}{\partial t}(-\frac{\partial \phi}{\partial p}) + u\frac{\partial}{\partial x}(-\frac{\partial \phi}{\partial p}) + v\frac{\partial}{\partial y}(-\frac{\partial \phi}{\partial p}) - \frac{\omega B}{g\rho^2} = \frac{1}{\rho c_p}\frac{d\phi}{dt} \ldots (13)$$

where, $\frac{d\phi}{dt}$ is the rate of increase of entropy due to diabatic processes and $B = -g\rho\frac{\partial \ln\theta}{\partial p}$

The geostrophic approximation enables the equation to be written as:

$$\frac{\partial}{\partial t}(\frac{\partial \psi}{\partial p}) + V.\nabla(\frac{\partial \psi}{\partial p}) + \frac{\omega B}{fg\bar{\rho}^2} = \frac{-1}{\bar{\rho}c_p t}\frac{d\phi}{dt} \qquad \ldots (14)$$

where, $\bar{\rho}$ represents the average density.

Philips (1956) specified the basic assumption which must be satisfied by the weather systems in the region where quasi-geostrophic models could be attempted:

i) $R_o << 1$

ii) $R_o^2 R_1 \sim 1$

iii) $L < a$

where, R_o is the Rossby number and is defined as ratio of internal force to coriolis force and is given by:

$$R_o = \frac{U}{f\,L} \qquad \ldots (15)$$

where, U is the basic zonal flow, f is the coriolis parameter and L is the characteristic horizontal length.

R_i is the Richardson number and is given by:

$$R_i = \frac{g}{\theta} \frac{\frac{d\theta}{dz}}{(\frac{\partial u}{\partial z})^2} \qquad \ldots (16)$$

where θ is the potential temperature.

Philips (1956) developed a simple 2-level quasi-geostrophic model which was confined to a portion of the global atmosphere which did not consider oceans, continents or mountains. Assuming a latitudinal distribution of zonally uniform heating, jet streams and zonal mean cells of the meridional circulation were simulated.

Though the model was not suitable for use with hydrologic models of land surface process because of the quasi-geostrophic approximation, it provided the basic structure based on which the later day developments were built up.

2.7.3 Primitive equation (PE) models

The baroclinic model although less restrictive than the barotropic model involves certain approximation especially the assumption of quasi-geostrophic motion. This restriction

could be removed easily by writing the equations in a more basic form namely the horizontal momentum equation:

$$\frac{\partial V}{\partial t} + V.\nabla V + \omega\frac{\partial V}{\partial p} + fk \times V = -\nabla\phi + F \qquad \ldots (17)$$

the continuity equation

$$\nabla. V + \frac{\partial \omega}{\partial p} = 0 \qquad \ldots (18)$$

the hydrostatic equation

$$\frac{\partial \phi}{\partial p} + \frac{1}{\rho} = 0 \qquad \ldots (19)$$

and the thermodynamic equation:

$$\frac{\partial}{\partial t}(-\frac{\partial \phi}{\partial p}) + V. \nabla(-\frac{\partial \phi}{\partial p}) - \frac{B\omega}{g_\rho 2} = \frac{1}{c_1 \rho}\frac{d\phi}{dt} \qquad \ldots (20)$$

With the primitive equation models care is needed such that the solutions are not swamped by spurious gravity or acoustic waves arising from errors in the initial data. For this reason time steps need to be considerably shorter than with quasi-geostrophic models with similar horizontal resolution. Primitive equation models, therefore, require much more computer time than comparable quasi-geostrophic models.

2.7.4 Boundary conditions

The boundary conditions required by atmospheric general circulation models are the distribution of surface topography (including the surface elevation and surface type or land use), the surface albedo and the distribution of sea surface temperature and see ice. The solar radiation at the top of the

atmosphere is usually either held fixed or assigned the normal daily and/or seasonal variation. Other physical parameters in an atmospheric general circulation model which are usually adjusted to more or less realistic values are the albedo of clouds, the diffusion coefficients for the horizontal and vertical turbulent mixing of heat, momentum and moisture by sub-grid scale processes.

2.7.4.1 inclusion of orography

Generally it is necessary for a model to take into account the varying height of the surface. In the isobaric coordinate system, where pressure is the vertical coordinate, the varying surface pressure due to the varying height of the surface is not easy to handle. For numerical models, therefore, σ coordinate system is employed which is defined as:

$$\sigma (x, y, t) = \frac{p(x, y, t)}{p_s(x, y, t)} \qquad \ldots (21)$$

where p_s is the surface pressure is a non-dimensional parameter. The lower boundary $\sigma = 1$ becomes a cordinate surface. In Table 1, the σ values at different pressure levels are given.

2.7.4.2 convection

As integration in the model proceeds, situations occur where the vertical temperature gradient is super adiabatic. To make allowance for the effect of convection, convective

adjustment is carried out in the models such that the temperature profile is adjusted to the dry adiabatic under conditions of low water vapour content and to the saturated adiabatic when the relative humidity is equal to or close to 100%.

2.7.4.3 Moisture

Water vapour evaporated from the surface and moved above by atmospheric motions plays a very significant part of the atmosphere's energy budget because of:

i) the release of latent heat of condensation, and

ii) the formation of clouds which alter the radiation budget because of reflectivity and absorption.

TABLE 1 Various Sigma Levels in the Vertical (p_s = 1000 mb)

Level		$\sigma = p / p_s$
1	TOP....	0
1/2		
1	.....	.01
2	.....	.08
3	.....	.21
4	.....	.37
5	.....	.54
6	.....	.71
7	.....	.86
8	.....	.96
9	frictional layer.....	1.00
	//////ground////////	

A numerical model, therefore, needs to keep track of the water content in vapour and liquid form.

2.7.5 Grid models

In this modelling, the entire globe is divided into grids of uniform size. The north-south separation between grid boxes remains constant and the number of the grid boxes along each latitude circle decreases poleward thereby giving nearly uniform horizontal grid resolution over the entire globe (Kurihara and Holloway, 1967; Holloway and Manabe,1971). There are some grid point global models where the number of points on each latitude circle remain same. But much of the difficulty arises because the grid size decreases as the meridians converge at poles; and a very small time step would be then required making numerical experiments very costly. To solve this problem, Fourier filtering is used in the latitudes near the poles. This allows one to use a uniform time step for the whole globe. The models which use this kind filtering are the models developed at UCLA (USA), UK Meteorological Office and LMD, Paris. The dynamic equations method and values of dynamic variable such as precipitation, temperature, humidity and other relevant parameters are computed on a network of discrete points. In the vertical direction, several (5, 9 or 11) finite difference levels are chosen so as to represent the structure of planetary boundary layer as well as that of stratosphere.

2.7.6 Spectral models

In the spectral models, the horizontal variations are represented in terms of a series of spherical harmonics. Spectral technique of evaluating the dynamical equations is a useful alternative to the finite difference technique especially for the upper atmosphere because of its ability to compute spatial derivatives accurately. However, full spectral technique has seldom been incorporated into high resolution general circulation models because of the computer time required for numerical time integration or spectral model increases rapidly with increasing spectral resolution. Therefore, semi-spectral model have been developed by Bourke (1974), Hoskins and Simmons (1975), Daley etal (1976), and Gordon (1979).

In the spectral models, the solutions predict spectral components rather than variables at grid point. The horizontal resolution in this technique is determined by the degree of truncation of the spherical components. Three truncation limits for climate models have been used namely: 15, 21 and 30, 42 waves, and these limits have been applied in both longitudinal and meridional directions (Manabe etal.,1979). The wave number refers to the number of complete cycles of a variation which occur around a latitude circle.

2.7.7 Comparison between grid and spectral models:

Comparisons of results from the spectral models with those from grid models show that spectral models are able to

outperform the grid models in simulating the large-scale sea level pressure distribution. In particular, the low resolution M15 spectral models performance is equal to or slightly better than that of the high resolution grid model.

The grid model's greatest asset is its ability to simulate the geographical distribution of the rate of precipitation, particularly in the tropical and subtropical regions. This is evidenced by the fact that the coarse resolution 500 km grid model is able to simulate some of the large scale precipitation features dispite its poor simulation of sea level pressure. On the other hand, large scale precipitation features are poorly simulated in the low resolution M15 spectral simulation. In general, the M30 spectral simulations equal the high level of performance of the 250 km grid model in simulating the hydrologic cycle. The geographical distribution of precipitation rate becomes more realistic with increasing spectral resolution. For example, the tropical rainbelt becomes narrower and is defined better and subtropical dryzones become broader as the spectral resolution is increased from M15 to M30. In the M15 spectral model simulation, only the large scale features of the geographical distribution of precipitation rate are simulated. The time step interval and amount of computer time required to time- integrate one model day for three spectral models with truncation wave 15, 21, 30 i.e. M15, M21, M30 and for the 500 km and 250 km grid models has been shown in table 2 (Manabe etal., 1979). This table

indicates that an entire year can be time integrated by the M15 spectral model in about 12 hours of CPU time. Similarly, only 36 hours of CPU time are required to simulate an entire year by M21 spectral model which performs at or above the level of the high resolution (250 km) grid model in many respects. The factor accounting for the higher computational speeds of the spectral models is the incorporation of the semi-implicit time integration scheme. Spectral models are best suited for climate simulation purpose.

TABLE 2 Relative Computational Speeds of Spectral and Grid Models

Model		t(min)	Advanced scientific computer CPU time (min/day)
Spectral	M15	30	2
	M21	20	6
	M30	15	18
Latitude/ Longitude Grid	500 km	9	7
	250 km	3.75	35

2.7.8 Characteristic input and output of general circulation models

The characteristic model input and output are listed in table 3 from the view point of the surface climate. The initial conditions are the distributions of the primary or basic variables at each model level. In a climate simulation

which typically extends over many months or year, the equilibrium climate statistics are essentially independent of the initial conditions (although the solution's approach to statistical equilibrium is generally delayed if unreasonable or inconsistent initial conditions are used). The observational studies are still limited by the lack of adequate observational systems. Consequently, in many instances, the fundamental data are lacking to grid the formulation of improved parameterizations or for providing sufficiently long global records of key climate parameters. The most immediate opportunity for a definitive global data set has been obtained from First GARP Global Experiment (FGGE)). The FGGE data sets have provided the best global view yet obtained of the general circulation of the entire atmosphere through out an annual cycle (Dec. 1978-Nov. 1979). The quality, consistency and global extent of the data has permitted improved regional, hemispheric and global analyses of the mass, momentum and energy budgets.

The output available from the general circulation models for the analysis of simulated climate includes the three dimensional distribution of the basic variables such as pressure, temperature, humidity, wind, cloudiness, soil moisture and the snow cover. These include the rates of precipitation and evaporation, the net surface flux of both short and long wave radiation, the turbulent flux of sensible heat at the surface, and the surface run-off. These qualities may in turn be used to reconstruct a variety of other

TABLE 3 Characteristic Input and Output of an Atmospheric General Circulation Model

INPUT

Initial conditions

- Pressure
- Temperature
- Humidity
- Wind
- Cloudiness
- Soil moisture
- Snow cover

Boundary conditions

(Principally at the earth's surface)

- Surface elevation
- Surface type (water, ice, land use)
- Surface albedo
- Sea surface temperature and sea ice
- Solar radiation (at model top)

Physical parameters

- Cloud albedo
- Diffusion coefficient(s)
- Ground water capacity
- Atmospheric composition

OUTPUT

Basic variables

- Pressure
- Temperature
- Humidity
- Wind
- Cloudiness
- Soil moisture
- Snow cover

Auxiliary variable processes

- Precipitation
- Evaporation
- Surface radiative flux
- Surface runoff

processes related to the specific climatic stresses or effects on the ecosystem, such as water use efficiency, many of which are not routiney observed.

2.7.9 Development of general circulation models (GCMs)

Smagorinsky (1963) succeeded in making a long term integration of general circulation model of the atmosphere with the so called primitive equations of motion. The geostrophic approximation was avoided in this model. Mintz (1965) constructed a general circulation model of the atmosphere with a global computational domain and realistic topography. A highly realistic distribution of the sea level pressure in the middle latitudes was obtained from this study, but the horizontal flow field was not very realistic. Particularly, the intertropical convergence zone was located too far from the equator and the intensity of convergence was also very weak.

The models mentioned earlier did not explicitly incorporate the processes associated with hydrologic cycle. Parameterizing the effects of moist convection by the so called 'moist convective adjustment' Manabe et al (1965) constructed a hemispheric model with moist convection processes assuming the surface uniformly wet. The zonal mean features of precipitation such as the tropical rainbelt, subtropical belt of meager precipitation and the mid-latitude rainbelt were reproduced satisfactorily. They demonstrated that the rainbelt in the model tropics resulted from many

centres of intense precipitation associated with synoptic scale disturbances, such as tropical cyclones and easterly waves, in agreement with features of the actual intertropical convergence zone. The process of surface hydrology was taken into account by Manabe (1969) when he investigated the climatic influence of the land-sea contrast in wetness by use of the model with limited computational domain and idealized geography. Many other investigators have also incorporated the hydrologic processes into their general circulation models with a global computational domain and realistic geography, and succeeded in simulating many large-scale characteristics in the geographical distributions of climate and hydrologic variables (Holloway and Manabe, 1971; Kasahara and Washington, 1971; Arakawa, 1972; Manabe and Holloway, 1975; Gates and Schlesinger, 1977; Somerville et al, 1974; Washington and Williamson, 1977; Corby et al, 1977). The climate of the earth embodies an enormously complex system in which strong interactions occur between the major components, viz., the atmosphere, the ocean, the cryosphere and the lithosphere. Mechanical and thermal inhomogeneties at the earth's surface created by the distribution of continental, land masses, oceans, ice and snow are believed to be a major factor in determining the climate of the earth throughout its geological history. The oceans with a much greater inertia than the atmosphere, is capable of integrating short period atmospheric influences, which seem to affect only the surface layer of the ocean, leaving the deeper part of the

ocean relatively undisturbed. On the other hand, the atmosphere receives from the ocean a major part of its heat and moisture and is exposed to the moderating effect of the ocean through the transport of heat by ocean currents. Also, because of the thermal capacity of the ocean, the diurnal and annual oscillations of the atmospheric temperature above the oceans is observed to be smaller than over the land. Therefore, in order to investigate a long term climate variability or sensitivity of climate to an external forcing, it is necessary to construct a combined ocean atmospheric model. Manabe (1969), Bryan (1969) and Wetherald and Manabe (1972) increased the understanding of the major mechanisms involved in the interaction between the various components of the coupled system. Manabe and Wetherald (1980) performed an experiment with a model that predicts cloud cover and extend the ocean domain to poles. An additional experiment with a quadrupling of CO_2 content showed a roughly linear response to temperature increase with increased radiative warming. One of the interesting aspect of this experiment was that prediction of cloudiness did not seem to change the sensitivity of model. Manabe and Stonffer (1980) used a spectral model with realistic geography and a simple mixed layer ocean 68 cm thick, which can approximate the seasonal heat storage of upper ocean. The mixed layer had a uniform temperature and a parameterization for formation and decay of sea-ice. The response to a quadrupling of CO_2 was found significantly smaller than that of other studies cited earlier. Washington

and Meehl (1983) used a spectral model with realistic geography and a different snow-sea ice albedo. The new radiation cloudiness scheme (Ramanathan et al., 1983) was incorporated in this study. The absorption formulation for CO_2 in this new radiation scheme was in excellent agreement with observed absorptance (Kiehl and Ramanathan, 1983). Analysis of globally averaged surface air temperature indicated increase of 1.3°C (fixed clouds) and 1.3°C (computed clouds) with a doubling of CO_2 and increase of 2.7°C (fixed clouds) and 3.4°C (computed clouds) for a quadrupling of CO_2. Zonal mean cross sections showed tropospheric warming of the order of 1-2°C and cooling in the stratosphere of up to 6°C for a doubling of CO_2 in both the fixed and computed cloud cases. Pitcher et al (1983) simulated Jan-July climate using NCAR spectral general circulation model. The most significant change in this model has been the incorporation of a cloud/radiations formulation described in detail by Ramanathan et al (1983). With the introduction of further modification for the evaluation of radiative transfer, the performance of the model improved. The most notable improvement was a more realistic simulation of the zonal wind profile. This model also predicted a separation between the winter time westerly jets in the troposphere and stratosphere. The zonal wind speeds in the model stratosphere are found in good accord with observations. During the last few years, several general circulation models have been improved to investigate the atmospheric response to the imposed sea surface temperature anomalies in the ocean as a meahingful step towards understanding atmospheric fluctuations before a dynamically

balanced ocean-astmospheric system is available (Spar, 1973; Houghton et al, 1974; Shukla, 1975; Huang; 1978). Lau (1978) investigated the effect of ocean on the seasonal variation of the general circulation using a coupled ocean-atmosphere model developed by Webster and Lau (1977). Manabe et al (1979) also simulated the climate using ocean-atmosphere model.

Washington and Meehl (1984) again indicated that stratospheric cooling and tropospheric warming is a result of increased CO_2. Zonal mean precipitation tends to increase in doubling CO_2 case, compared with control, which is mainly due to warming of sea surface temperatures, causing greater evaporation which increase the moisture of atmosphere and therefore, rainfall. In the tropics this is associated with an increase in the intensity of the tropical meridional circulation and a strengthening of the upper level zonal winds in the subtropics.

In table 4 a summary of the General Circulation Models is given.

2.7.9.1 limited area fine mesh modelling

Limited area modelling is now regarded as the application of global modelling concepts to regional problems with increased horizontal resolution. Recently the limited area fine mesh modelling gained an important place both in operational numerical prediction and in meteorological research and development. Gilchrist et al (1982) and Dell'Osso (1983) have implemented such techniques in case of GATE and ALPEX respectively. For FGGE and MONEX much of the relevant numerical modelling was carried out using global models, but regional studies were under

TABLE 4 - Summary of General Circulation Models

	Centre	Vertical representation	Horizontal representation	References
1.	Atmospheric environment service, Canadian Climate Centre, Downsview, Ontario	5 levels	Spectral 20 waves rhomboidal truncation	Boer and McFarlane (1979)
2.	Australian Numerical Meteorology Research Centre, Melbourne	9 levels	Spectral 15 waves rhomboidal truncation	Bourke et al (1977) McAvaney et al (1978,79)
3.	Computing Centre, Siberian Academy of Sciences, Novosibirsk	3 or 5 levels	Finite difference 5^{o} or 10^{o} latitude-longitude	Marchuck et al (1979)
4.	Geophysical fluid Dynamics Laboratory/ NOAA, Princeton, New Jersey	9 levels	Finite difference irregular latitude-longitude approx. 500 km (N24) or 250 km (N48)	Holloway and Manabe (1971) Manabe and Terpstra (1974)
		11 levels	Finite difference irregular latitude-longitude approx. 250 km(N48)	Manabe, Hahn and Holloway (1974), Manabe and Holloway (1975)
		18 levels	Finite difference irregular latitude longitude approx. 500 km (N24)	Miyakoda and Sirutis (1977)
		9 levels	Spectral 15, 21 or 30 waves rhomboidal truncation	Manabe et al (1979)

	Centre	Vertical representation	Horizontal representation	References
5.	European centre for Medium Range Weather Forecasts	15 levels	Spectral 42 waves rhomboidal truncation	Cubasch et al (1985)
6.	Goddard Space Flight Centre, Laboratory for Atmospheric Sciences, NASA, Greenbelt, Maryland	9 levels	Finite difference 4° latitude by 5° longitude	Halem et al (1979)
7.	Laboratoire de Meteorologie Dynamique, Paris	11 levels	Finite difference 2° latitude by 5° longitude	Sadourny and Laval (1984)
8.	Meteorological Bracknell, England	5 levels	Finite difference irregular latitude-longitude approx. 330 km. (N30)	Corby et al (1977) Gilchrist (1979)
		11 levels	Approx. 220 km (N45)	Saker (1975) Carson and Cunnigton (1979)
9.	National Centre for Atmospheric Research, Boulder, Colorado	9 levels	Spectral 30 waves rhomboidal truncation	Washington et al (1979)
10.	The Rand Corporation Santa Monica, California	2 levels	Finite difference 4° latitude by 5° longitude	Gates and Schlesinger (1977)
11.	Department of Atmospheric Sciences, University of California, Los Angeles, California	3 and 6 layers	Finite difference 4° latitude by 5° longitude	Arakawa (1972)
		6 and 12 layers	Finite difference 4° latitude by 5° longitude	Arakawa and lamb (1977)

taken using limited area models (Leslie et al, 1981; Krichak, 1981). Experiments have shown that certain aspects of prediction and simulation are improved using the higher horizontal resolutions which are possible in limited area fine mesh models. The importance attached to regional modelling is also indicated by the activities of the European Working Group on Limited Area Modelling (EWGLAM) and also in published reviews (Anthes, 1983)

Sharma and Sadourny (1985) have also made simulation of the onset of the 1979 Indian monsoon using fine mesh in a GCM with FGGE data. The feasibility of using fine mesh in the Indian Ocean region for efficient regional forecasts in the medium range was investigated, in parallel with the former experiments using standard LMD model. It was concluded that the fine mesh thus appears as a promising method to increase the efficiency of numerical models over a specific region. Further, the potential benefits of the increased horizontal resolution were also assessed by Gadd (1984) in terms of sea level pressure, surface wind, precipitation and the representation of fronts. These are the most important aspects, strongly linked with short range forecasts for public services, aerodrome forecasts and coastal marine services.

2.7.9.2 simulation of hydrologic parameters

Washington and Kasahara (1970) constructed a two level general circulation model with realistic orography and reproduced some of the zonal mean features of the hydrologic cycle. Further, Kasahara and Washington (1971) repeated this study

with a six level general circulation model which simulated some of the geographical distributions of precipitation. Manabe and Holloway (1975) made efforts to compute global distribution of the various hydrologic variables and compared with climatic data. A brief review of simulated hydrologic parameters is presented here. (Manabe and Holloway, 1975).

Precipitation : The general features of the tropical rainbelt are well simulated by the model[figure 11(a)]. The areas of heavy precipitation in the tropical oceans approximately coincide with regions of warmer sea surface temperatures. The rainfall rates were found lower where sea surface temperatures are relatively low.

In the western part of the continents the model produced the area of very low rainfall rate, such as in Sahara desert and in south-western United States, in agreement with nature. In the subtropics of the southern hemisphere, the distribution of precipitation have not been found obviously, partly because of the smaller size of the continents. Nevertheless, the model simulates the major aridregion in the Australia and the belt of moderate precipitation along the east coasts of the Australia and Africa. The low rate of precipitation was also simulated in the neighbourhood of the Great Western Desert in North America. This meager rainfall, however, extends too far into Texas, as compared with the observed distributions.

In the middle latitudes of the northern hemisphere, the computed rate of precipitation over oceans was significantly larger than the rate over the continents[figure 11 (b)].

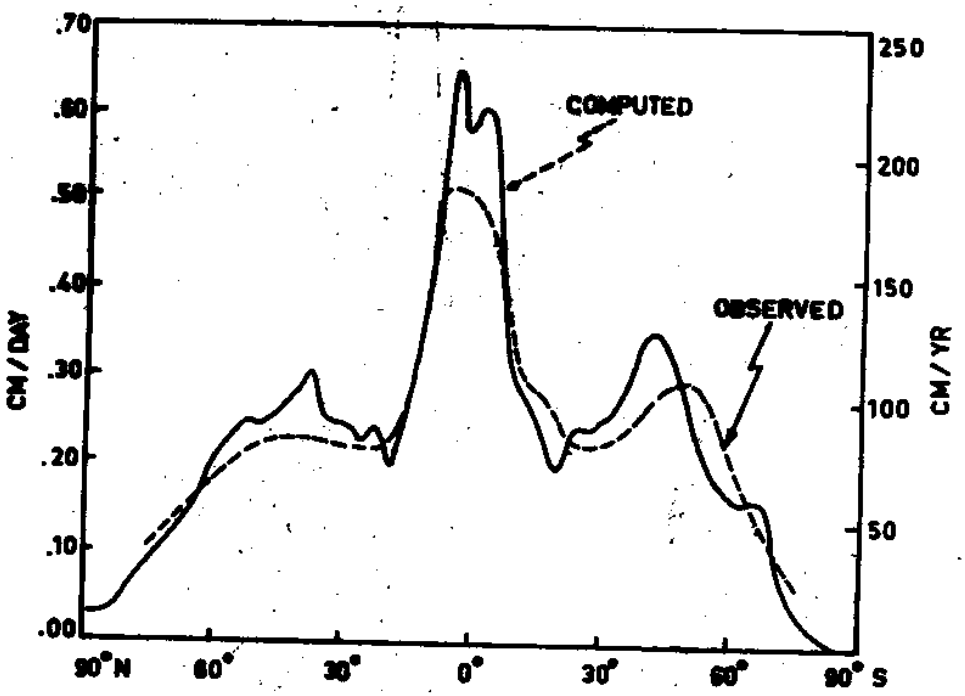

FIGURE 11(a) - LATITUDINAL DISTRIBUTION OF THE ANNUAL MEAN RATE OF PRECIPITATION COMPUTED BY THE MODEL (SOLID LINE) AND OBSERVED (DASHED LINE) BUDYKO, 1956).

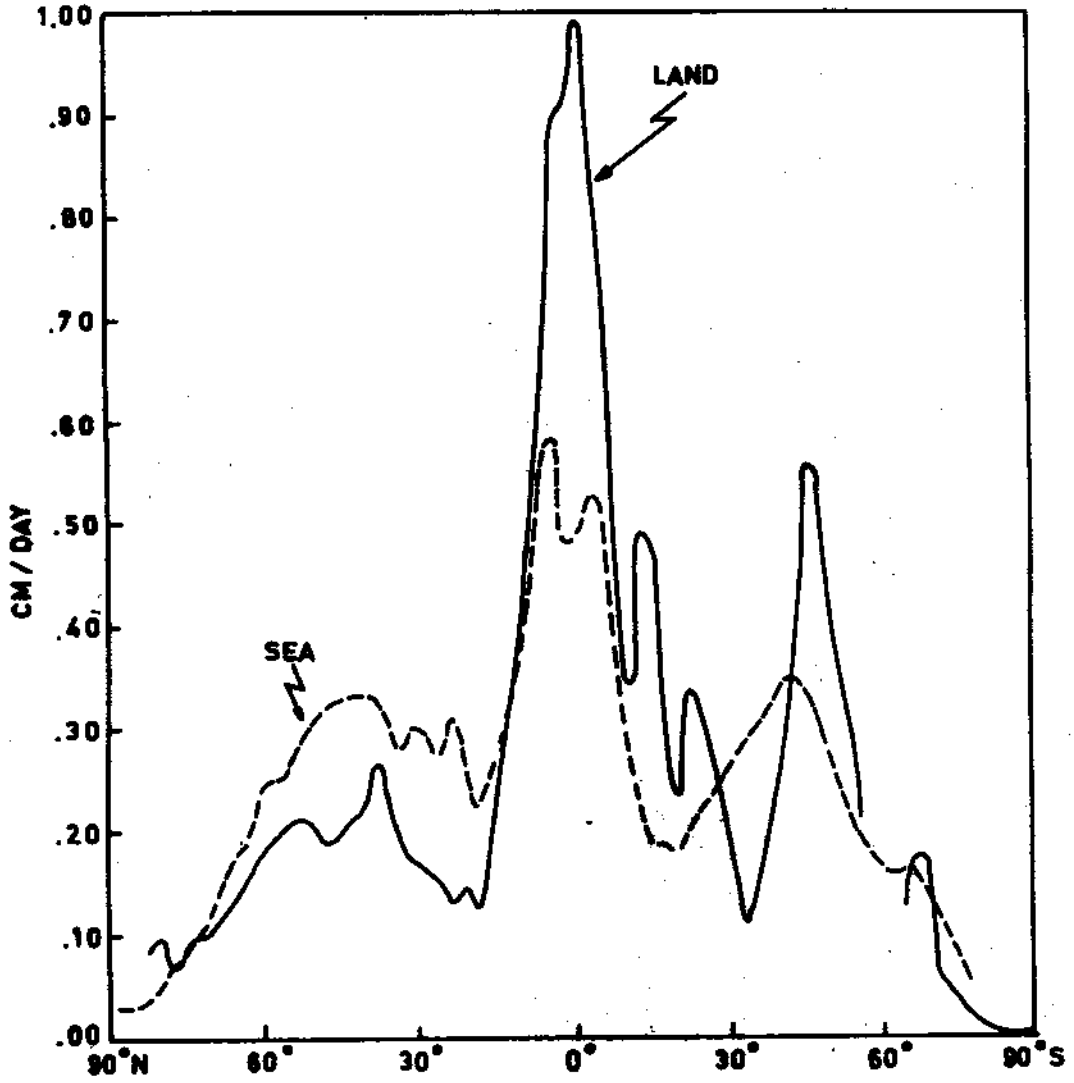

FIGURE 11(b) - LATITUDINAL DISTRIBUTION OF THE ANNUAL MEAN SIMULATED PRECIPITATION RATE BROKEN DOWN INTO ZONAL MEANS OVER LAND (SOLID LINE) AND OVER SEA (DASHED LINE).

Obviously, this results partly from the difference in surface wetness and according from the difference in evaporation rate between land and sea. Over the continents, the meager precipitation produces the area of dry soil. The low evaporation rate in such regions suppresses further precipitation. A similar positive feed back mechanism does not exist over oceans which always have a sufficient supply of moisture for evaporation. Although the model successfully simulates the monsoon phenomena, it fails in producing sufficient rainfall in northern India. It is understood that it is probably due to failure of the model to deal with steep southern slope of Himalayas (Hahn and Manabe, 1975). Similarly, the simulation over the south America was also poor partly because of the difficulty in coping with the steep Andes mountain range.

Evaporation :

The simulation of evaporation was also made by Manabe and Holloway (1975). The effect of soil moisture on evaporation was considered in a very simple manner (Budyko, 1956). When the soil does not contain a sufficient amount of water, the evaporation was smaller than that from the sea or a perfectly wet surface. The sea surface sets the upper limit for evaporation over a land surface under given surface wind and humidity conditions. If the soil moisture was greater than a certain critical percentage (75% in Manabe and Holloway, 1975 case) of the maximum soil capacity, the evaporation was assumed to equal the maximum rate. Otherwise, evaporation from the land was considered to be linearly proportional to the soil moisture

up to this critical value. The rate of sublimation from the surface of snow or ice was computed under the assumption of water vapour saturation at the surface.

It was shown by Manabe and Holloway (1975) that maximum computed rate of evaporation occured in the oceans of the subtropics, especially in the western part of these oceans, where the water is warmest. Such results were found to be in good qualitative agreement with Budyko (1963) distribution. A band of minimum evaporation was simulated on the earth along the equator between the subtropical belts in both the hemispheres. This equatorial strip of low evaporation rate results from cooler sea surface temperatures directly at the equator than at adjacent latitudes to the north or south. In the middle latitudes the evaporation rate was greatest along the east coasts of continents, where the warmer ocean currents, such as the Gulf Streams, prevail. At high latitudes of both hemispheres, evaporation rates were computed to be lowest because of low sea surface temperature or weak insolation available for the latent heat of evaporation.

A comparison of computed and observed rate of evaporation is shown in figure 12 (a). It was found that computed evaporation was systematically greater than the observed values in the tropics. It is understood that the greater computed evaporation rates in the tropics were due to greater evaporation over both oceanic and continental regions as shown in figure 12(b).

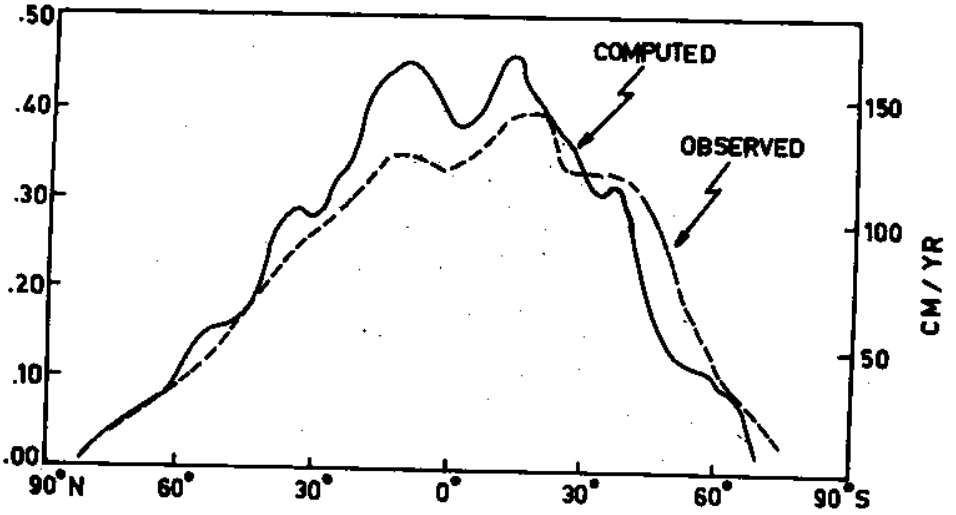

FIGURE 12 (a) - LATITUDINAL DISTRIBUTION OF ANNUAL MEAN RATE OF EVAPORATION COMPUTED BY THE MODEL (SOLID LINE) AND DERIVED FROM THE OBSERVED DATA (BUDYKO, 1963) (DASHED LINE) (REPRODUCED FROM MANABE & HOLLOWAY,1975).

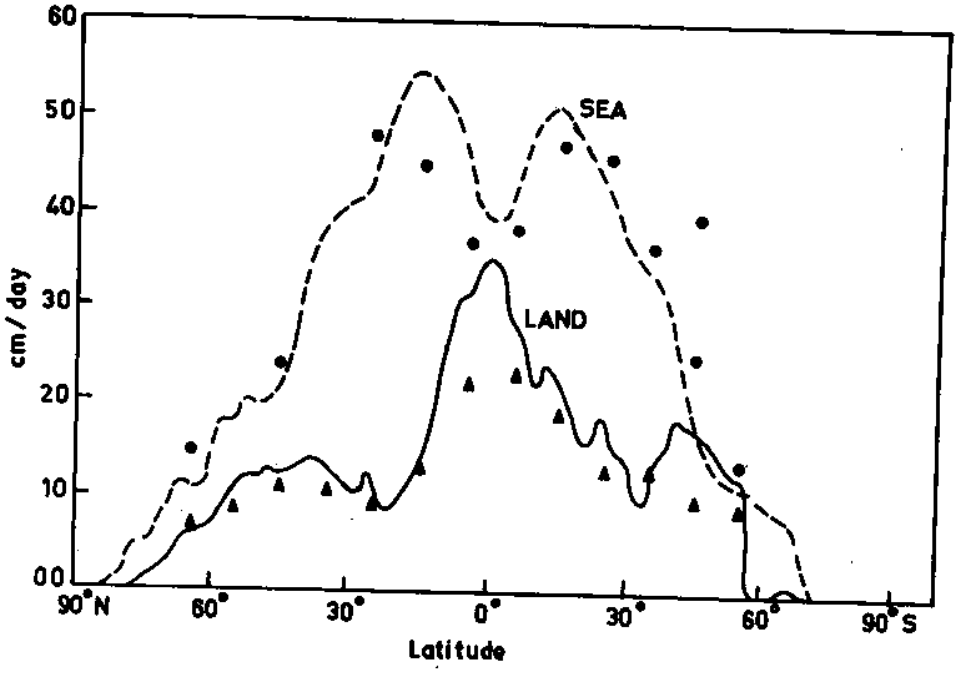

FIGURE 12 (b)- LATITUDINAL DISTRIBUTION OF SIMULATED ANNUAL EVAPORATION RATE BROKEN DOWN INTO MEANS OVER LAND (SOLID LINE) AND OVER SEA (DASHED LINE). FOR COMPARISON, VALUES FOR LAND AND SEA DERIVED FROM OBSERVED DATA (BUDYKO, 1963) ARE INDICATED BY TRIANGLES AND DOTS RESPECTIVELY.

Runoff

The maximum amount of water that can be stored in the ground called field capacity of the soil, depends upon a number of characteristics of the ground surface and thus varies considerably throughout the world. For simplicity, Manabe and Holloway (1975) set the field capacity of the soil to 15 cm over all land areas. A budget of the soil moisture was kept at each land grid points. The changes in the soil moisture were computed as the residual of the contributions from processes that increase the soil moisture (i.e. rainfall and snowmelt) and those which decrease it (i.e. evaporation and sublimation). Runoff was predicted only at the grid points, if a computed change in soil moisture would result in a water depth exceeding the field capacity. Moreover, runoff was assumed to flow directly to the sea via rivers without affecting the soil moisture at any other grid points. The snow melt rate was calculated from the surface heat budget under assumption that the temperature of the snow surface does not exceed the freezing point and that the conductivity of snow is zero.

The global distribution of computed annual mean rate of runoff was compared with the observed runoff rate derived by Lvovitch and Ovtchinnikov (1964)[figure 12(c and d)]. In general, regions of large runoff rate corresponded to areas of heavy precipitation particularly in the tropical rainbelt. The model simulated the high rate of runoff in Indonesia and the Philippines qualitatively which agreed with the observations. Further, runoff was completely missing from the Sahara Desert

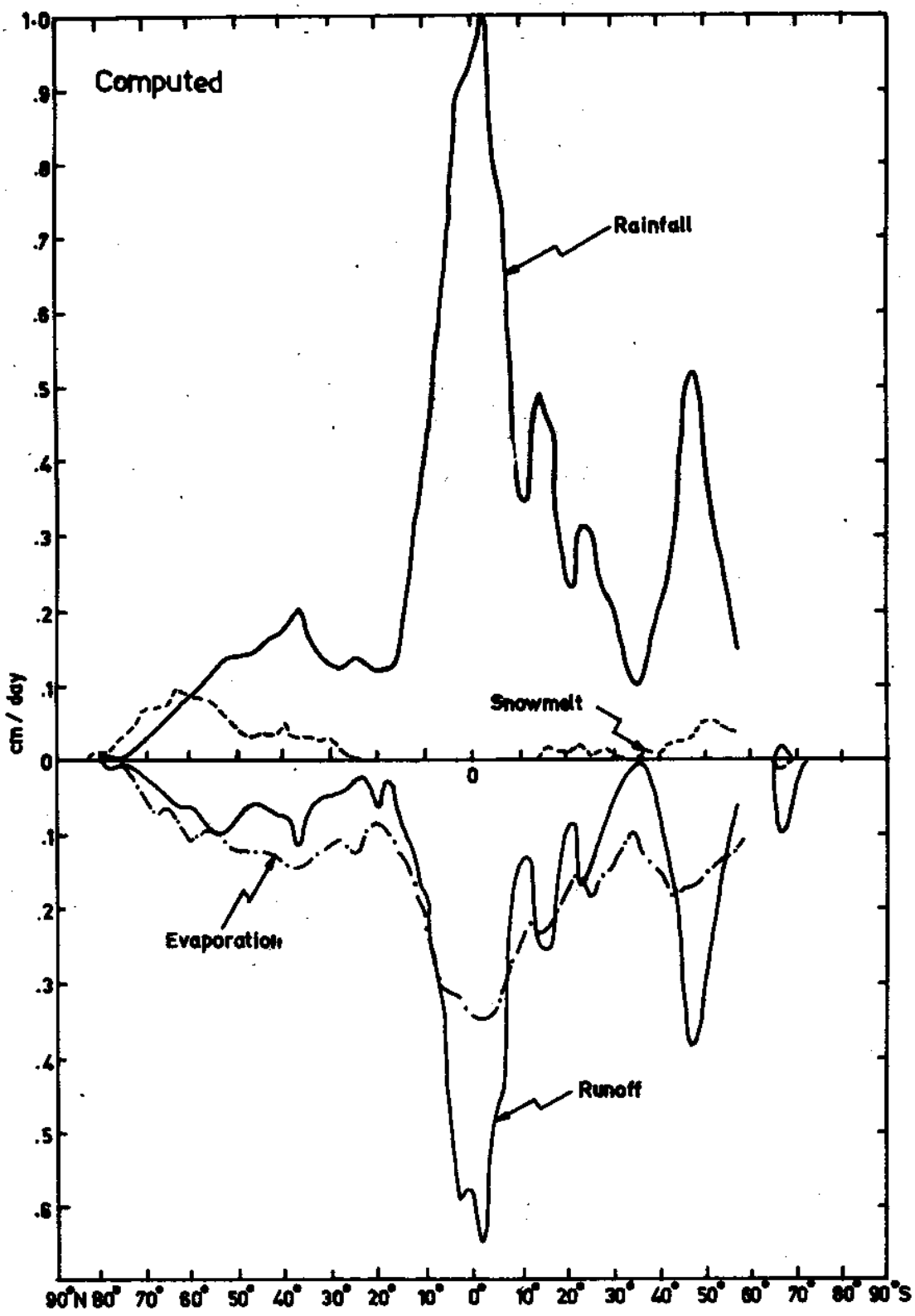

FIGURE 12(c) - ZONAL MEAN COMPONENT OF WATER BUDGET OVER LAND COMPUTED BY MODEL (REPRODUCED FROM MANABE AND HOLLOWAY, 1975).

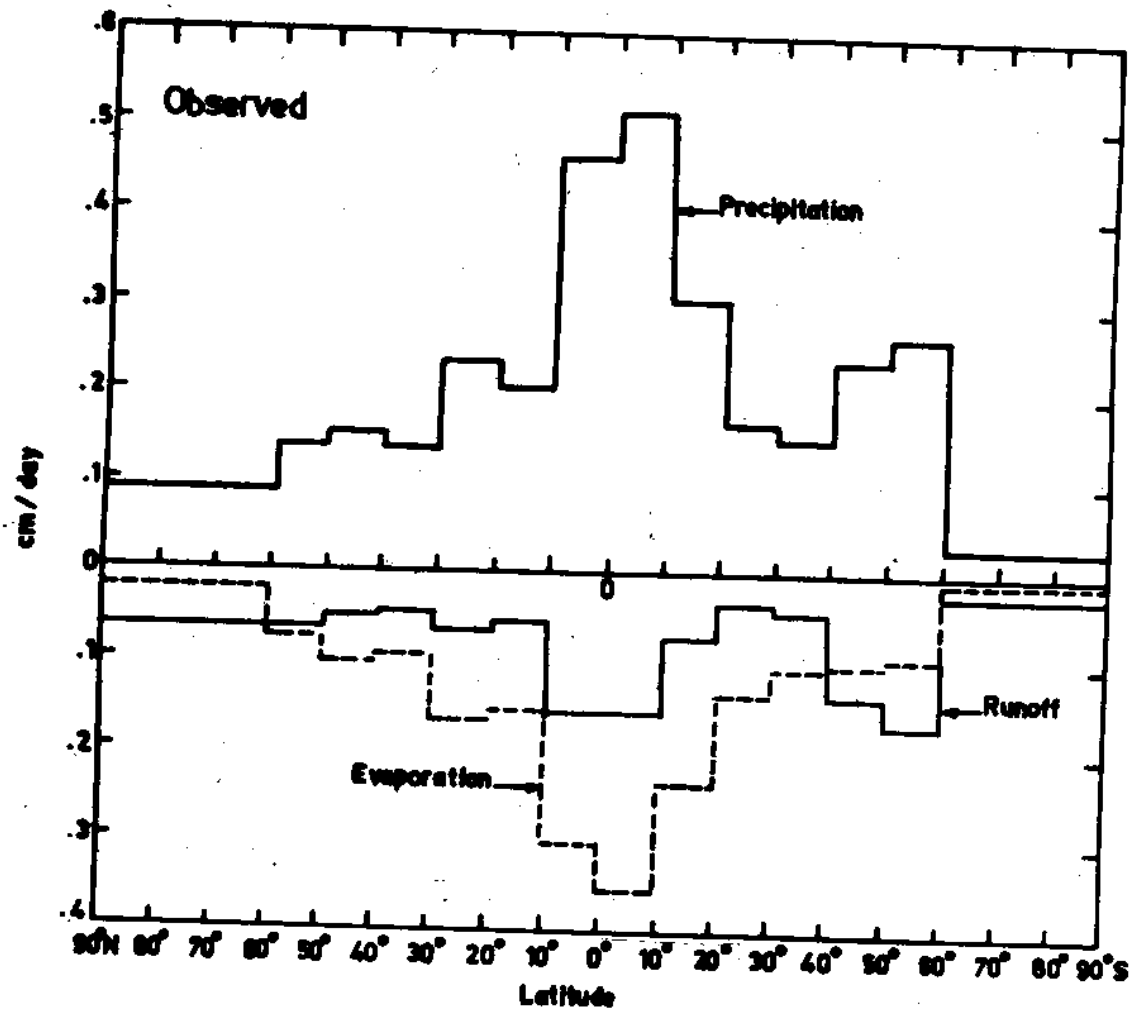

FIGURE 12(d) - ZONAL MEAN COMPONENTS OF THE WATER BUDGET OVER LAND ESTIMATED FROM THE OBSERVED DATA BY LVOVITCH AND OVTCHINNIKOV (1964) (REPRODUCED FROM MANABE AND HOLLOWAY, 1975).

and the deserts of Arabian Peninsula, as well as from most of Australia, in agreement with observations.

In general, the model failed to simulate the observed distribution of runoff in regions where its simulation of precipitation was poor. For example, the model markedly underestimates the runoff in the south-eastern China, Southern United States, and northern India, and it also failed to simulate the small scale features of the distribution of runoff along the west coast of south America. On the other hand, the model successfully reproduced moderately large runoff over Canada, Siberia and Europe. Although the rate of precipitation was not very large in these high altitude regions, the rate of evaporation or sublimation was very small due to weak insolation available . It was also concluded that snowmelt on the Tibetan Plateau contributed to the centre of the large runoff rate north of India where the Indus and Ganges rivers originate.

According to a combined view of precipitation, evaporation and runoff, it was noticed that the simulated tropical rainfall was far too heavy over continents of the model compared with observations[figure 12(c)].

Consequently, greater rain resulted in greater runoff in the model tropics. Further, the computed evaporation in the tropics agreed with observations, but the runoff rate in the model was nearly double the rate of evaporation. This is opposite to that observed over the continental areas in the actual tropics. Although the estimate of the true runoff in the tropics may not be very accurate, figure 12 (c)suggests that

the model tends to exaggerate the amount of runoff over the tropical parts of the continents.

2.8 General Circulation of Atmosphere Over India and Adjoining Areas

The seasonal reversals in the atmosphere circulation associated with the monsoon are closely linked with the seasonal march of solar insolation over the tropics and subtropics. The winter and summer circulations over the Asian monsoon areas are illustrated by the mean monthly upper air charts for January and July at 850 and 200 mb level (figure 13 and 14).

In January, the subtropical high pressure systems of the two hemispheres have practically the same intensity. The ridges in both the hemispheres tilt towards the equator from 850 to 200 mb.

In July, the southern hemisphere ridge has nearly the same latitudinal location as the northern hemisphere ridge in January and the intensities are also comparable. The northern hemisphere subtropical ridge dominates the upper troposphere in July. Over the Indian area of the tropics both winds and pressure gradients are stronger in the summer monsoon months as compared with the rest of the tropics. Comparison of the zonal components of the winds over the Indian peninsula and the Bay of Bengal with the geostrophic winds calculated from pressure gradients between pairs of stations located along certain meridians revealed that the flow was sub-geostrophic both in the lower troposphere and in the upper troposphere south of

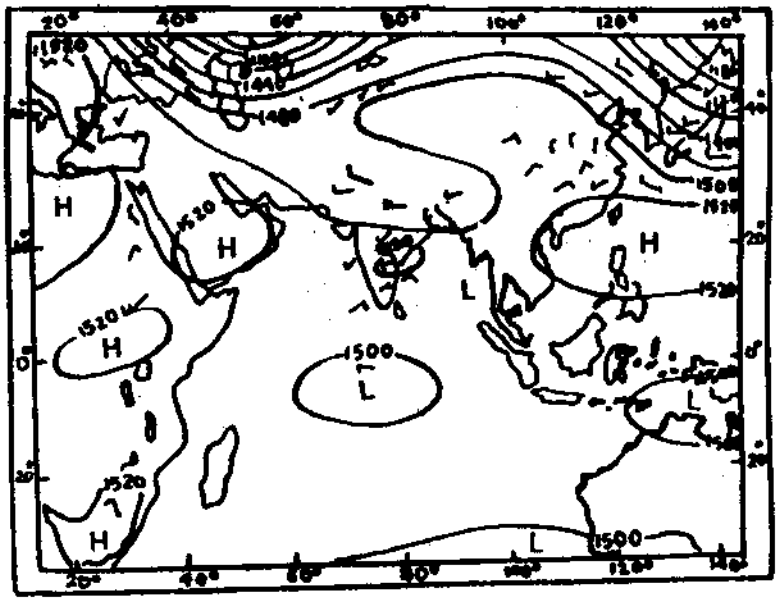

FIGURE 13(a)- CONTOUR AND WIND PATTERNS: JANUARY 1964 AT 850 mb (REPRODUCED FROM ANANTHAKRISHANAN, 1965).

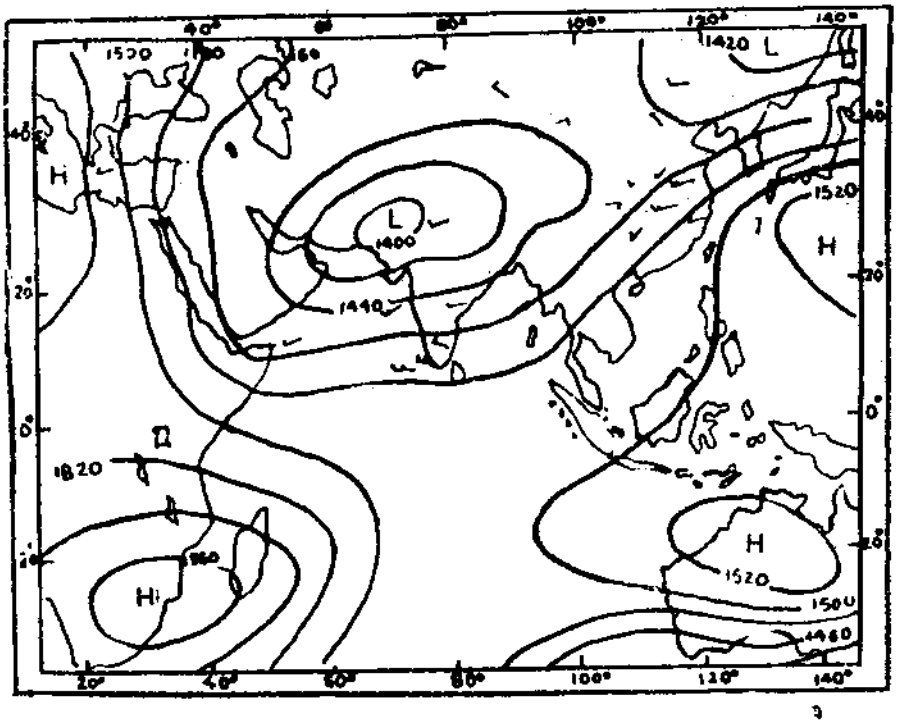

FIGURE 13(b)- CONTOUR AND WIND PATTERNS: JULY 1964 AT 850 mb (REPRODUCED FROM ANANTHAKRISHANAN, 1965).

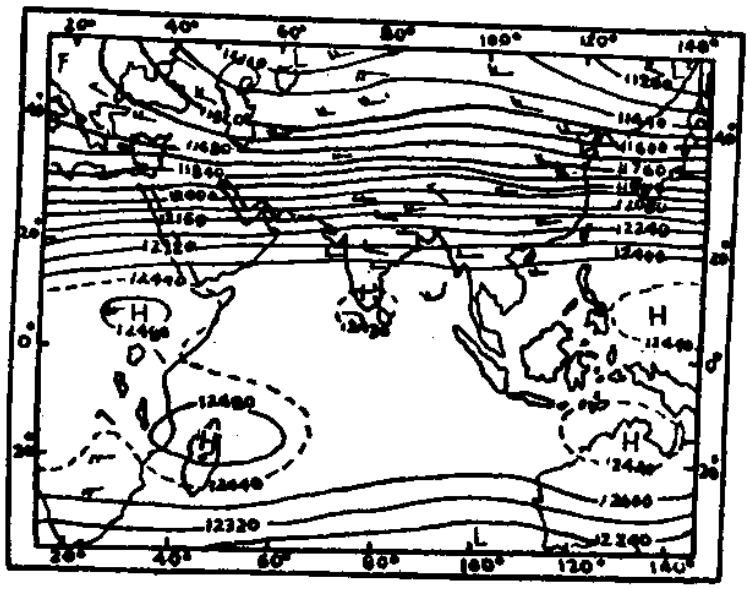

FIGURE 14(a)- CONTOUR AND WIND PATTERNS: JANUARY 1964 AT 200 mb (REPRODUCED FROM ANANTHAKRISHANAN, 1965).

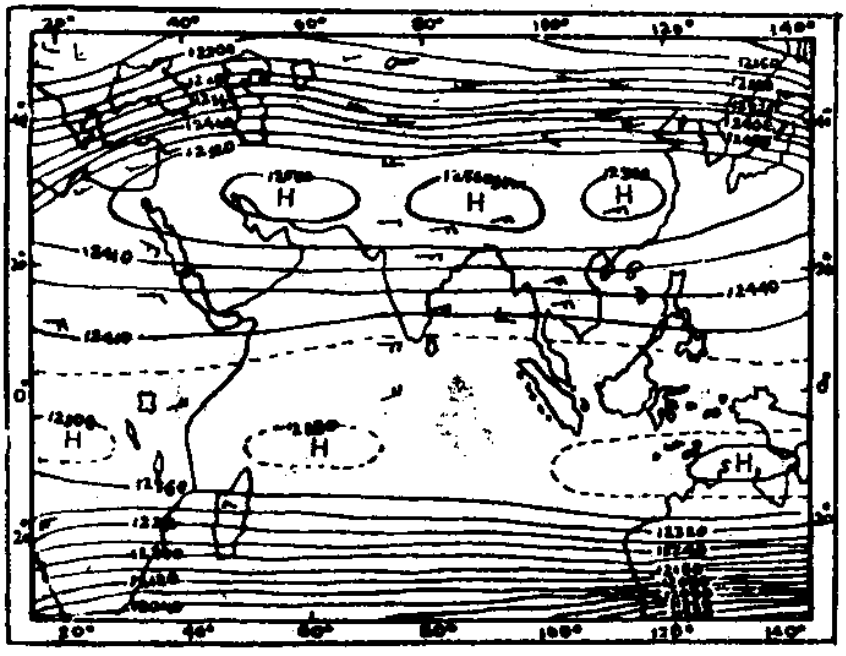

FIGURE 14(b)- CONTOUR AND WIND PATTERNS: JULY 1964 AT 200 mb (REPRODUCED FROM ANANTHAKRISHANAN, 1965).

latitude 15°N (Ananthakrishnan, 1965). This has indicated the existence of meridional accelerations directed from south to north in the lower troposphere and from north to south in the upper troposphere. Evidence for the existence of a Hadley type of circulation over the area to the east of 70°E was thus obtained. The belt 10°N-15°N appeared to be the central part of the Hadley cell with ascending motion along the latitudinal belt 25°N to 35°N and descending motion over the oceanic areas in the equatorial regions of the southern tropics.

Rao (1962) using Rawin data at 12 Indian stations and data from Colombo, Nairobi, Aden, Bahrein and Tashkent presented the meridional circulation over India during monsoon season [figure 15 & 16].

During January, Northerlies of the direct cell prevail from the surface upto 300 mb and southerlies aloft. The southerlies and northerlies are stronger near the equator. The northerlies weaken in the mid troposphere. The indirect circulation was noticed at Tashkent (42°N) but the transition from lower southerlies to northerlies is near 250 mb.

In July, the direct cell is well marked at both Bahrein and Aden along 40°E. The direct cell circulation commences only at 750 mb below which southerlies of the southwest monsoon are present. In the Indian Longitudes, direct cell circulation is noticed in the middle and upper layers at 30°. But towards the equator this is not noticed. Because of the presence of Himalayas north of 30°N, the centre of the meridional circulations are lifted sufficiently and this explains the level of

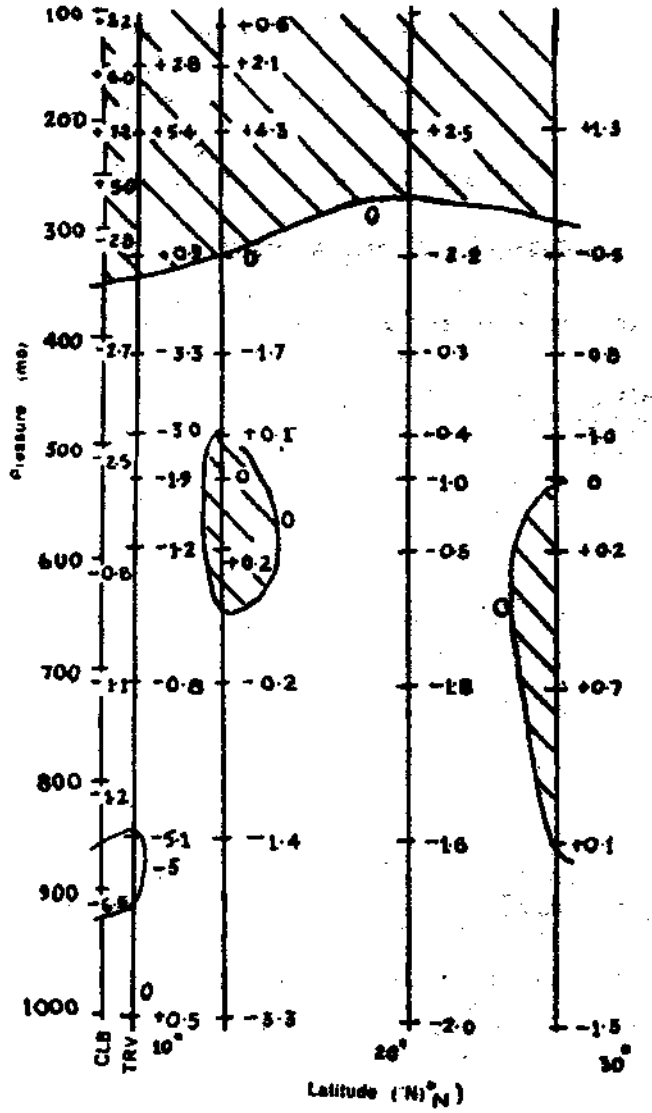

FIGURE 15 - MEAN MERIDIONAL COMPONENTS (kt) FOR JANUARY (INDIAN LONGITUDE). COMPONENT FROM SOUTH IS POSITIVE AND HATCHED (REPRODUCED FROM RAO, 1962).

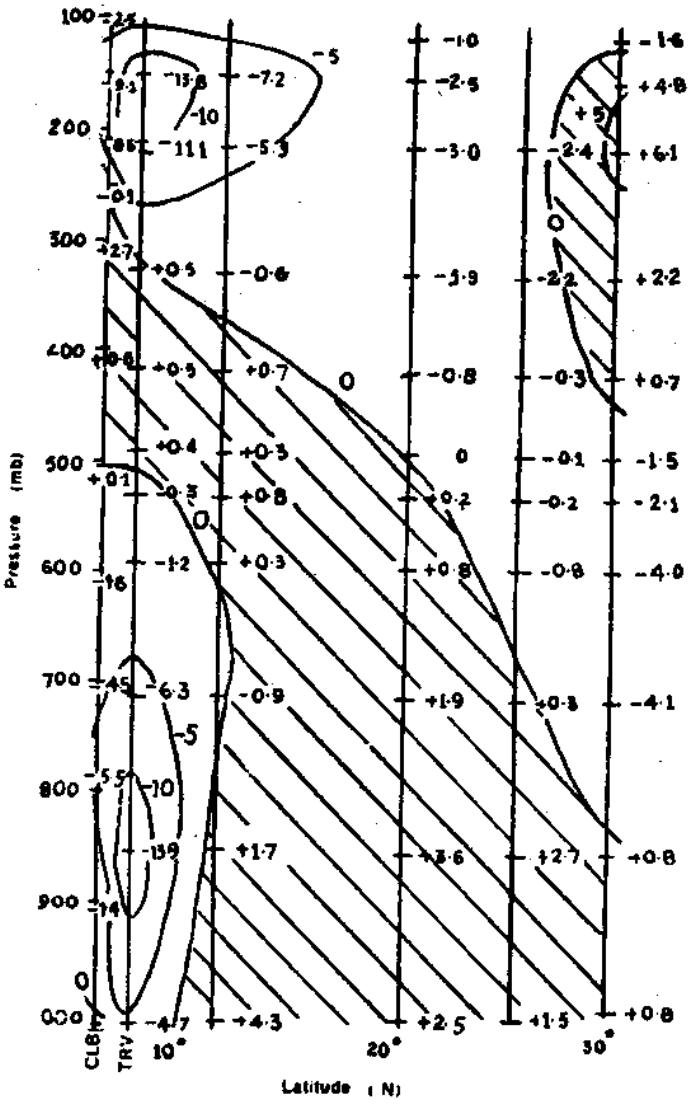

FIUGRE 16 - MEAN MERIDIONAL COMPONENTS (kt) FOR JULY INDIAN LONGITUDE). COMPONENT FROM SOUTH IS POSITIVE AND HATCHED (REPRODUCED FROM RAO, 1962).

transition being around 300 mb in both the direct and indirect cells over the Indian area. Modelling of regional circulation features over the Indian region :

The general circulation models have recently been applied to the summer and winter monsoons of Indian sub-continent and other monsoon regions of Africa and south Asia (Temperton et al, 1983).

Das (1962) used a 10 layer quasi-geostrophic model to compute the mean vertical motion for a typical monsoon month (July) and his results suggested that there is an area of ascent over northeast India and subsidence over northwest India. The model besides being able to bring out the structure of circulation over the monsoon through, was also able to explain the extensive precipitation over northeast India and the little or no rainfall over Rajasthan and adjoining areas.

This, and the later study by Das et al. (1971) using the 10 layer quasi geostrophic model indicated the possibility of using geostrophic models in a monsoon regime to compute large-scale vertical velocity. While the model was able to represent the rainfall patterns fairly satisfactorily during well marked synoptic situations like monsoon depressions, it was not sensitive to situations of weak or active monsoon not accompanied by well marked synoptic features like depressions.

Mukherji and Datta (1973) attempted quantitative forecast of precipitation by using a 4 layer quasi geostrophic model. The equations of baroclinic flow were written as:

$$\nabla^2 \frac{\partial z}{\partial t} + (z, \quad + f) - (f^2/g) \frac{\partial \omega}{\partial p} = 0 \qquad \ldots (22)$$

$$\sigma \nabla^2 \omega - (f^2/g) \frac{\partial^2 \omega}{\partial p^2} = (g/f) \nabla^2 J(z, \frac{\partial z}{\partial p}) - \frac{\partial}{\partial p} J(z, \zeta + f)$$

for computing the vertical velocity ω and contour heights for different atmospheric levels.

where

∇^2 = Horizontal Laplacian operator

Z = Geopotential height

$J(\phi, \psi)$ = Horizontal Jacobian operator

σ = Coefficient of static stability

d = Grid length

Δp = Constant increment of pressure along the vertical

The three dimensional grid had a length of 381 km true at 22 1/2°N and is same in x and y directions. Except in the computation of vorticity, a constant value of f has been used. Vale of f was taken corresponding to 25°N. The distance in vertical Δp was taken as 200 mb. The initial values of ω at 1000 mb and 200 mb were taken as zero.

As the authors themselves had indicated, the chief limitations of the model besides the geostrophic assumption were:

i) rather large grid length (381 km) because of which some of the small scale (local) systems were not noticed,

ii) effect of radiation was considered to be negligible,

iii) consideration of non-adiabatic process, and

iv) non-consideration of the effect of topography on the vertical velocity

Mukherji and Datta (1975) improved on this model by incorporating all such effects neglected in the 1973 study excepting radiation. The model was able to forecast the movement of large scale synoptic systems and cyclogenesis.

Awade and Keshavamurty (1975) had computed the vertical motion field in the Indian monsoon region using a quasi-geostrophic ω equation. Besides forcings due to thermal and differential vorticity advection, the vertical motion due to orography and friction have been included. The vertical motion due to the different forcing functions was computed. Two contrasting situations of good and bad (weak) monsoon days in July have been studied.

In the quasi-geostrophic omega equation

$$\sigma\nabla^2\omega + f_o^2 \frac{\partial^2 \omega}{\partial p^2} = g \frac{\partial}{\partial p} J(Z, \eta) - \frac{g^2}{f_o} \nabla^2 J(Z, \frac{\partial Z}{\partial p}) \qquad \ldots (23)$$

The first term on the right hand side is the forcing due to vorticity advection, while the second term is forcing due to thermal advection.

The equation was solved by a three dimensional relaxation with 2.5° grid. The conversion from potential to kinetic energy associated with the circulations of the monsoon were computed. The ω field and the associated energy conversions had indicated

large fluctuations between good and weak monsoon conditions.

The meridional circulation was well marked on the strong monsoon day and was accompanied by conversion of potential energy to kinetic energy. On weak monsoon day there was descent with no energy conversion whatsoever.

Although the quasi geostrophic models were generally successful for forecasting in middle and high latitudes because of the conditional instability and near saturate humidity conditions in the tropics especially during monsoon season, convective heating in some form needed to be introduced into the models.

Ramanathan and Bansal (1976) had developed over the quasi-geostrophic model of Mukherjee and Datta (1973 and 1975) by improving upon:

a) Boundary conditions

b) Orographic effects, and

c) Moisture processes

Their model used constant boundaries on an extended coarse grid model at 5^{o} interval on a domain from 0^{o} to $140^{o}E$ and 0^{o} to $60^{o}N$ to compute boundary values for each step for ω and $\partial z/\partial t$ for the boundaries of a fine mesh model at 2.5^{o} interval from 5^{o} to $42.5^{o}N$ and 40^{o} to $120^{o}E$. The values obtained from coarse mesh integration were used for integration with the fine mesh.

The lower boundary condition was applied at the pressure level nearest to the terrain pressure at the grid point instead of 1000 mb.

The static stability parameter σ has been used alongwith an additional forcing due to diabatic heating at the grid points.

In the forcing function:

$$-\nabla^2 Q = -\frac{R}{C_p P}\nabla^2 H$$

H is the rate of heating per unit mass of air per second. In the model H was taken to include only the effect of release of latent heat in free atmosphere omitting the sensible heat transfer from water surface and radiation effects. The results of the study by inclusion of cumulus scale heating were reported to be encouraging.

It was generally recognised that during the movement of storm there was little conversion of kinetic energy into potential energy and, therefore, the storm movement could be modelled by two-dimensional barotropic model. Ramanathan and Saha (1972) used a barotropic primitive equation model to forecast the movement of western disturbances.

Sikka (1975) used a non-divergent barotropic model for forecasting tropical storms in the Bay of Bengal and Arabian Sea.

The governing equation was the usual vorticity equation for the horizontal non-divergent flow applied at 500 mb.

$$\nabla^2\left(\frac{\partial \psi}{\partial t}\right) = J(\nabla^2\psi + f, \psi) \qquad \ldots(24)$$

The stream function ψ was obtained by:

$$\nabla^2 \psi = \zeta = \frac{\partial u}{\partial x} - \frac{\partial u}{\partial y} \qquad \ldots (25)$$

The input data for all the cases considered in the study were the 00 GMT wind analysis at 500 mb. The stream function derived from the analysis of the observed wind field have been used to forecast the storm for 24 hour and 48 hours in advance. The forecasted tracts were compared with observed tracks. There was no particular bias in the forecasts and they were either way of the observed tracks. In case of storms with recurvature, the forecast was generally later by 24 hrs.

Ramanathan and Bansal (1977) had used a primitive equation barotropic model to forecast the storm tracks in the Arabian sea and Bay of Bengal. The model equation adopted on a mercator projection in cartesian coordinates were:

$$\frac{\partial u}{\partial t} + m\left(u\frac{\partial u}{\partial a} + v\frac{\partial u}{\partial y} + g\frac{\partial h}{\partial x}\right) - fv = 0$$

$$\frac{\partial v}{\partial t} + m\left(v\frac{\partial}{\partial x} + v\frac{\partial}{\partial y} + g\frac{\partial h}{\partial y}\right) + fu = 0 \quad \ldots (26)$$

$$\frac{\partial h}{\partial t} + m\left[u\frac{\partial h}{\partial x} + v\frac{\partial h}{\partial y} + h\left(\frac{\partial u}{\partial x} + \frac{\partial v}{\partial y}\right)\right] - vh\frac{\partial m}{\partial y} = 0$$

where,

m is map scale factor, and

h is height of free surface

The model was applied to a number of cases in 1970. The grid size of 2.5^{o} adopted was too coarse for defining the initial position of storm accurately. The initial position of the vortex centre was said to be in error by 60 km in some cases. Reduction of the grid size to 1.25^{o} enabled a better positioning of the vortex centre. From experiments with

analytical symmetrical vortex, it was realised that the basic flow was more important than the disturbance intensity. The basic flow was, therefore, separated by double fourier analysis and integrated treating the vortex as a point and advecting the point along with the basic flow. The authors felt that better forecasts would be possible if the grid size was reduced further say to 55 km to reduce truncation errors.

Singh and Saha (1978) used a quasi-Lagrangian advection scheme for forecasting the movement of monsoon depressions using a primitive equation barotropic model. The prediction equations used in cartesian coordinates in the Mercator projection were

$$\frac{Du}{Dt} = fv - mg\frac{\partial h}{\partial x}$$

$$\frac{Dv}{Dt} = -fu - mg\frac{\partial h}{\partial x} \qquad \ldots (27)$$

$$\frac{Dh}{Dt} = -mh\left(\frac{\partial u}{\partial x} + \frac{\partial v}{\partial y}\right)$$

where $\frac{D}{Dt} = \frac{\partial}{\partial t} + \frac{\partial}{\partial x} + \frac{\partial}{\partial y}$ represents the Lagrangian advection operator.

The basic input to the model was the observed wind using which the stream function was obtained. A 2^{o} lat/long grid was used to study two cases (i) a monsoon depression of Aug 1968 and (ii) a tropical cyclone of October 1971. The results obtained for both the cases suggested that the forecasts upto 48 hours were encouraging but deteriorated for further length of periods.

Saha (1983) had also used a single level primitive equation barotropic model for predicting the movement of monsoon depressions over the Arabian Sea and Bay of Bengal. The initial input to the model was the subjectively analysed wind field from which geopotential field was derived. The movement of three depressions during the summer monsoon of 1979 was studied. The study has shown that a single level primitive equation barotropic model was able to predict the movement of monsoon depressions to a limited degree of accuracy. This could be broadly due to the fact that a barotropic model might not be able to represent the conditions of a highly baroclinic atmosphere characteristic of the monsoon depression field.

Das and Bedi (1976) and Bedi et al (1976) had developed a regional primitive equation model for the Indian region. The model was regional variant of the baroclinic hemispherical model developed by Krichak and Rabinovich (1972). To account for the effect of Himalayas, orography has been introduced in the Indian model which has led to truncation errors along the edges of the mountains. To overcome this Das and Bedi (1978) had followed the procedure suggested by Philips wherein the pressure gradient force is evaluated on a constant pressure surface instead of a sigma surface. The results indicated considerable reduction in the truncation errors. The model was able to simulate the monsoon trough and also demonstrate the shift of and intensification of the monsoon trough with the variation of the albedo over Rajasthan. Other important observations from the study were

i) initial zonal flow with shear generated a low pressure area resembling the monsoon trough at the 500 mb and

ii) anticyclonic circulation resembling the subtropical ridge was generated at 300 mb after 120 hours due to advection of cold air from the north of Himalayas.

Mohanty and Madan (1985) have evolved a systematic approach to solve some of the problems arising out of integrating simple barotropic models for forecasting the tropical systems such as depressions and cyclones. Dynamic initialization was carried out for selective smoothing of high frequency wave spectrum. The improvement in the efficiency of the model by incorporating the dynamic initialization and filtering techniques was demonstrated by applying the model for the forecast of tropical cyclones in Bay of Bengal. As in earlier studies it has been realized that the geopotential field could be derived from the observed wind field and the observed wind field was a reasonable representation of the input data for the primitive equation model. Other important conclusions from the study were:

i) the dynamic initialization made the model more stable for a long time integration and substantially improved the quality of the forecast and

ii) a space filter besides the dynamic initialization was essential to supress the two grid waves to obtain a realistic forecast of the meteorological fields.

Shaw (1978) applied a limited version of an 11 layer global model (developed at the Dynamical Climatology branch of the Meteorological Office, U.K.) to the Indian monsoon region.

The model is a primitive equation, finite difference model incorporating the moisture and topography. Physical processes of radiation, convection and surface exchanges were also simulated by the model using a 2^{o} grid. Using the objective analysis (optimum interpolation) technique the geopotential and wind field were analysed independently. During the initialization all sources and sinks of energy including latent heat release were ignored.

Bedi (1985) presented the results of integration of a multilevel global spectral model being developed at India Meteorological Department. The model has been limited to six fourier waves in the zonal direction and six zeros of associated legender functions between poles in the meridional direction. In the vertical, the model extended from the earth's surface to the top of the atmosphere with three equally spaced layers in the sigma coordinate system. It does not include the physical features like topography, radiation and moisture nor the boundary aspects. Originally, the model was written with equations for horizontal flow in momentum form but subsequently was modified to the vorticity and divergence form.

The basic input for the model were the spectral amplitudes of geopotential field which were obtained by spectral decomposition of geopotential field interpolated at sigma surface at 5^{o} lat./long. interval over the whole globe. More details of the spectral representation were given by Bedi (1976 and 1979).

In spite of not considering the physical features like

topography, radiation and moisture, the model was reported to have retained the essential features of the circulation.

2.8.1 Modelling of monsoons

Monsoons are large scale seasonal wind systems blowing over vast areas of the globe, persistently in the same direction with reversal with change of season. In the summer monsoon which is very important for large parts of India, huge mass of air including that from the southern hemisphere is drawn into circulation. The south-east trades of the south equatorial Indian Ocean after crossing the equator, due to the action of Coriolis Force, become south-westerly and that is why the summer monsoon is also known as the south-west monsoon.

The summer monsoon, with its characteristic south-westerly current at lower levels and a marked easterly flow above 500 mb, is an important component of the general circulation of the atmosphere in tropics which serves as a large scale mechanism of re-distribution of excess of heat from the equatorial regions to higher latitudes.

With the onset of monsoon the whole atmosphere over the south-Asian region undergoes conspicuous and sudden changes. The moist south-westerlies of the monsoon extend upto 6 km replacing the prevailing north-easterly winds. The mean upper air wind pattern in July at 200 mb level is shown in figure 17. At the surface level, the Inter Tropical Convergence Zone (ITCZ) shifts from the winter position near equator to about 20^{o} to 25^{o}N. This is the monsoon trough which runs through the Indo-Gangetic

plains. The subtropical westerly jet stream shifts to north heralding the onset of monsoon.

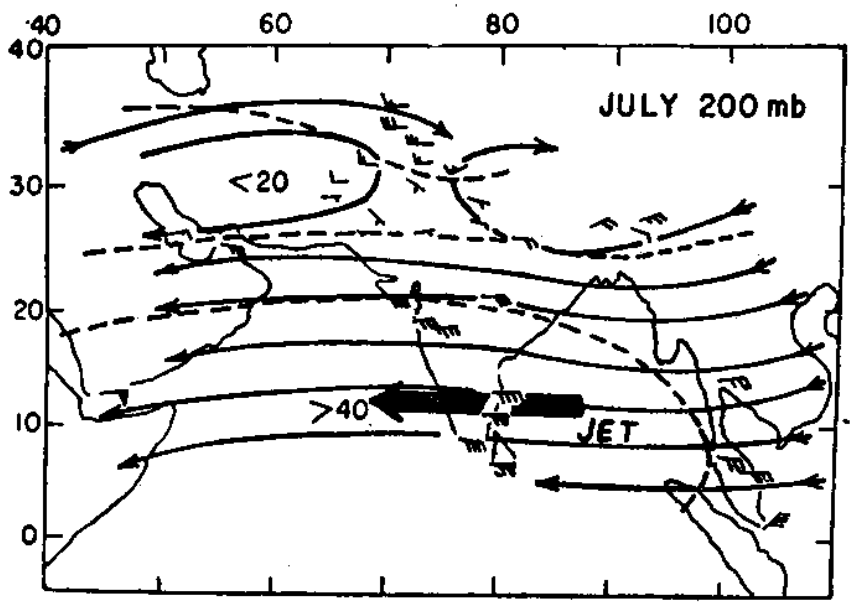

FIGURE 17 - MEAN UPPER WINDS OVER INDIA AND NEIGHBOURHOOD AT 200 mb

Flow south of lat 20°N is westerly upto 500 mb and easterly aloft with winds of jet speed between 150 and 100 mb. Two easterly jet streams, characteristic of the south-west monsoon appear over peninsular India.Koteswaram (1958) suggested that the easterly jet results from the thermal effects of the elevated Tibetan Plateau on the general circulation in summer. The monsoon trough to the south of the Himalayas helps in augmenting the circulation by liberation of condensation heat. Koteswaram (1958) suggested a model for the circulation during the south-west monsoon(figure 18). The tropical circulation (Hadley cell) is replaced by two cells of opposite circulation during the monsoon season. The common source of heat is the Tibetan Plateau and Sinks over Siberia and equatorial regions respectively. Two jet streams one each in the poleward

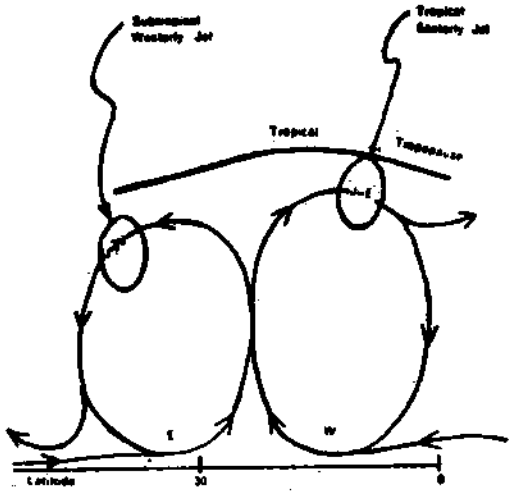

FIGURE 18 - SCHEMATIC MODEL OF THE VERTICAL CIRCULATION IN THE ASIAN SUMMER MONSOON.
(REPRODUCED FROM KOTESWARAM,1958).

westerlies and equator-ward easterlies were indicated.

The chief synoptic features of the monsoon are:

i) the monsoon trough in the Indo-Gangetic plains,

ii) tropical storms originating in the Bay of Bengal which move over the land,

iii) break in the monsoon with the movement of monsoon trough towards the foot of Himalayas

iv) trough in westerlies, and

v) mid tropospheric low pressure systems

Early attempts to establish relationships between monsoons and atmospheric behaviour employed statistical analysis without much regard for physical justification. Lack of upper air data has also to some extent precluded a proper physical understanding of the association. Sir Gilbert Walker attempted about 50 years ago, although inconclusively, to explain in physical

terms a statistical relationship between the April and May pressure in South America and June to September Indian monsoon rainfall. Walker's work led to the discovery of the phenomenon which he called 'the southern oscillation'. This was characterised by a tendency for air to be removed from pacific area around the same time as air moves into the Indian ocean area and vice-versa. This phenomenon was evidenced by not only in values of surface pressure but also in temperature and rainfall records of India, Indonesia and Australia (Walker, 1972).

Godbole et al (1970) conducted a numerical experiment in simulating monsoon in a two dimensional meridional plane along 80^{o}E extending from the equator to the pole. In the horizontal 18 grid points at 5 degrees latitude intervals were used. To facilitate inclusion of topography, in the vertical, the atmosphere was divided into eight layers in sigma coordinate system with the top of the turbulence layer coinciding with the level '$8\frac{1}{2}$'. The ground was represented by level '9'.

Observationally determined distribution of water vapour, carbon dioxide, ozone and cloud amount were used for computing the heating due to short and long wave radiation. Albedo at the earth's surface was determined by considering the cloud amount, precipitation and surface conditions,seasonal variation of monsoon circulation, interaction between the southern and northern hemispheres, effect of Asian continent and oceanic currents have been disregarded.

Roughness parameters appropriate to sea, land and mountains have been applied, to estimate the forced convection.

Vertical distribution of temperature was adjusted to dry or wet adiabatic lapse rate depending on whether the humidity being less or more than 100%. Sea surface temperature was kept constant at 300°K (27°C), the value observed normally. The initial state was considered as calm. Integration over a period of 80 days using 10 minute time steps, determined the zonal profile. Lower tropospheric westerlies and upper easterlies were developed in the model which showed speeds of the same order of magnitude as in climatic normals. When the mountain effect was not included, westerlies were less than 10 kt and easterlies 20 kt, like the conditions to the east of Himalayas.

Godbole (1973) made further computations for the following sets of conditions:

i) with moisture and with the Himalayas

ii) Without moisture and with Himalayas

iii) Without moisture and without Himalayas

iv) With moisture and without Himalayas

Experiment (iii) was carried out with two values of sea surface temperature 300° and 290°K. Experiment (iv) was carried out for two different surface mixing ratio values namely 80 and 40 per cent of saturation mixing ratio at the surface and also by the assumption that condensation occured at 80 per cent relative humidity.

In the wet model with Himalayas (Experiment (i)) the simulated tropical easterly jet has a core speed of 36 m/sec. at a height of 12 km at 20°N as against the observed speeds of 35 m/sec. at 14 km at 15°N. In the dry model with Himalayas

(Experiment (ii)) while simulation circulation pattern remained as in the case of wet model, the jet had a core speed of 25 m/ sec. Results with wet and dry model experiments indicates that moisture was not important in controlling the monsoon circulation. Higher amounts of water only contributed to higher precipitable water but not higher rainfall.

The experiments with and without Himalayas indicated the dominant role of the Himalayas in the development of monsoon circulation. Variation of sea surface temperature by $10^{o}C$ did not make any material difference. Some of the simulation with the wet model with Himalayas is shown in figure 19.

As the author himself had pointed out, the zonally symmetric model which operates in the two dimensional vertical plane, might be having some limitations in taking into account the eddies, monsoon depressions and lows and middle latitude troughs in westerlies.

Hahn and Manabe (1975) using a global general circulation model developed at the GFDL, U.S.A. carried out what would be termed a most comprehensive numerical simulation of the monsoon. A sigma coordinate system with eleven unevenly spaced finite difference levels from the planetary boundary layer upto 31 km are used. The model has been tried with and without the mountain topography of south Asia. The mountain model (M model was time integrated for 3.5 years. The experiment with no mountain (NM model) was started from 25 Mash of M model by setting the initial pressures every where at 988 mb.

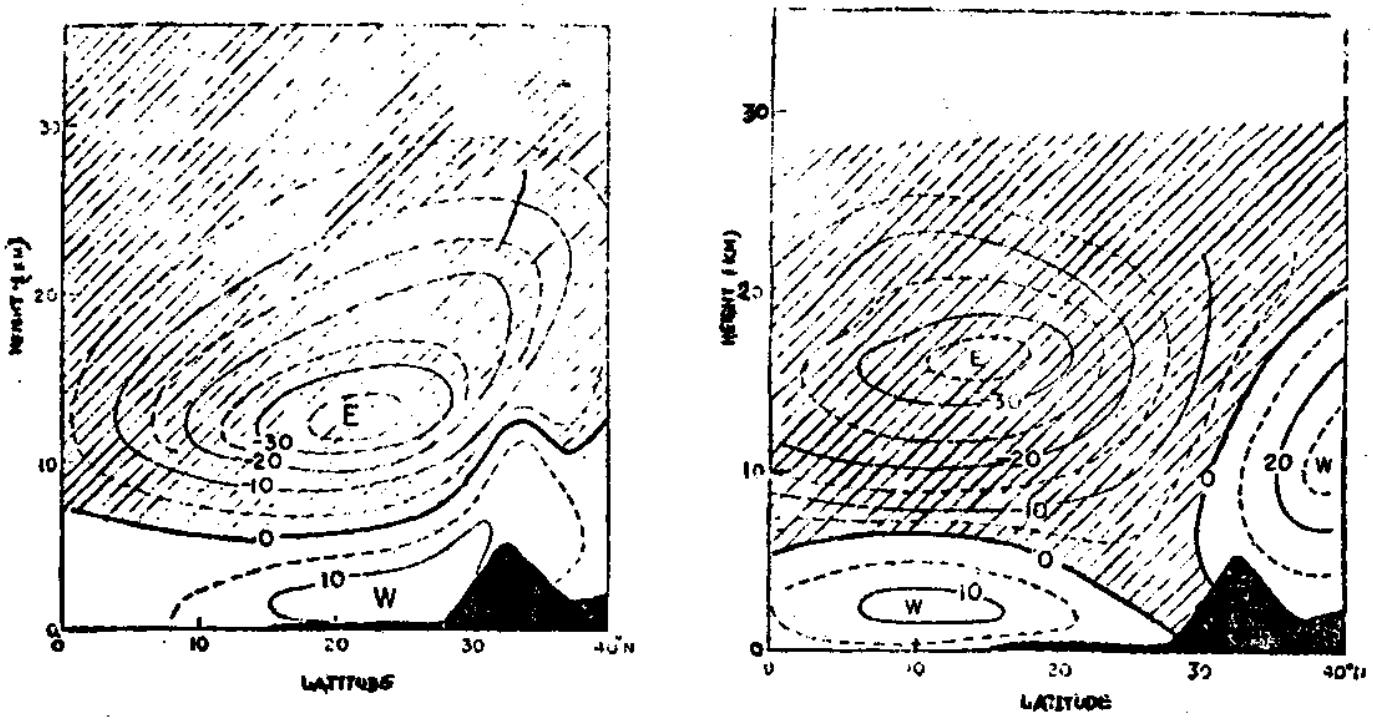

FIGURE 19(a) - SIMULATED AND THE OBSERVED ZONAL WIND FOR THE WET MODEL (REPRODUCED FROM GODBOLE, 1973).

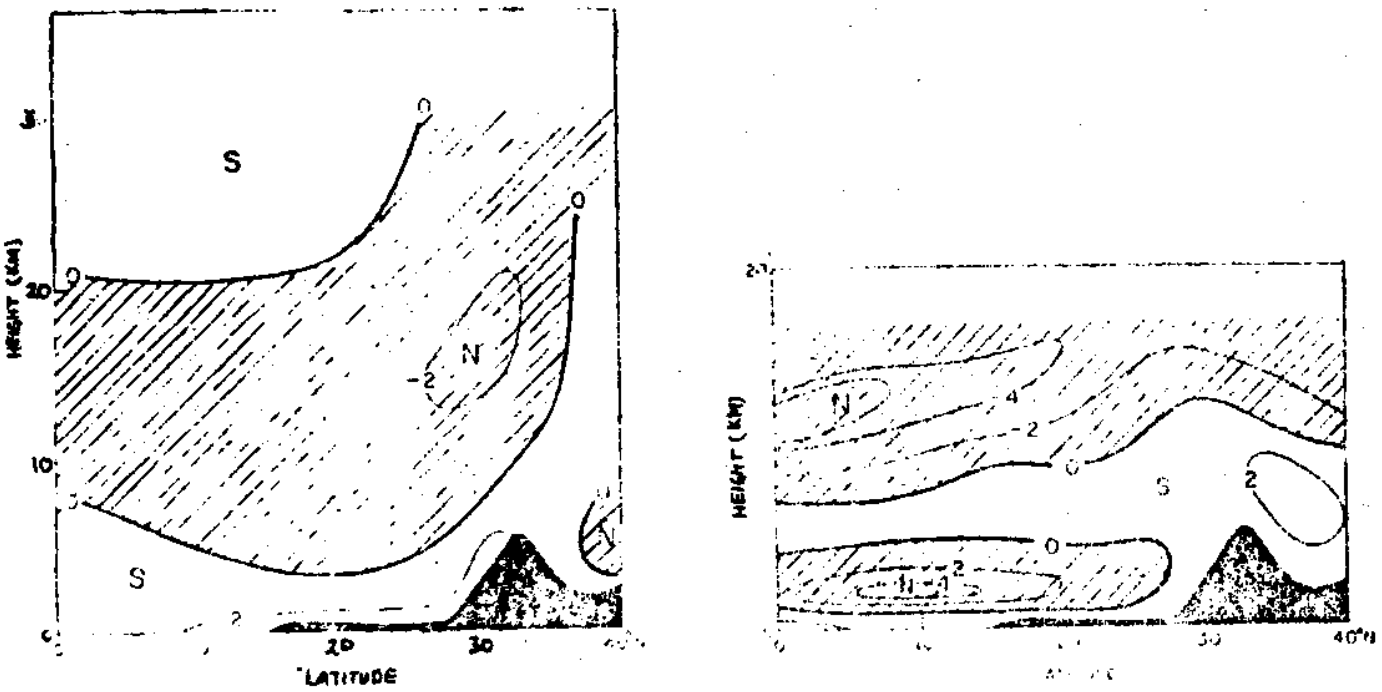

FIGURE 19(b) - SIMULATED AND THE OBSERVED MERIDIONAL WIND FOR THE WET MODEL (REPRODUCED FROM GODBOLE, 1973).

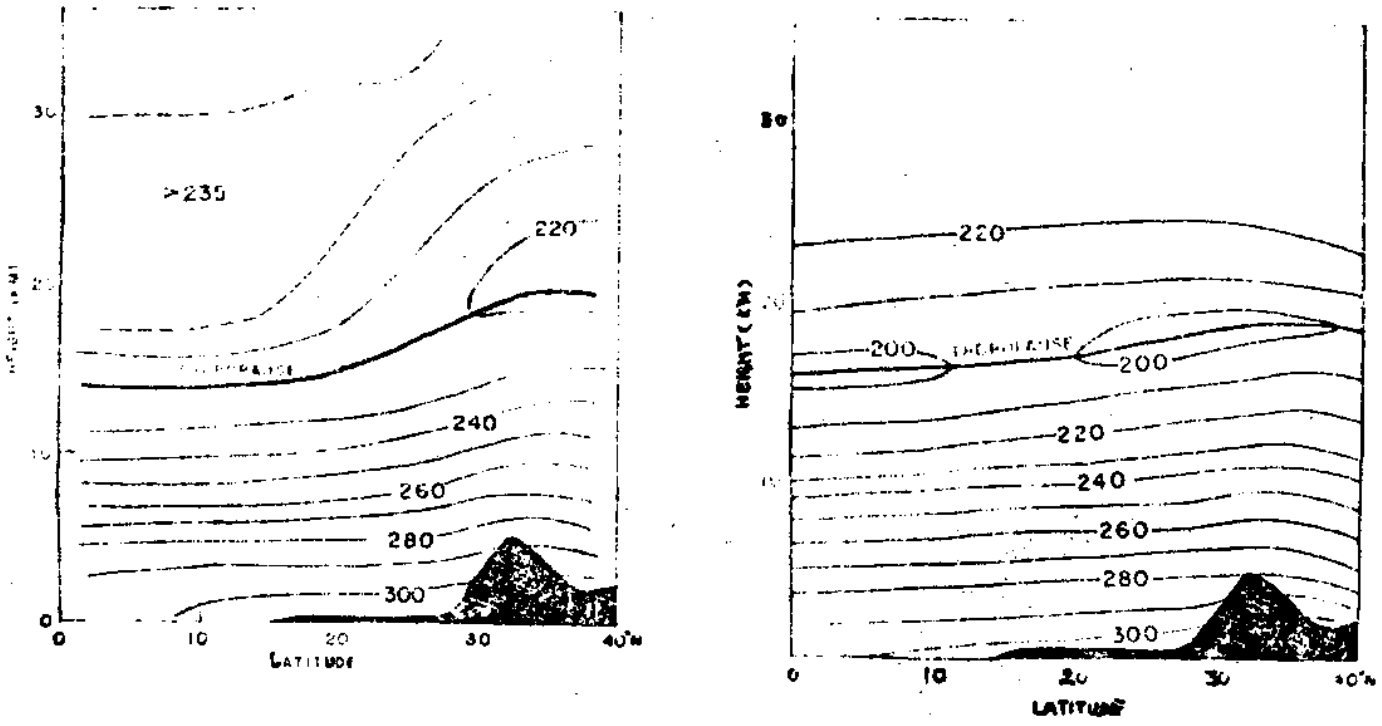

FIGURE 19(c) - SIMULATED AND OBSERVED TEMPERATURES WITH THE WET MODEL (REPRODUCED FROM GODBOLE, 1973).

The M model was successful in simulating important features of the south Asian monsoon circulation. The onset of the monsoon was studied with day to day computations. All the features associated with the onset of monsoon were generally simulated but by a lag of 10 to 15 days after the normal dates of onset of monsoon. Other discrepancies noticed were:

i) The lowest pressure was near the highest point of the Tibetan Plateau

ii) The seasonal low over Pakistan was weaker by 5 mb.

iii) Monsoon depressions which normally move west north westward, move northeast-ward in the model

iv) Large scale anticyclone over the low pressure belt was brought out but the 190 mb anticyclone was 5^{o} too far south .

The major discrepancy was in terms of the rainfall computed. The western ghats and northeast India get no rainfall in the model while the peninsula gets very high rainfall. The region around the northwest Bay of Bengal gets almost the same amount of rainfall as in the western desert regions.

In the NM model, the upper tropospheric anticyclone lies south of Tibet. Both the westerly and easterly jets are stronger in the NM model. The centres were displaced by about 10^{o} to south. A narrow band of intense upward motion was centred at 10^{o}N with descending motion on both sides.

In both the models, maximum latent heat release was responsible for highest mid-tropospheric temperature. The ITCZ between the two Hadley cells was located at 15^{o}N in the

M model and at 12°N in the NM model.

In the NM model a desert like climate was simulated over South Asia while in the M model substantially good rainfall was simulated over the same region. An important feature indicated by the models was that the dynamics which produce rainfall just south of the equator may be important for temporal variations in the monsoon to the north over South Asia. Also, without the mountains, the South Asian low pressure belt and the monsoon trough would not have existed.

The global general circulation model of the GFDL has been integrated by Shukla (1975) with and without a cold sea surface temperature anomaly over the Somali coast and the western Arabian Sea with a view to assess the possible effects of the anomalies on the fluctuations in the monsoon. A schematic representation of the air - sea interaction over the Arabian Sea is given in figure 20 which shows the effects of the air - sea interaction on the evaporation, cross equatorial moisture flux and rainfall over the Indian region.

During the Indian summer monsoon, strong northward airflow takes place near the Somali coast of Africa and western Inian ocean. Wind speeds reaching 100 to 150 km/hr are usually found at about 1.5 km height a.s.l. This wind is usually referred to as the 'Somali Current' which causes large scale upwelling in the western Arabian sea. Studies by several workers has shown that

i) warmer sea surface temperature (sst) anomalies and stronger winds may cause higher evaporation and consequent

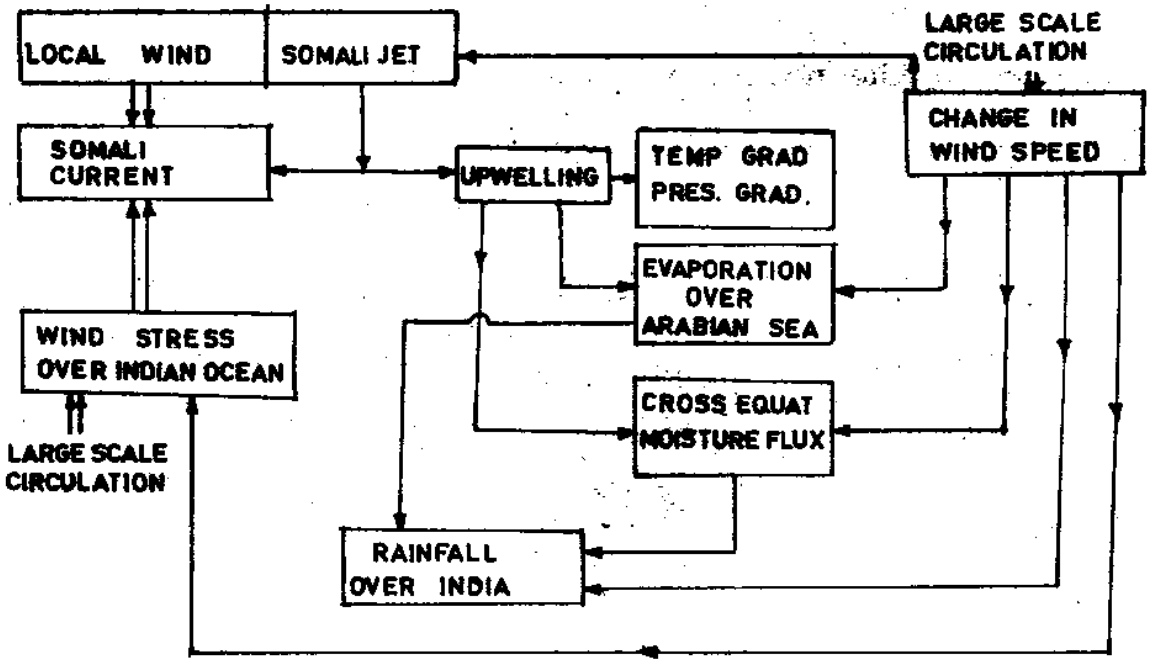

FIGURE 20 - SCHEMATIC REPRESENTATION OF AIR-SEA INTERACTION OVER THE ARABIAN SEA (REPRODUCED FROM SHUKLA, 1975)

increase in moisture and instability of monsoon air over the region.

ii) colder anomalies may cause reduction in cross equatorial moisture flux and consequent reduction in rainfall over India.

The eleven layer primitive equation model in the sigma system developed at the GFDL has been used in this study. The results of the study have shown that evaporation would be less for colder sst (as was to be expected). The reduction in evaporation could be also partly due to the reduction in the wind speed. Because of colder sea surface, the cross equatorial moisture flux has also reduced and the reduction in rainfall over India and adjoining areas could be explained as partly due to this. The study has broadly indicated the possibility that colder sst anomalies over Somali coast and west Arabian Sea might cause reduction in monsoon rainfall over India and neighbouring areas.

Washington (1970) experimented with a 5^{o} lat/long version of the National Center for Atmospheric Research (NCAR) GCM showing the basic features of the monsoon. The strong cross-equatorial jet near Somalia, the formation of the tropical easterly jet and the low level westerly flow in the vicinity of India were simulated satisfactorily. The precipitation pattern was incorrect, especially over land. This was partly due to the assumption of the saturated surface conditions. Later versions of the model (Washington, 1974 and Washington and Williamson, 1977) included a simplified ground hydrology to account for the

variable soil moisture conditions of the ground surface.

Gilchrist (1977 a) also simulated the Asian summer monsoon using a 5 layer general circulation model which has a irregular grid mesh of 330 km. The sigma coordinate were used in the vertical. Considering the importance of diabatic heating in the monsoon circulation, the diabatic heat sources and sinks have been considered in the model. The model has simulated maximum amounts of precipitation over the Indian ocean and Burma regions which were in confirmity with the observations of Moller (1951).

Gilchrist (1977b) simulated the southwest monsoon using a 11 layer high resolution GCM with 220 km grid length. In contrast to the 5 layer model, the 11 layer model incorporated an interactive ground hydrology with a running total of soil moisture at each grid point in the model. The soil moisture is subjected to increase or decrease due to rainfall, downward water vapour flux, melting snow and evaporation. The 11 layer model appeared to have performed better over the 5 layer because of the large scale low level flow from the Bay of Bengal and the presence of the Himalayas over which the moist flow was forced to ascend.

Druyan (1981) reviewed the Global circulation models in the study of the Indian monsoon. It has been shown that the gross features of Indian monsoon are simulated as a matter of course by the global models because this phenomena represents such an important aspect of the planetary climate. It has been pointed out that simulation of hydrological cycle has many

important ramifications. Many models, although not all, consider the formation of clouds whenever and wherever the air becomes saturated. These clouds, in turn, reflect much of the solar radiation away from the ground by day while constituting a tropospheric source of infrared radiation day and night. A parameterization of ground hydrology which take the precipitation rate into account, fixes the availability of water for evaporation from the surface thus providing this significant cooling mechanism for the ground which operates in the nature. The simulation of mean sea level pressure, and precipitation by the various GCMs over the Indian subcontinent are shown in figures 21 - 24.

Druyan (1981, 82) also discussed the performance of a course-mean general circulation model in studies of the Indian summer monsoon. The 5- layer primitive equation model developed at NASA, Goddard Institute for Space Studies (GISS) was used in the simulation of climate parameters over South Asia. It was inferred that Himalayas are responsible for the observed northwesterly flow aloft over northern India before onset and the delay in the precipitation onset there until late June or July. Sea surface temperature anomalies, which were held constant throughout the four months of simulations, affect local precipitation computation via changes in stability.

2.8.2 Modelling of break monsoon conditions

Breaks in southwest monsoon occur during July and more often in August when rainfall generally decreases over the peninsula, Central India and north Indian plains. The break

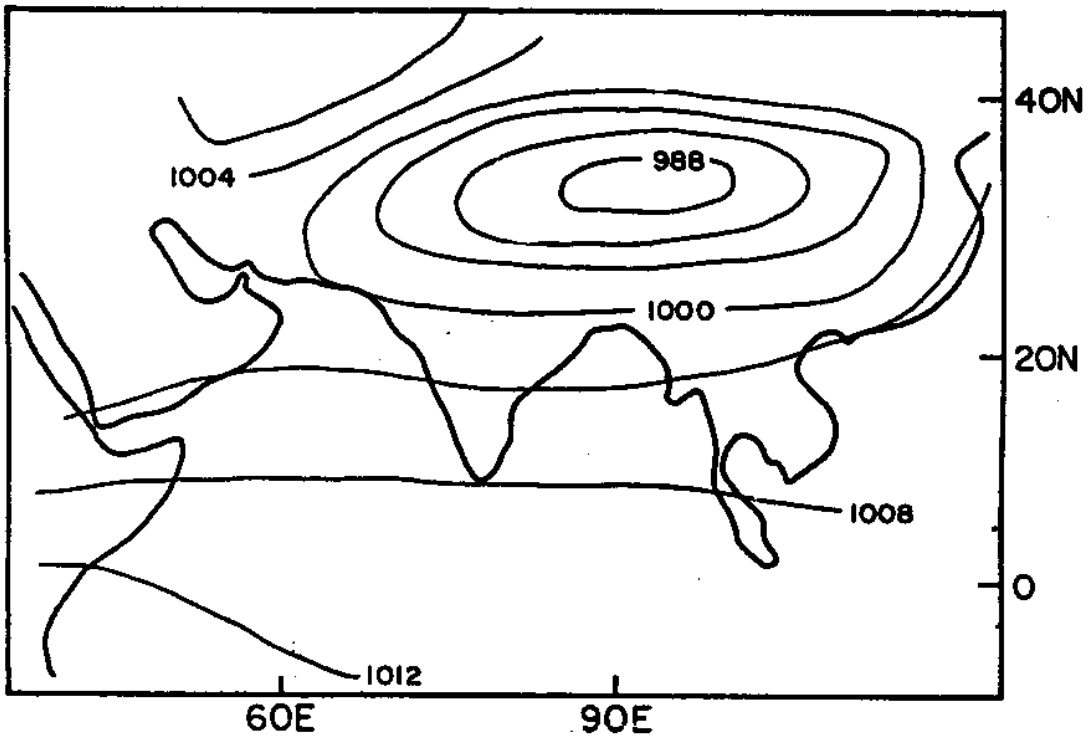

FIGURE 21(a) - MODEL SIMULATED MEAN SEA-LEVEL PRESSURE (mb) DISTRIBUTION FOR JULY (STONE ET AL, 1977).

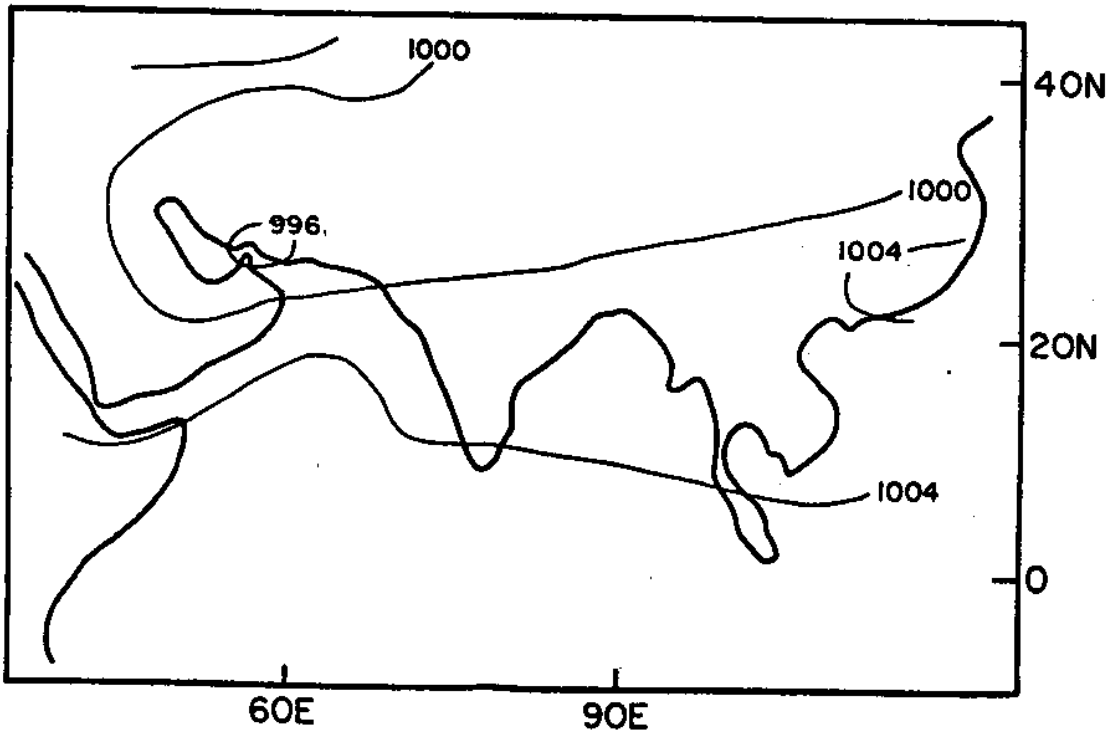

FIGURE 21(b) - MODEL SIMULATED MEAN SEA-LEVEL PRESSURE (mb) DISTRIBUTION FOR JULY (GILCHRIST, 1977).

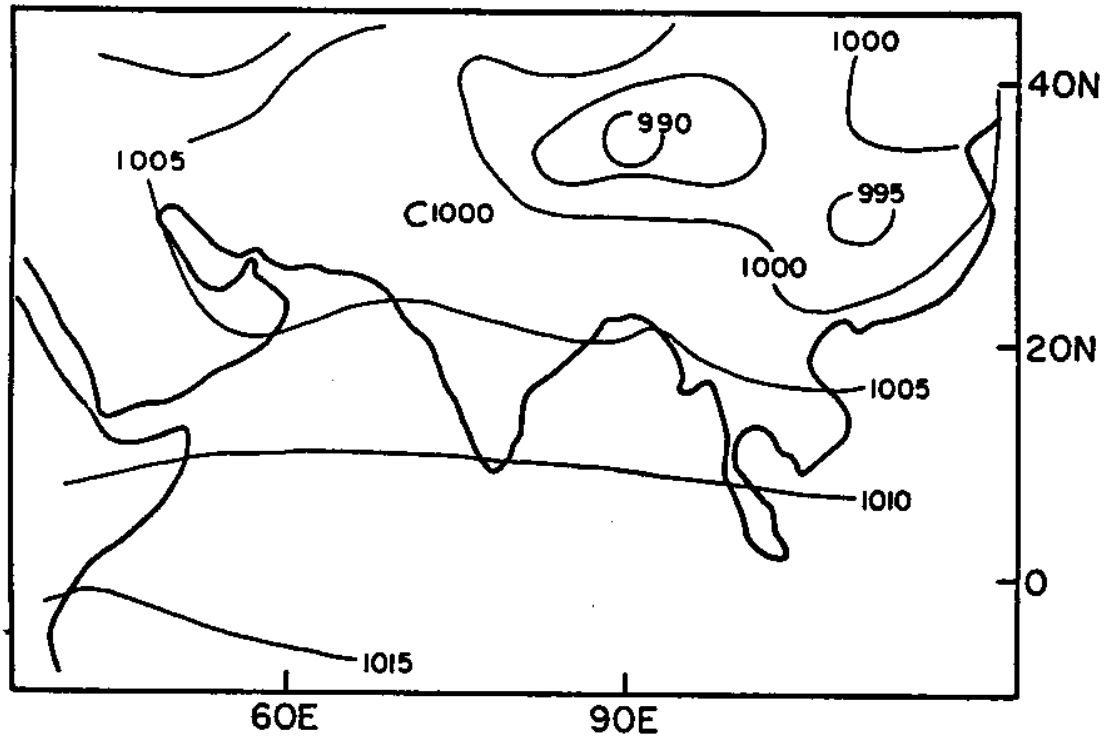

FIGURE 21 (c) - MODEL SIMULATED MEAN SEA-LEVEL PRESSURE (mb) DISTRIBUTION FOR JULY (HAHN AND MANABE, 1975)

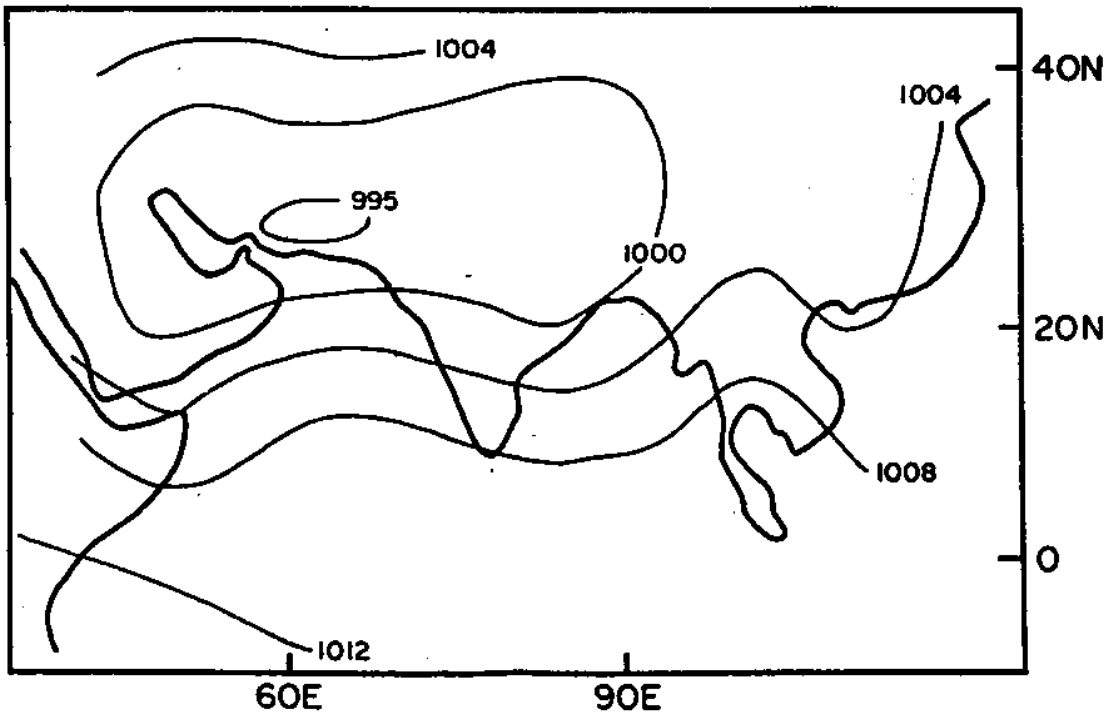

FIGURE 21(d) - OBSERVED MEAN SEA LEVEL PRESSURE (mb) DISTRIBUTION FOR JULY.

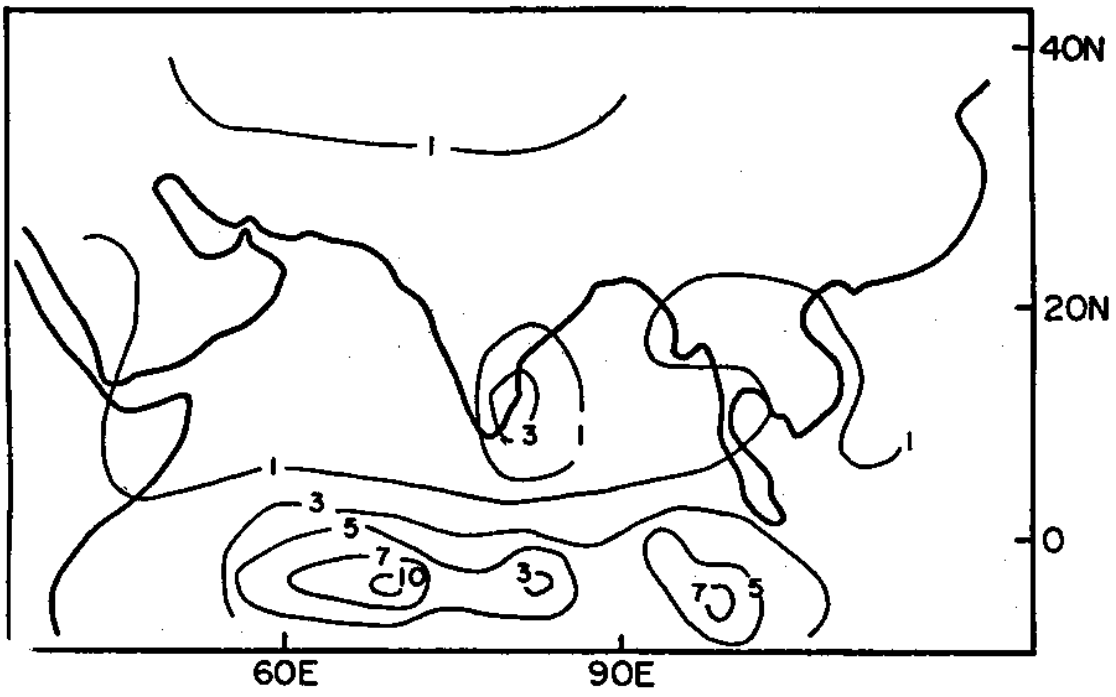

FIGURE 22(a) - GISS MODEL SIMULATED MEAN PRECIPITATION RATIO (mm/day) FOR JANUARY (STONE ET AL, 1977).

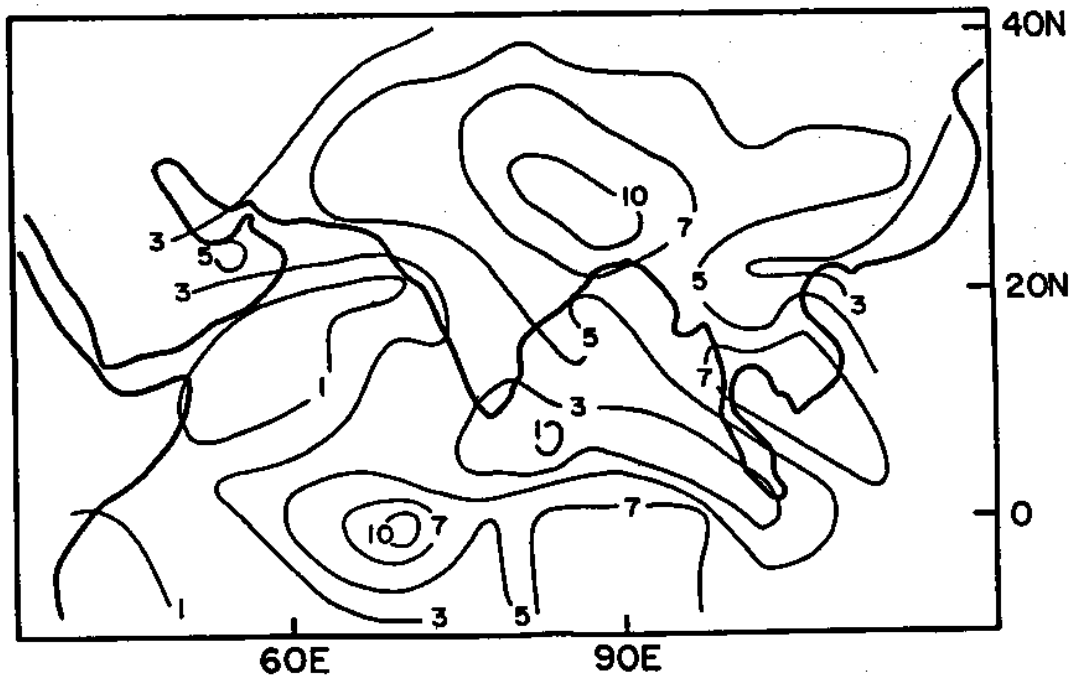

FIGURE 22(b) GISS MODEL SIMULATED MEAN PRECIPITATION RATIO (mm/day) FOR JULY (STONE ET AL, 1977)

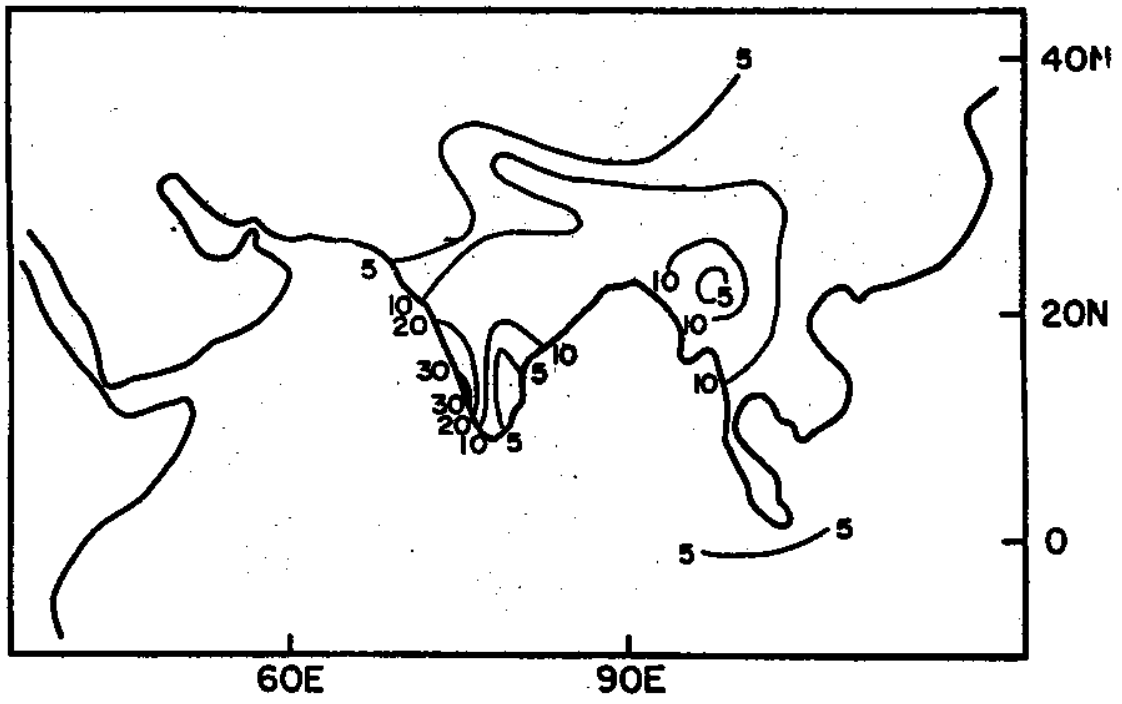

FIGURE 22(c) - OBSERVED OVER LAND DISTRIBUTION OF MEAN PRECIPITATION RATIO (mm/day) FOR JULY BASED ON DATA FROM WERNSTEDT 1972).

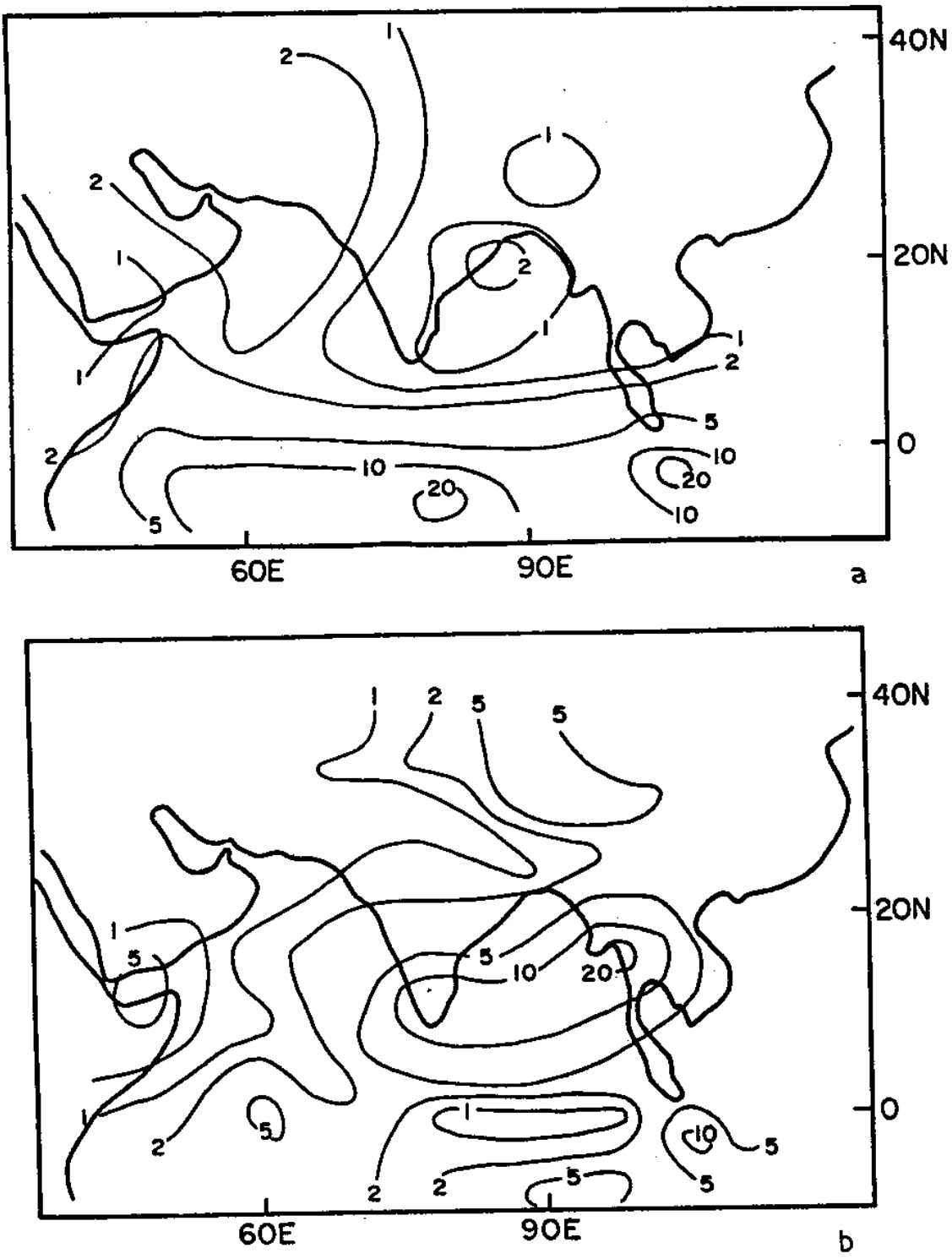

FIGURE 23 - GFDL MODEL SIMULATED MEAN PRECIPITATION RATES (mm/day) FOR (a) WINTER (b) SUMMAR(FROM MANABE ET AL 1974).

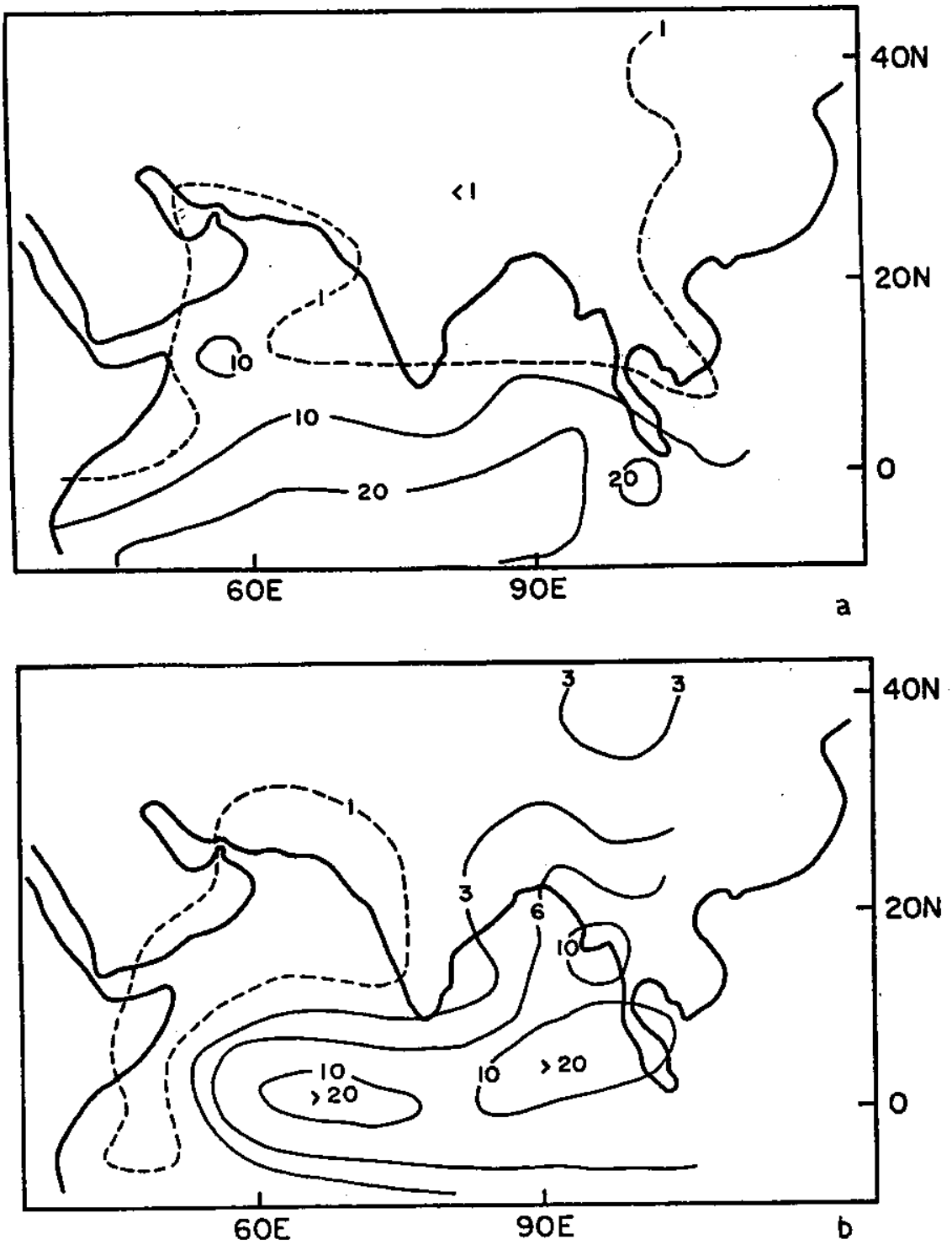

FIGURE 24 - NCAR MODEL SIMULATED MEAN PRECIPITATION RATES (mm/day) FOR (a) JANUARY FROM WASHINGTON, 1976, (b) JULY (FROM WASHINGTON AND DAGGUPATY 1975).

generally lasts for one week to two weeks but may extend upto three weeks in some cases. During the breaks westerly wind speeds over the peninsula decrease considerably confining only to lower levels of troposphere. On the other hand they spread over northern India replacing the monsoon easterlies and in the process shift the monsoon trough towards the Himalayas.

Other features include:

i) movement of mid troposphere lows

ii) troughs in mid tropospheric westerlies

iii) second westerly maxima in upper troposphere, and

iv) occurrence of double easterly jet maxima one around 10^{o}N and other near 20^{o}N.

Raghavan (1973) suggested a model for break monsoon conditions but it was not consistent with observed circulation features. Krishna Rao and Datta (1975) proposed a circulation model for the break monsoon conditions which was claimed to be consistent with observed conditions. The model is shown in figure 25. It is seen that in the lower troposphere south of 10^{o}N there are westerlies, weak westerlies between 10^{o}-20^{o} N and easterlies north of 20^{o}-30^{o} N. In the mid troposphere, weak westerlies are indicated from equator to 30^{o}N. The upper troposphere has easterlies from Himalayas down towards equator with two jet maxima. Two areas of ascent, one around 10^{o}N and the other around 30^{o}N with subsidence around 20^{o}N is also indicated.

Study of 1972 break monsoon by Kesavamurty (1974) indicated that the north-south meridional circulation weakens and shifts to the north and the east-west Walker circulation becomes more intense.

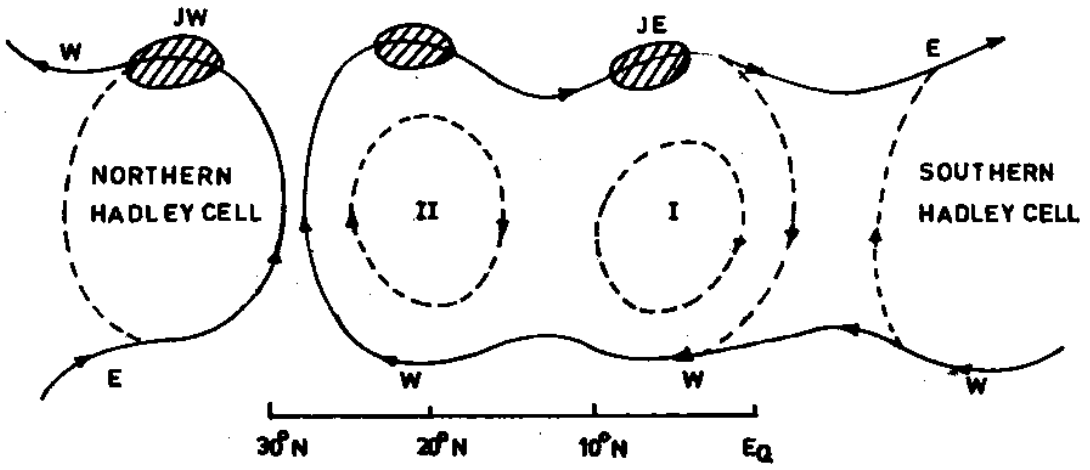

FIGURE 25 - CIRCULATION MODEL FOR 'BREAK MONSOON' (REPRODUCED FROM KRISHNA RAO AND DATTA, 1975).

Datta and Mukerji (1975) computed the vertical velocity for the monsoon seasons of 1966 and 1967 using a five layer quasi-geostrophic model. 1966 was a drought year and had break monsoon during August. A comparison of the vertical velocity distribution with height during the active monsoon and break monsoon conditions has indicated that during active monsoon, the vertical velocity undergoes a reversal near about 600 mb level, south of 20°N but such reversal does not take place in break monsoon condition. However, when an average situation made up of both active and break conditions were considered only a single vertical cell as in Koteswaram (1960) is observed.

Sikka and Gadgil (1978) studied the changes in the large-scale rainfall during the monsoon seasons of 1972 and 1973 and related them to the daily veriation of the large-scale vorticity abov the frictional boundary layer. The 1972 monsoon season

was characterized by prolonged break while 1973 was a good monsoon year.

During an average monsoon season, the lower level vorticity is cyclonic and concentrated in the belt between $20^{o}N$ and $28^{o}N$. The dominant component of this vorticity is the meridional variation of the zonal wind. The major fluctuations in the vorticity are restricted to the northern regions. The vorticity in these regions is high and cyclonic in active monsoon spells and anti-cyclonic during break monsoon conditions. Thus, the meridional shear of the zonal wind in the northern belt was considered to be related to rainfall distribution over the plains under normal and extreme (good and bad) monsoon conditions.

The rainfall index used in the study was:

$$\text{Rainfall index} = \frac{100 \times \text{Daily Rainfall over Plain stations}}{\text{Normal daily rainfall over the stations}}$$

The shear of the zonal wind at 900 mb between $12^{o}N$ and $20^{o}N$ along $80^{o}E$ was considered to represent the large scale vorticity over the southern peninsula. Similarly computations for the latitudes $20^{o}N$ to $28^{o}N$ was considered to represent the large scale vorticity on the plains of India.

The major difference in the upper tropospheric circulation of the two seasons was in the meridional component which was southerly over larger regions of India in the drought year 1972 and northerly in the active monsoon year 1973. Other important conclusions from the study were:

i) the magnitudes of the changes in the lower level vorticity were much larger than those in the upper level vorticity and as such the lower level vorticity becomes anticyclonic during the break monsoon whereas it reamined anticyclonic throughout the season in the upper levels. The anticyclonic vorticity decreases during breaks and decreases markedly at the end of break.

ii) the kinetic energy of the upper tropospheric westerlies was maximum during the break and weak monsoon conditions as in 1972 and 1973.

The study revealed that the meridional advection of vorticity in the upper troposphere largely determines the divergence in the upper levels and consequently lower level convergence and the active rainfall situation.

Rao et al (1978) studied the influence of the fluctuations of energy budget of north Indian ocean on the general behaviour of Indian summer monsoon during July. The parameters used in the study were:

i) monthly heat gain by the ocean,

ii) solar radiation absorbed by the ocean,

iii) net infrared radiational exchange at the surface,

iv) latent heat flux, and

v) sensible heat flux.

The first three parameters were computed using the Budyko' method and the later by bulk aerodynamic method. The

differences in the energy budget components of north Indian ocean between normal July conditions and break monsoon period of 15-31 July 1972 were examined to assess the influence of oceanic surface on the behaviour of monsoon system.

The main conclusions of the study were:

i) The net radiation during break monsoon conditions in July was more than the corresponding under normal conditions,

ii) during break monsoon, higher energy losses occur over Arabian sea than in Bay of Bengal i.e. to say the Bay of Bengal gains heat and Arabian sea losses heat.

3.0 REMARKS

Most of the regional and general circulation models especially those based on the primitive equation Barotropic model were able to reproduce some of the broad large scale characteristics of the seasonal variations of climate. The simulation, however, generally suffer from spurious features where large scale orography such as Himalayas or Rockies were involved. It is generally recognised that among the lot of models available, each model was able to reproduce certain of the characteristics better than the other. However, it could not be definitively concluded which of the processes or parameters cause the difference in the performance among the various models.

Some of the attempts at the Geophysical Fluid Dynamic Laboratory have provided the necessary impetus for inclusion of the land surface, in other words the hydrological processes into the general circulation models. Studies by Charney (1977) and others have indicated the importance of the land surface parameters such as albedo, soil moisture in influencing the atmospheric general circulation and in broadly determining the climate of the world and the year to year phenomena like floods and droughts. It is well known that the albedo and soil moisture of the land surface are directly related to the vegetative cover which in turn partly controls the amount of moisture being put into the atmosphere through evapotranspiration. It is, therefore, very vital that future general circulation

models should include appropriate parameters to represent the land surface processes.

In India, considerable progress in the modelling of the atmosphere over the monsoon region has been made in the last 10 to 15 years. It is encouraging to note that the spectral models which are known to behave well for global representation are in the process of development and testing. As indicated by Bedi (1985), the spectral models need further refinement by inclusion of moisture processes, sub-grid convective process and boundary layer energy exchanges whereupon this could be used for general circulation modelling in the Indian ocean region.

To fulfill the objective of using the climate information for hydrological forecasts some studies are to be carried out in the immediate future. These include

i) Parameterization of the infiltration for general circulation model studies.

ii) Sensitivity study regarding the change in soil moisture to assess the impact of soil moisture on monsoon circulation and precipitation.

iii) Response of GCM forecasting on surface water hydrologic models for the Indian sub-continent and use of GCM output for real time flood forecasting.

iv) Estimation of water yield from a drainage basin.

v) Modelling for hydrological forecast of the water resources system in the operation for irrigation, hydropower and flood control.

REFERENCES

1. Abbott, D.A., (1973), 'Scale Interactions of Forces Quasistationary Planetary Waves at Low Latitudes', Tech. Report No. 73-2, Department of Meteorology, Florida State University, pp. 190.

2. Ananthakrishnan, R. (1965), 'General Circulation of the atmosphere over the Indian Ocean and adjoining areas', Proc. Symp. on Meteorological results of the IIOE, Bombay pp. 105-114.

3. Anthes, R.N. (1983), 'Regional Models of the Atmosphere in Middle Latitudes', Mon. Weath.Rev., 111, pp.1306-1335.

4. Arakawa, A. (1972), 'Design of the UCLA General Circulation Model', Numerical Simulation of Weather and Climate', Tech. Report No.7, Department of Met. UCLA.

5. Arakawa, A., and V.R. Lamb (1977), 'Computational Design of the Basic Dynamical Processes of UCLA General Circulation Model', Methods in Computational Physics, 17, pp. 173-263, Academic Press. New York.

6. Asnani, G.C. (1972), 'An experiment with barotropic quasi-geostrophic model for the Indian region', Indian Journal of Meteorology and Geophysics, Vol. 23, No.2, pp. 173-175.

7. Awade, S.T. and R.N. Kesavamurty (1975), 'Vertical Motion in the Indian Summer Monsoon, Ind. Jour. Met. Hydrol. Geophys. Vol. 26, 384-390.

8. Bedi, H.S. (1976), 'Spectral representation of Hemispheric flow patterns', Indian Jour. Meteoro., Hydro. and Geophy., Vol.27, No.4, pp. 397-408.

9. Bedi, H.S. (1985), 'A primitive equation spectral model for study of planetary scale atmospheric flow', Mausam, Vol. 36, No.3, pp. 295-300.

10. Boer, G.J. and N.A. McFarlane, (1975), 'The AES Atmospheric General Circulation Model', Report of the JOC study conference on Climate Models, GARP Publication Series No.22, Vol. I, pp. 409-460.

11. Bourke, W. (1974), 'A multi-level model(I)formulation and hemispheric integrations' Mon. Weath. Rev., 102, pp. 688-701.

12. Bourke, W.,B. McAdvaney, K Puri and R Thurling, (1977), 'Global Modelling of Atmospheric Flow by Spectral Models', Methods in Computational Physics, 17, pp.267-324. Academic Press, New York.

13. Bryan, K. (1969), 'Climate and Ocean Circulation'-3, The Ocean Model', Weath. Rev., 97, pp. 806-827.

14. Budyko, M.I. (1956), 'The Heat Balance of the Earth's Surface', Gidrometeorologicheskoe Izdatel' stvo, Leningrad.

15. Budyko, M.E. (1963), 'Atlas of the Heat Balance of the Earth', USSR Glavnaia Geofizicheskaia Observations, Moscow.

16. Carson, D.J. and W.M. Cunnington, (1979), 'General Circulation Experiments with an 11-layer Model', GARP Programme on Numerical Experimentation, Research Activities in Atmospheric and Oceanic Modelling, Report No.19, pp. 85-89.

17. Charney, J.G., P.H. Stone, and W.J. Quirk, (1975), 'Drought in Sahara: A biogeophysical feedback mechanisam', Science, 187, pp. 434.

18. Charney, J.G., W.J. Quirk, S. Chow, J. Kornfield, (1977), 'A comparative study of the effects of Albedo change on Drought in Semi-arid Regions', J. Atmos. Sci., 34, pp. 1366.

19. Corby, G.A., A.Gilchrist and P.R. Rowntree, (1977), 'United Kingdom Meteorological Office Five Level General Circulation Model', Methods in Computational Physics, 17, pp. 67-110, Academic Press, New York.

20. Cubasch, V., S. Tibaldi and F. Molteni, (1986), 'Deterministic Extended Range Forecast Experiments Using Global ECMWF Spectral Model', Proceedings of the First WMO Workshop on the Diagnosis and Prediction of Monthly and Seasonal Atmospheric Variations over the Globe, College Park Maryland, U.S.A., 29 July-2 August 1985. WMO Long -Rang Forecasting Research Report Series, 6, Vol. II. pp. 581-589.

21. Daley, R., C. Girard, and J. Hendersen, (1976)'Short Term Forecasting with a multi-level Spectral Primitive Equation model Part I-Model Formulation', Atmosphere, Vol. 14, 98-116.

22. Das, P.K. (1962), 'Tellus', Vol. 14, pp. 212-220.

23. Das, P.K., R.K. Datta and B.M. Chhabra (1971), 'Diagnostic study of a tropical storms using a quasi geostrophic baroclinic model', Indian Jour. of Meteor. and Geoph., Vol. 22, No.4, pp. 331-336.

24. Das, P.K. and H.S. Bedi (1978), 'Inclusion of Himalayas in a primitive equation Model', Indian Jour. of Meteor. Hydro. and Geophy., Vol. 29, No.1 and 2, pp.

25. Datta, R.K. and T.K. Mukerji, (1975), 'Vertical Velocity patterns over India and neighbourhood during break monsoon and active monsoon periods', Indian Jour. Meteor. Hydro. and Geophy., Vol. 26, No.3, pp. 399-404.

26. Deardorff, J., (1978), 'Efficient Prediction of Ground Temperatures and Moisture with Inclusion of a Layer of Vegetation', J. Geophy. Res. 83, pp. 1889-1903.

27. Dell'Osso, L. (1983), 'High Resolution Experiments with ECWMF Model', A Case Study, ECMWF Tech. Report No.37.

28. Douglas, H.A., R. Hide and B.J. Mason, (1972), 'An Investigation of the Structure of Baroclinic Waves using three-level streak photography', Q.J. Roy, Met. Soc.98, pp. 247-263.

29. Druyan, L.M. (1981), 'Review : The use of Global circulation Models in the Study of the Indian Monsoon', Journal of Climatology, Vol. 1, pp. 77-92.

30. Druyan, L.M., (1982), 'Studies of the Indian Summer Monsoon with a Coarse Mesh General Circulation Model', Jour. of Climatology, Vol. 2. pp. 127.

31. Druyan, L.M., (1982), 'Studies of the Indian Summer Monsoon with a Coarse-Mesh General Circulation Model, Part II, Jour. of Climatology, Vol. 2, pp. 347-355.

32. Ellis, R.S. (1952), 'Preliminary Study of a Relation Between Surface Temperatures of the North Indian Ocean and Precipitation over India', M.S. Thesis, Department of Meteorology, Florida State University.

33. Gadd, A.J. (1985), 'Extra-tropical Limited Area Fine Mesh Modelling', GARP Special Report No.43.

34. Gates, W.L. and M.E. Schlesinger, (1977),'Numerical Simulation of the January and July Global Climate with a Two-Level Atmospheric Model', J. Atmos. Sci., 34, pp. 36-76.

35. Gilchrist, A., (1977a), 'The simulation of the Asian Summer Monsoon', Pure and Applied Geophys., 115, pp. 1431-1438.

36. Gilchrist, A., (1977b), 'Simulation of the Asian Summer Monsoon by a 11-layer General Circulation Model', Monsoon Dynamics edited by S.J. Lighthill and R.P. Pearce, Cambridge University Press, Cambridge, pp. 131-145

37. Gilchrist, A., (1979),'The meteorological Office 5-layer General Circulation Model', Report of the JOC Study Conference on Climate Models, GARP Publication Series No.22, Vol. 1, pp. 254-295.

38. Gilchrist, A., P.R. Rowntee, and D.B. Shaw, (1982), 'Large Scale Numerical Modelling', The GATE Monograph, GARP Publication Series No.25.

39. Godbole, R.V., (1973), 'Numerical simulation of the Indian Summer Monsoon', Indian Jour. of Meteo. and Geophy. Vol. 24, No.1, pp. 1 to 14.

40. Godbole, R.V. and J. Shukla, (1981), 'Global Analysis of January and July Sea Level Pressure', NASA Technical Memorandum 82097.

41. Hadley, G., (1735), 'Concerning the cause of the General Trade Winds', Philosophical Transactions, Royal Society', Vol. 29, pp. 58.

42. Hahn, D.G., and S. Manabe, (1975), 'The Role of Mountains in the South Asian Monsoon Circulation: A comparison of Two Global General Circulation Model Experiments', GFDL/NOAA, Princeton.

43. Halem, M., J. Shukla, Y. Mintz., M.L., Wu,R. Godbole, G. Eerman, and Y Sud, (1979), 'Comparison of Observed Seasonal Climate Features with a Winter and Summer Numerical Simulation Produced with GLAS General Circulation Model', Ibid, pp. 207-253.

44. Hide, R., (1969), 'Some laboratory experiments of Free Thermal Convection in a Rotating Fluid Subject to a Horizontal Temperature Gradient and their Relation to Theory of the Global Atmospheric Circulation', In Corby G.A. (editor), The Global Circulation of the Atmosphere, London, Roy. Met. Soc., pp. 196.

45. Hide, R. and B.J. Mason, (1970), 'Baroclinic waves in a Rotating Fluid Subject to Internal Heating', Philosophical Transactions, Royal Society, 268,pp.201.

46. Holloway, J.L., Jr. and S. Manabe, (1971), 'Simulation of Climate by a Global General Circulation Model', Mon. Weath. Rev., 99, pp. 335-370.

47. Holloway, J.L., Jr. and S Manabe, (1971), 'Simulation of Climate by a Global General Circulation Model I, Hydrologic Cycle and Heat Balance', Mon. Weath. Rev., 99, pp. 335-370.

48. Hoskins, B.J., and A.J. Simmons, (1975), 'A Multi-level spectral model and the semi-implicit method', Quart. Jour. Roy. Meteorol. Soc., 101, pp. 637-655.

49. Houghton, D.D., J.E. Kutzbach, M. McClintock, and D. Suchman, (1974), 'Response of a General Circulation Model to a Sea Temperature Perturbation', Jour. Atmos. Sci., 31, pp. 857-868.

50. Huang, J.C.K., (1978), 'Response of the NCAR General Circulation Model to North Pacific Sea Surface Temperature Anomalies', J. Atmos. Sci., 35, pp.1164-1179

51. Kasahara, A. and W.M. Washington, (1971), 'General Circulation Experiments with a six-layer NCAR Model, Including Orography, Cloudiness and Surface Temperature Calculations', Jour. Atmos. Sci., 28, pp. 657-701.

52. Kiel, J.T. and V. Ramanathan, (1983), 'CO_2 Radiative Parameterization Used in Climate Models: Comparison with Narrow Band Models and with Laboratory Data', J. Geophy. Res., 88, pp.5191-5202.

53. Koteswaram, P. (1958), 'The Asian Summer Monsoon and the General Circulation over the Tropics', Proc. of International Symp. on Monsoons of the World, New Delhi, pp. 105-110.

54. Krichak, S.O., (1981), 'Experimental Forecast of the Meteorological Elements over the Summer Monsoon Area Using the Diabatic Primitive Equation - Limited Area Model', Proc. of the International Conference on Early Results of FGGE and Large Scale Aspects of its Monsoon Experiments, Jalla Hassee, January.

55. Krishna Rao, D. and R.K. Datta (1975), 'Circulation during 'Break' in the Indian Southwest monsoon - A proposed model'. Indian Jour. of Meteor., Hydrology and Geophysics, Vol. 26, No.3 pp. 405-409.

56. Kurihara, Y., and J.L. Holloway, Jr., (1967),'Numerical Integration of a Nine Level Global Primitive Equations Model Formulated by the Box Method', Mon. Weath Rev., 95 pp. 509-530.

57. Krishnamurti, Ruby, (1977), 'Laboratory Modelling of theOceanic Response to Monsoonal Winds', Monsoon Dynamics edited by S J Lighthill and R.P. Pearce, Cambridge University Press, Cambridge , pp. 557-578.

58. Lau, Ka, N.W., (1978), 'Experiment with a Simple Ocean - Atmosphere Climate Model : The Role of the Ocean in the Global Climate', J. Atmos. Sci., 35: pp. 1144-1163.

59. Lieslie, L.M., G.A. Mills,,and D.J. Gauntlett, (1981), The impact of FGGE Data Coverage and Improved Numerical Techniques in Numerical Weather Prediction in the Australian Region', Q J Roy. Met. Soc., 107: pp. 629-642.

60. Lvovitch , M.I., and S.P. Ovtchinnikov, (1964), 'Physical Geographical Atlas of the World', Academy of Sciences USSR, Department of Geodesy and Cartography, State Geodetic Commission, Moscow.

61. Marchuk, G.I., V.P. Dymnikov, V.N. Lykosov, V.Y. Galin, I.M. Bobyleva, and V.L. Perov, (1979), 'Numerical Simulation of the Global Circulation of the Atmosphere', Report of the JOC Study Conference on Climate Models, GARP Publications Series No.22, Vol. I, pp. 318-370.

62. Manabe, S., (1969), 'Climate and the Ocean Circulation, (I)The Atmospheric Circulation and the Hydrology of the Earth's Surface', Mon. Weath. Rev., 97, pp. 739-774.

63. Manabe, S., D.G. Hahn and J.L. Holloway, Jr. (1974), 'The Seasonal Variation of the Tropical Circulation as Simulated by a Global Model of the Atmosphere', Ibid, 31, pp. 43-83.

64. Manabe, S., D.G. Hahn and J.L. Holloway, Jr. (1979), 'Climate Simulation with GFDL Spectral Models of the Atmosphere: Effect of spectral Truncation', Report of the JOC Study Conference on Climate Models, GARP Publication Series No.22, Vol. I, pp. 41-94.

65. Manabe, S., and J.L. Holloway, Jr., (1975), 'The Seasonal Variation of the Hydrologic Cycle as Simulated by a Global Model of the Atmosphere', Jour. Geophys., Res., 80, pp. 1617-1649.

66. Manabe, S., J. Smagorinsky and R.F.Strickler, (1965), 'Simulated Climatology of a General Circulation Model with the Hydrologic Cycle', Mon. Weath. Rev.,93, pp. 769-798.

67. Manabe, S., and R.J. Stouffer, (1980), 'Sensitivity of a Global Climate Model to an Increase of CO_2 Concentration in the Atmosphere', J. Geophy. Res., 85, pp. 5529-5554.

68. Manabe, S., and T.B. Terpstra, (1974), 'The effects of Mountains on General Circulation of the Atmosphere as Identified by Numerical Experiment', Jour. Atmos. Sci., 31, pp. 3-42.

69. Manabe, S. and R.T. Wetherald, (1980), 'On the Distribution of Climate Change Resulting from an Increase in CO_2-content of the Atmosphere', J. Atmos. Sci., 37, pp. 99-118.

70. McAvaney, B.J., W. Bourke, and K Puri, (1978), 'A Global Spectral Model for Simulation of General Circulation', Jour. Atmos. Sci., 35, pp. 1557-1583.

71. McAvaney, B.J., W. Bourke and K. Puri, (1979), 'A Simulation of the January Global Circulation Using a spectral Model', Report of the JOC Study conference on Climate Models, GARP Publication Series No.22 Vol.I pp. 296-317.

72. Mintz, Y., (1965), 'Very Long-term Global Interation of the Primitive Equations of Atmospheric Motion', WMO Tech. Note No.66, pp. 141-167.

73. Miyakod, K. and J Sirutis, (1977), 'Comparative Integrations of Global Models with various Parameterized Processes of subgrid-scale vertical Transport: Description of the Parameterization, Beitrage Zur Physik der Atmosphere, 50, pp. 445-447.

74. Mohanty, U.C. and S.C. Madan, (1985), 'Certain aspects on the realization of primitive equations forecasting model in the low latitudes', Mausam, Vol.36, No.2, pp. 127-134.

75. Moller,F., (1951), 'Vierteljahrskarten des Niederschlags fur die ganze Erde', Petermanns Geogr. Mitt., 95, pp. 1-7.

76. Mukerji, T.K. and R.K. Datta (1973), 'Prognosis by four layer quasi-geostrophic model', Indian Jour., of Meteor. and Geophy., Vol. 29, No.2, pp. 93-100.

77. Mukerji, T.K. and R.K. Datta, (1975), 'An experiment in forecasting with diabatic baroclinic model over India and neighbourhood', Indian Jour. of Meteor., Hydrol., and Geophys., Vol. 26, No.3, pp. 326-332.

78. Phillips, N.A., (1956), 'The General Circulation of the Atmosphere: A Numerical Experiment', Q.J. Roy. Met. Soc., 82, pp. 123-164.

79. Pitcher, E.J., R.C. Malone, V. Ramanathan, M.M. Blackman, K. Puri, W. Bourke, (1983), 'January and July Simulation with a spectral General Circulation Model', J. Atmos. Sci., 40, pp. 580-604.

80. Raghavan, K. (1973), 'Monthly Weather Review, Vol.101, No.1, pp. 33-43.

81. Ramage, C.S., and C.R.V. Raman, (1972), 'Meteorological Atlas of the International Indian Ocean Expedition', Vol.2, Upper Air,National Science Foundation, Washington, D.C.

82. Ramanathan, Y. and K.R. Saha, (1972), 'Application of a primitive equation barotropic model to predict movement of western disturbances', Jour. Appl. Met. Vol. 11, pp. 268-272.

83. Ramanathan, Y. and R.K. Bansal (1977), 'On the Application of a primitive equation barotropic model for the prediction of storm tracks in the Indian region', Indian Jour. Meteo., Hydro. and Geophy., Vol. 26, No.2, pp. 169-176.

84. Ramanathan, V., E.J. Pitcher, R.C. Malone, and M.L. Blackmou, (1983), 'The Response of the Spectral General Circulation Model to Refinements in Radiative Processes', J. Atmos. Sci., 40, pp. 605-630.

85. Rao, Y.P. (1962), 'Meridional circulation associated with the monsoon of India, Indian Jour. of Meteorology and Geophy. Vol. 13, No.2, pp. 157-166.

86. Rao, R.R., S.V.S. Somanadham and Syed Nizamuddin, (1978), 'Study of the influence of surface energy budget of north Indian ocean on the behaviour of Indian Summer Monsoon', Indian Jour. of Meteor., Hydrol., and Geophy. Vol. 29, No.1 and 2, pp. 253-258.

87. Rowntree, P.R. (1972), 'The influence of Tropical East Pacific Ocean Temperature on the Atmosphere', Q.J.Roy. Met. Soc., 98, pp. 290-321.

88. Saha, S (1983), 'Behaviour of monsoon depressions in Primitive equation barotropic model', Mausam, Vol. 34, No. 1 pp. 27-32.

89. Saker, N.J., (1975), 'An 11-layer General Circulation Model', Ibid, Met 020, Tech Note No.II/30.

90. Sikka, D.R. (1975), 'Forecasting the movement of tropical cyclones in the Indian seas by non-divergent barotropic model', Indian Jour. of Meteoro., Hydrol. and Geophy., Vol. 26, No.3, pp. 323-325.

91. Sikka, D.R. and Sulochana Gadgil (1978), 'Large-scale rainfall over India during the summer monsoon and its relation to the lower and upper tropospheric vorticity', Indian Jour. of Meteor., Hydrol., and Geophy., Vol. 29, No.182, pp. 219-231.

92. Singh, S.S. and K.R. Saha, (1978), 'Numerical experiment with primitive equation barotropic model using quasi-Lagrangian advection scheme to predict the movement of monsoon depression and tropical cyclone', Indian Jour. of Meteor., Hydrol. and Geophy., Vol. 29, No. 1 and 2, pp. 367-374.

93. Sharma, O.P. and R. Sadourny (1985), 'Numerical Experimentation with FGGE Data: Simulation of the 1979 Indian Monsoon Onset using a Stretched - Coordinate Version of the LMD GCM', GARP Special Report No.44.

94. Shaw, D.B., (1978), 'Numerical prediction experiment in the monsoon region', Indian Jour. of Meteorl. Hydrol., and Geophy., Vol. 29, No. 182, pp. 361-366.

95. Shukla, J., (1975), 'Effect of Arabian Sea-Surface Temperature Anomaly on Indian Summer Monsoon: A Numerical Experiment with the GFDL Model', J. Atmos. Sci., 32, pp. 503-511.

96. Shukla, J. and B.M. Misra, (1977), 'Relationships between sea-surface Temperature and Wind speed over the Central Arabian Sea and Monsoon Rainfall Over India', Mon. Weath. Rev., 105, pp. 998.

97. Somerville, R.C.J., P.H. Stone, M. Halem, J.E. Hansen, J.S. Hogan, L.M. Druyan, G. Russel, A.A. Lacis, W.J. Quirk, and J. Tennenbaum, (1974), 'The GISS Model of the Global Atmosphere', J. Atmos. Sci., 31, pp. 84-117.

98. Smagorinsky, J., (1963), 'General Circulation Experiments with the Primitive Equations', Mon. Weath. Rev., 91, pp. 99-164.

99. Spar, J., (1973), 'Some Effects of Surface Anomalies in Global General Circulation Model', Mon. Weath. Rev. 101, pp. 91-100.

100. Stone, P.H.,S. Chow, and W.J. Quirk, (1977),'The July Climate and a Comparison of the January and July Climates Simulated by the GISS General Circulation Model', Mon.Weath. Rev., Vol. 105, pp. 170.

101. Temperton, C., T.N. Krishnamurti, R. Pasch and T.Kitade, (1983), 'WGNE Forecast Comparison Experiment', Report No.6, Numerical Experimentation Programme, WRCP, WMO.

102. Vettin, L. (1885), 'Experimentelle Darstellung Von Lufybewegungen unter Dem Einfluss von Temperaturunterschieden und Rotationsimpulsen', Meteorologische Zeitschrift, 2, pp. 172.

103. Walker, J.M. (1972) 'Monsoons and the global Circulation', The Meteorological Magazine, Vol. 101, No. 1205 pp. 349-350

104. Washington, W.M. (1970), 'On the Simulation of the Indian Monsoon and Tropical Easterly Jet Stream with the NCAR General Circulation Model', Proceedings of the Symp. on Tropical Meteorology, 2-11 June 1970, University of Hawai , Honolulu, Hawaii.

105. Washington, W.M. (1974), 'Brief Descripiton of NCAR Global Circulation Model', In Modelling for the First GARP Global Experiment, GARP Publication Series No.14, pp. 61-78.

106. Washington, W.M., (1976), 'Numerical Simulation of Asian African Winter Monsoon', Mon.Weath. Rev., 104, pp. 1023.

107. Washington, W.M. and S.M. Dagupaty, (1975), 'Numerical Simulation with the NCAR Global Circulation Model of the Mean conditions during the Asian-African Summer Monsoon', Mon. Weath. Rev., 103, pp. 105-114.

108. Washington, W.M., R Dickinson, V Ramanathan, T Mayer, D.L. Williamson, G. Williamson, and R. Wolski, (1979), 'Preliminary Atmospheric Simulation with the Third Genration NCAR General Circulation Model: January and July', Report of the JOC Study Conference on Climate Models, GARP Publication Series No.22, Vol. I, pp. 95-138.

109. Washington, W.M. and A Kasahara, 'A January Simulation Experiment with Two-Layer Version of the NCAR Global Circulation Model', Mon. Weath. Rev., 98, pp. 559-580.

110. Washington, W.M. and G.A. Meehl, (1983), 'General Circulation Experiments on the Climatic Effects due to a Doubling and Quadrupling of CO_2 Concentration', J. Geophys. Res., 88, pp. 6600-6610.

111. Washington, W.M. and G.A. Meehl, (1984), 'Seasonal Cycle experiment on the climate sensitivity due to a doubling of CO_2 with an Atmospheric General Circulation Model Coupled to a simple Mixed-Layer Ocean Model', J. Geophys., Res., 89, pp. 9475-9503.

112. Washington, W.M. and D.L. Williamson, (1977), 'A description of the NCAR Global Circulation Models', Methods in Computational Physics, 17, pp. 111-172, Academic Press, New York.

113. Webester, P.J. and K.M.W. Lau (1977), 'A simple Large-scale Ocean-Atmosphere Interaction Model Basic Model and a Simple Experiment', J. Atmos. Sci., 34, pp. 1063-1084.

114. Wernstedt, F., (1972), 'World Climate Data', Climatic Data Press, Lemont, Pennsylvania.

115. Wetherald, R.T., and S. Manabe, (1972), 'Response of the Joint Ocean-Atmosphere Model to the Seasonal Variation of the Solar Radiation', Mon. Weath. Rev., 100, pp. 42-59.